NOAA NA16RC0116
NSF ATM-9115184

EVIDENCE OF A STRATOSPHERIC QBO MODULATION OF TROPICAL CONVECTION

by John A. Knaff

P.I.–William M. Gray

Colorado State University

DEPARTMENT OF ATMOSPHERIC SCIENCE

PAPER NO. 520

EVIDENCE OF A STRATOSPHERIC QBO MODULATION OF TROPICAL CONVECTION

By
John A. Knaff

Department of Atmospheric Science
Colorado State University
Fort Collins, CO 80523

January, 1993

Atmospheric Science Paper No. 520

ABSTRACT

Evidence is presented of a modulation of deep tropical convection by the Stratospheric Quasi-Biennial Oscillation (SQBO) in convective anomalies, precipitation and pressure in the Western Tropical Pacific region. In particular, the SQBO, by creating differing amounts of upper tropospheric (200 mb) to lower stratospheric (50 mb) zonal wind shear, appears to modulate deep tropical convection. Results suggest that in the tropical West Pacific region, strong values of this vertical shear act to suppress convection, limit rainfall and often raise surface pressures. During the west phase of the SQBO, areas of least 200 mb to 50 mb shear are located in off-equator regions. In contrast, during the east phase of the SQBO, minimum 200 mb to 50 mb zonal wind shear is located along the equator. These differences result in convection being preferred off (on) the equator during the west (east) phase of the SQBO. Because the SQBO creates opposing patterns of this 200 mb to 50 mb zonal wind shear during the east and west phases, convection is modulated by each of these patterns for a prolonged (6-18 month) period, thus allowing time for gradual change in the West Pacific general circulation. The convection, rainfall, pressure, and circulation patterns associated with the differing phases of the SQBO are discussed along with a preliminary theory for these patterns. Furthermore, evidence is presented that the west phase of the SQBO favors cold ENSO events whereas the east phase favors warm ENSO events.

TABLE OF CONTENTS

LIST OF SYMBOLS AND ACRONYMS

CAC : Climate Analysis Center

DJF : December-January-February

DMSP : Defense Meteorological Satellite Program

ENSO : El Niño/Southern Oscillation

HRC : Highly Reflective Clouds

ITCZ : Inter–Tropical Convergence Zone

JJA : June-July-August

MAM : March-April-May

NCAR : National Center for Atmospheric Research

NOAA : National Oceanic and Atmospheric Administration

OLR : Outgoing Longwave Radiation

OND : October–November–December

PV : Potential vorticity

QBO : Quasi-Biennial Oscillation

SO : Southern Oscillation

SOI : Southern Oscillation Index

SON : September–October–November

SPCZ : South Pacific Convergence Zone

SQBO : Stratospheric Quasi–Biennial Oscillation

SST : Sea Surface Temperature

ZWA : Zonal Wind Anomaly

Chapter 1

INTRODUCTION

Interannual variations of deep tropical convection are of primary importance to short term climate variability. The latent heat released in the tropics in association with deep convection supplies much of the energy driving the earth's general circulation. Moreover, recent studies have shown a fundamental and characteristic biennial or quasi-biennial modes of variation in many tropospheric and ocean parameters which are either directly or indirectly related to the variation of deep convection in the tropics. The latter studies include evidence of (quasi-) biennial oscillations in the ultra-long waves of the Southern Hemisphere (Trenberth, 1980); the equatorial intra-seasonal (30-60 day) oscillation (Kuma, 1990); the Indian monsoon (Mukherjee *et al.*, 1985); tropospheric winds and temperatures (Yasunari, 1989); global precipitation (Lau and Sheu, 1988); tropical cyclones (Gray, 1984, 1988); equatorial Sea Surface Temperatures (SST) (Barnett, 1989, 1990, 1991; Meehl, 1987) and; the El Niño/Southern Oscillation (ENSO) (Angell, 1992; Gray *et al.* 1991, 1992a, 1992b; Rasmusson *et al.*, 1990). The large number of tropospheric and ocean parameters which have underlying biennial signals suggest that there may be a single direct or indirect cause of this apparent fundamental mode of climate oscillation. These and other findings suggesting a biennial or quasi-biennial mode of climate variability led us to look at possible linkages between the Stratospheric Quasi-Biennial Oscillation (SQBO) and tropospheric parameters which might be related to these biennial oscillations of climate.

The argument for a direct link between the SQBO and the ocean/tropospheric system have been proposed by Gray *et al.* (1991,1992a, 1992b), Shapiro (1989), Gray (1984, 1988), Angell (1992), Yasunari (1989), Knaff (1991), Kuma (1990), Mukherjee *et al.* (1985) and

Muruyama (1991). That most climate variability can be linked to variations in tropical convection has directed this study to the search for direct relationships between the SQBO and deep tropical convection. It is hypothesized that the variations of the stratospheric zonal winds associated with the SQBO effectively modulate deep convection by creating prolonged periods of strong (> 15 m/s) and weak (< 15 m/s) vertical wind shear between the upper troposphere (12 km, 200 mb) and lower stratosphere (20 km, 50 mb). Such a SQBO-convection relationship is of great potential importance to climate research and seasonal forecasting and has many relevant implications. In addition to offering a partial explanation of (quasi-) biennial oscillations in tropospheric and oceanic parameters, a SQBO-convection modulation effect may require that present convective parameterizations be further refined by the inclusion of SQBO related affects and that seasonal predictions for the tropics, including monsoon strength/duration and ENSO, might be improved.

This paper presents evidence that the SQBO does modulate deep tropical convection manifested as precipitation, pressure and convective anomalies. This convection modulation is accomplished by the SQBO through varying rates of upper tropospheric to lower stratospheric (e.g., 200 mb to 50 mb) zonal wind shear, such that small (< 15 m/s) values of shear promote deep convection and large (> 15 m/s) values of this shear act to suppress deep convection. This modulation is also shown to have distinct spatial modes. During the east phase of the SQBO when this 200 mb to 50 mb shear is lowest **on** the equator, convection is shown to be favored **on** the equator (0° to 7°) whereas during the west phase of the SQBO when this shear is lowest **off** the equator, convection is shown to be favored in **off** equator regions (8° to 18°). Furthermore, this **on** versus **off** equator modulation results in prolonged periods of contrast such that circulation changes related to this convective modulation could play an important role in shaping anomalous seasonal circulation patterns associated with monsoons, the 30 to 60 day oscillation and thus ENSO. In agreement with this argument, observations suggest that cold ENSO episodes are favored during the west phase of the SQBO and warm ENSO episodes favored during the east phase of the SQBO. With these ideas in mind, the following chapter will describe the

temporal and spatial aspects of the SQBO and the variable aspects of upper tropospheric to lower stratospheric shear. Subsequent chapters present discussions of the relationships between convection, precipitation, surface pressure, and the general circulation.

Chapter 2

THE STRATOSPHERIC QUASI–BIENNIAL OSCILLATION OF ZONAL WINDS

The east and west phases of tropical stratospheric zonal winds associated with the Stratospheric Quasi-Biennial Oscillation (SQBO) create prolonged periods of contrasting upper tropospheric (200 mb) to lower stratospheric (50 mb) zonal wind shear. These contrasting shear patterns are primarily manifested as large regions of relatively small shear along the equator (±7°) during the east phase of the SQBO and as relatively small shear in areas 8° to 18° off the equator during the west phase of the SQBO. In this chapter, the latitudinal variation of the zonally symmetric SQBO that forces these contrasting vertical shear patterns and the associated spatial 200 mb to 50 mb shear patterns in the equatorial West Pacific region will be discussed.

2.1 The Latitudinal Variation of Lower Stratospheric Zonal Winds

Seasonal-latitudinal profiles of 50 mb zonal winds shown in Fig. 2.1 were created from 35 years of daily rawinsonde station data. Station data for latitude belts were averaged to obtain zonal means for typical east and west SQBO periods from which the latitudinal variations of the 50 mb zonal winds can be studied. These zonal means were then interpolated every 2.5° of latitude from 25°N to 25°S for all seasons. These values are then used to create the 50 mb to 200 mb zonal wind shear profiles discussed later in this chapter.

The variability of zonal wind in the stratosphere actually entails two distinct time scales, a zonally symmetric quasi–biennial signal that is very strong near the equator and an annual cycle which is strongest in the subtropics (Dunkerton and Delisi, 1985).

The effect of the annual cycle of stratospheric winds is to superimpose easterlies on the summer hemisphere and westerlies in the winter hemisphere. During the equinox, however, there is little evidence of the annual signal in the stratospheric zonal winds; the winds appear nearly symmetric about the equator during both the spring and the fall. The net affect of the stratospheric annual cycle is a reduction (enhancement) of the westerlies (easterlies) during the west phase (east phase) of the SQBO in the summer hemisphere, and a enhancement (reduction) of the westerlies (easterlies) in the winter hemisphere. This latter point is important as observational evidence suggests the 200 mb to 50 mb shear forced by the SQBO represents a modulating link between the troposphere and the lower stratosphere.

The 50 mb zonal wind speeds for typical east and west phase cases of the SQBO during December-January-February (DJF) are shown in Fig. 2.1a. During the east phase, zonal winds are easterly from 25°N to 25°S with a maximum occurring in the Southern (summer) Hemisphere. This is much different from the situation during the west phase. The zonal winds for the west phase of the SQBO for DJF have a distinct westerly maximum at the equator, westerlies in the Northern Hemisphere to 25°N, and weak westerlies near the equator that become easterly near 7° in the Southern (summer) Hemisphere.

During March-April-May (MAM), the zonal wind pattern at 50 mb becomes more symmetric about the equator, as shown in Fig. 2.1b. In this case, the east phase of the SQBO has an equatorial easterly maximum that weakens poleward (on both sides) of the equator, especially in the Northern Hemisphere. However, the west phase zonal winds show a distinct equatorial westerly maximum which fades quickly on both sides of the equator, becoming easterly near ±7°.

During June-July-August (JJA), Fig. 2.1c, the east phase of the SQBO again has easterly zonal winds extending from 25°S to 25°N with a maximum in the Northern (summer) Hemisphere near 10°N. During the westerly SQBO periods, the zonal winds at 50 mb have a westerly maximum at the equator which weakens poleward. Much as in DJF, the west phase for JJA is associated with a rapid decrease of the westerlies poleward in the

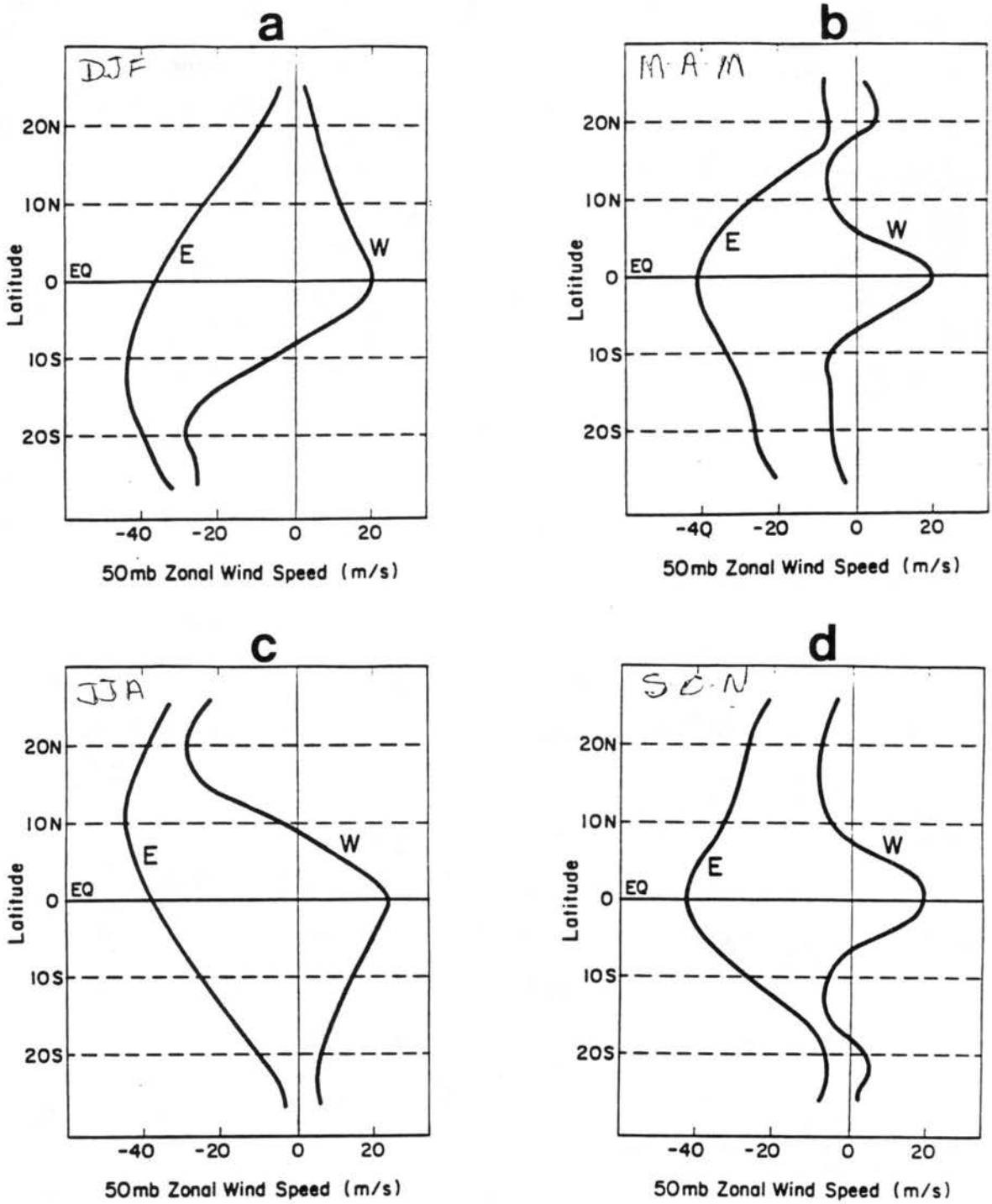

Figure 2.1: The absolute mean zonal wind at 50 mb for a) December-January-February, b) March-April-May, c) June-July-August, and d) September-October-November for typical east (E) and west (W) SQBO periods. Note that even though the anomalies are westerly/easterly the annual cycle forces more easterlies in the summer hemisphere and more westerlies in the winter hemisphere.

Northern (summer) Hemisphere with a transition from westerlies to easterlies occurring near 7°N.

The September-October-November (SON) transition season 50 mb zonal winds (Fig. 2.1d) are much like the conditions during MAM season. The east phase of the SQBO has an easterly maximum on the equator with strong easterlies extending through the Northern Hemisphere and somewhat weaker easterlies into the Southern Hemisphere. This profile is greatly different from the situation that exists during the west phase. During west phase SQBO periods there is a westerly wind maximum along the equator that weakens and becomes easterly on both sides of the equator.

This study of the latitudinal variations of 50 mb zonal winds shows that during the SQBO west phase, these winds are generally weakest (< 10 m/s) over regions that support large upper tropospheric ridges such as the monsoons. This placement causes the upper troposphere (200 mb) to lower stratospheric (50 mb) shears to be lowest in these regions during the west phase of the SQBO. By contrast, during the east phase of the SQBO, strong stratospheric easterly winds (< -30 m/s) along the equator occur above regions where similarly strong easterly zonal flow exists in the troposphere. The net result of this configuration during the east phase is small upper tropospheric to lower stratospheric shear along the equatorial zones. The spatial distribution of the shear patterns forced by the oscillating SQBO will be discussed further in the next section.

2.2 Magnitude of the Upper Tropospheric to Lower Stratospheric Wind Shear

The absolute value of the zonal wind shear between the upper troposphere (200 mb) and lower stratosphere (50 mb) shows distinct variations. A 10-year (1979 to 1988) zonal wind climatology for the troposphere was created at the Climate Analysis Center for a 2.5° by 2.5° grid. This climatological tropospheric data was subtracted from the 50 mb zonal wind values derived from 35 years of rawinsonde station data, thereby forming a 200 mb to 50 mb shear data set. The absolute value of this shear is then examined for both east and west phases of the SQBO. The following discussion will focus on the observed

seasonal differences of 200 mb to 50 mb shear patterns for both the east and the west phases of the SQBO. In this comparison, the shear will be considered strong if its absolute value is greater than 15 m/s and weak if the absolute value is less than 15 m/s.

The absolute values for upper tropospheric to lower stratospheric shear in the West Pacific region during the DJF season for a typical SQBO west phase situation are displayed in Fig. 2.2 (top). In this figure, there is an area of very strong shear centered on the equator over most of the West Pacific from 8°N to 8°S. This shear maximum is the result of strong equatorial westerlies at 50 mb and the strong easterly 200 mb equatorial jet associated with the Australian Monsoon. Figure 2.2 (top) also shows a rapid decrease in the value of the shear poleward on either side of the equator, with a minimum at about 20° from the equator. Hence, the DJF west phase shear patterns are characterized by (1) extremely strong shear on the equator extending to ±8°, and (2) minimum shears located approximately 20° off either side of the equator.

The shear patterns associated with the east phase of the SQBO during DJF are nearly opposite those of the west phase situation. During the east phase (Fig. 2.2, bottom), the lowest values of shear are located over Indonesia and the northern parts of New Guinea, with low shear values extending to near the Dateline. This shear is again the result of the strong easterly monsoon jet located near the equator at 200 mb. In Fig. 2.2 (bottom), the regions poleward of the equator have greater values of shear. This increase of shear is more evident in the Northern Hemisphere than in the Southern Hemisphere. Thus, the east phase of the SQBO causes 200 mb to 50 mb shear patterns characterized by (1) very small shear values near the equator extending to approximately ±8°, (2) maximum values of shears located approximately 20° off the equator, and (3) nearly opposite shear patterns as those of the west SQBO case (Fig. 2.2, top).

During the MAM season, the absolute value of 200 mb to 50 mb shear for the west phase of the SQBO (shown in Fig. 2.3, top), has a nearly symmetric shear pattern spanning the equator. The largest shear values are located along the equator and in the extreme Northwest Pacific. The shear minimums are again located off the equator approximately

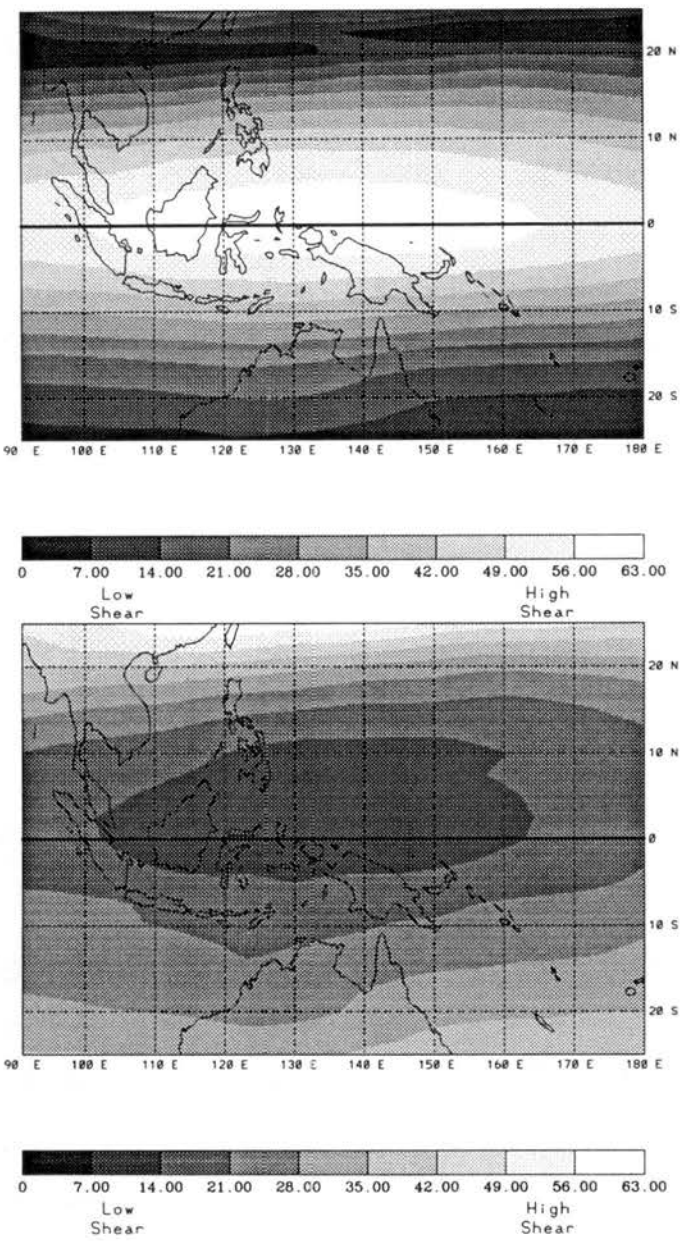

Figure 2.2: The absolute value of the zonal wind shear (m/s) for the DJF season between the upper troposphere (200 mb) and the lower stratosphere (50 mb) during the west phase (top) and east phase (bottom) of the stratospheric quasi-biennial oscillation at 50 mb. Areas with least shear are dark shaded; unshaded areas have strong shear.

at 10°N and at 15°S, much like the DJF west phase case. It is also interesting to note that in moving east along the equator, a relative minimum value of shear occurs near the Dateline. The west phase of the SQBO forces 200 mb to 50 mb shear patterns during MAM that are thereby characterized by (1) off-equator minimums located approximately at 13°S and 10°N, and (2) a relative maximum shear value over the equatorial Indonesia.

The shear patterns forced by the east phase of the SQBO during the MAM season (shown in Fig. 2.3, bottom), have broad regions of relatively strong shear throughout most the West Pacific. A relative minimum is located over the Northern Philippines whereas the greatest shear maximum is located near the Dateline. Although the shear forced by the SQBO east phase is very uniformed and strong in the West Pacific, it is much different than the west phase shear case (Fig. 2.3, top), wherein there were two distinct minimum shear regions on either side of the equator. Thus, 200 mb to 50 mb shear during the MAM season forced by a typical easterly east phase of the SQBO is characterized by (1) fairly strong values of shear throughout the West Pacific region, and (2) a relative shear minimum located from approximately 12°N to 20°N.

With the migration of the monsoon trough to the Indian region during JJA, 200 mb to 50 mb zonal shear patterns forced by the west SQBO are again fairly symmetric around the equator. The maximum values of shear during the JJA west phase case (Fig. 2.4, top), are along the equator but are not nearly so strong as in the DJF case (Fig. 2.2, top). However, broad areas of comparatively weak shear occur relatively close to the equator. In the Southern Hemisphere, a large area of near zero shear exists in a band roughly from 13°S to 16°S, extending throughout the West Pacific. In the Northern Hemisphere, another band of relatively minimum shear exists from roughly 5°N to 12°N. The main features of the west phase JJA shear patterns are thus characterized by (1) two very pronounced minima, one on either side of the equator located at 13°S and 10°N, respectively, and (2) a relative maximum located on the equator in the vicinity of Borneo and Malay in association with the strong 200 mb equatorial easterly jet.

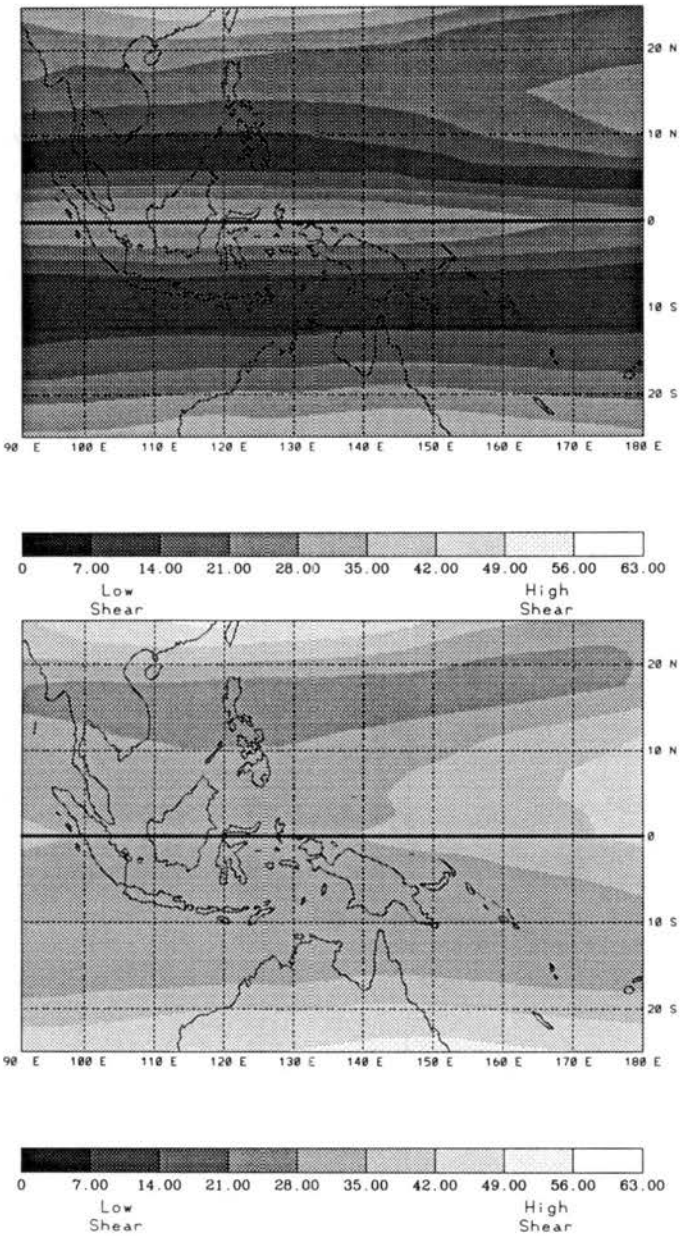

Figure 2.3: The absolute value of the zonal wind shear (m/s) for the MAM season between the upper troposphere (200 mb) and the lower stratosphere (50 mb) during the west phase (top) and east phase (bottom) of the stratospheric quasi-biennial oscillation at 50 mb.

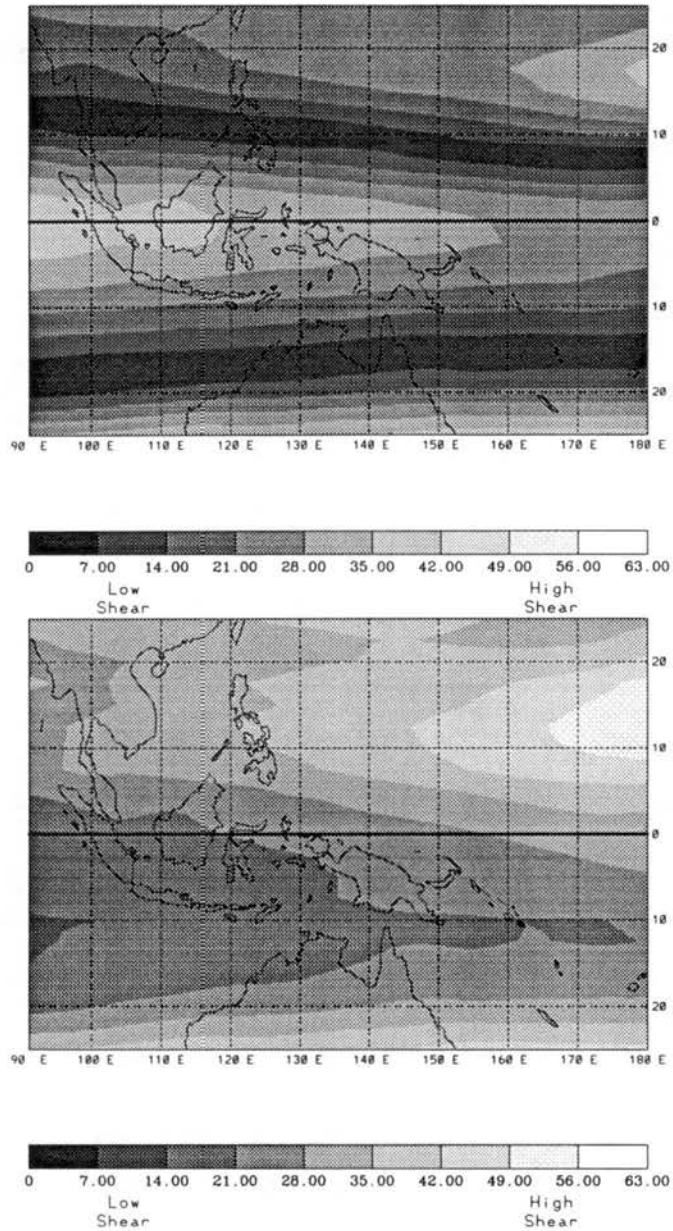

Figure 2.4: The absolute value of the zonal wind shear (m/s) for the JJA season between the upper troposphere (200 mb) and the lower stratosphere (50 mb) during the west phase (top) and east phase (bottom) of the stratospheric quasi-biennial oscillation at 50 mb.

During the same JJA season, the east phase of the SQBO causes the 200 mb to 50 mb shear patterns which are not equatorially symmetric, as shown in Fig. 2.4 (bottom). The maximum values of shear in this figure are located in the northwest tropical Pacific near 10°N where a band of strong tropospheric westerlies are located. The minimum shear values are located in the South Indian Ocean at about 10°S. This large region of minimum shear is associated with a strong tropical 200 mb ridge that extends roughly from Africa to North Australia during this season. The shear patterns associated the east phase of the SQBO during the JJA result in (1) relatively strong shear throughout the entire Northwest Pacific region with the strongest maximum near the Dateline and 13°N, and (2) a region of relatively minimum shear extending from the Indian Ocean continuing across Southern Indonesia in the Southern Hemisphere.

During SON, the west phase of the SQBO causes upper tropospheric to lower stratospheric zonal wind shear patterns which are again fairly symmetric about the equator. These shear values as shown in Fig. 2.5 (top), have very broad areas of minimum shear in both the Northern and Southern Hemispheres. The largest of the two minimum shear areas is located from 8°N to 15°N from 90°E to 165°E. In the Southern Hemisphere; another area of minimum shear extends across the West Pacific from 8°S to 12°S. Along the equator, there again is an area of maximum shear extending throughout the West Pacific. The SON west phase shear maps again show symmetry about the equator as was observed for the DJF, MAM and JJA seasons. The west phase SQBO 200 mb to 50 mb shear patterns can thus be characterized by (1) broad areas of minimum shear, one on either side of the equator, located at approximately 10°S and 12°N, and (2) a narrow area of relatively large shear located over the Western Indonesian region along the equator.

Finally, during the east phase of the SQBO in the SON season, stratospheric winds at 50 mb create 200 mb to 50 mb shear patterns much like those of the MAM season (Fig. 2.3, Bottom). As shown in Fig. 2.5 (Bottom), the east phase shear patterns for SON are rather strong throughout the entire West Pacific Region. Maximum values are situated

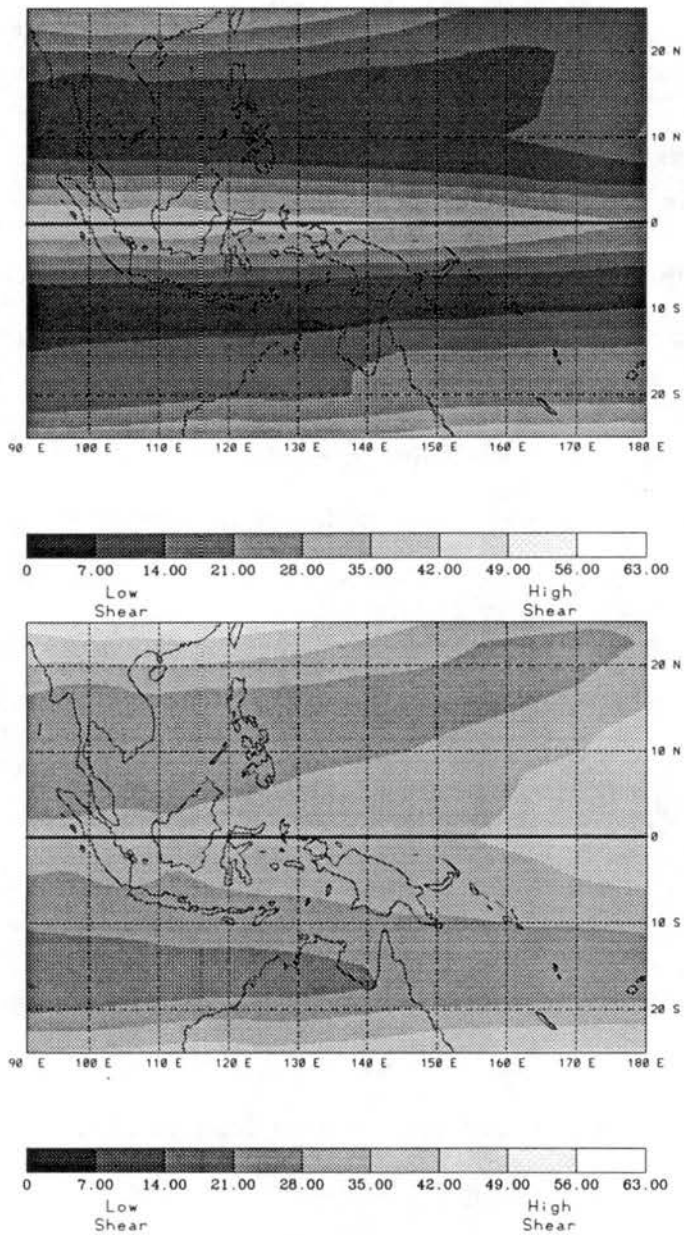

Figure 2.5: The absolute value of the zonal wind shear (m/s) for the SON season between the upper troposphere (200 mb) and the lower stratosphere (50 mb) during the west phase (top) and east phase (bottom) of the stratospheric quasi-biennial oscillation at 50 mb.

near the Dateline and minima are located in the 90°E to 140°E region at about 15° off the equator. However, all of these shear values are rather large, being greater than 21 m/s. The east phase SQBO upper tropospheric to lower stratospheric shear pattern during SON can be characterized as being (1) rather strong throughout the West Pacific region with (2) relative shear minima located on either side of the equator, covering the Malay Peninsula and the Philippines in the Northern Hemisphere, and North Australia and the parts of the Indian Ocean in the Southern Hemisphere, and (3) a relative maximum located on the Dateline.

The foregoing results have shown how the QBO of zonal winds in the lower stratosphere cause quite different upper tropospheric to lower stratospheric zonal wind shear patterns during each phase. These shear patterns manifest themselves during the west phase of the SQBO as fairly symmetric minimum shear areas that are displaced slightly to either side of the equator. In contrast, during the east phase of the SQBO, shear is generally stronger everywhere except during DJF, with maximum shear values located off the equator and minimum shear along the equator.

The east phase versus west phase differences can also be illustrated using vertical profiles of zonal wind. Figure 2.6 schematically illustrates the estimated vertical profile of zonal winds in the vicinity of 130°E during the DJF season at (a) 12°N, (b) the equator, and (c) 12°S. At the off-equator location (Fig. 2.6 a and c), shear differences between east and west phases of the SQBO are relatively small, but with the west phase 50 mb zonal winds creating smaller values of 200 mb to 50 mb vertical wind shear in both Hemispheres. In contrast, the equatorial location in Fig. 2.6b has very large 200 mb to 50 mb shear values during the west phase of the SQBO and relatively small values of this shear associated with the easterly phase. Similar vertical profiles of zonal winds are shown for the JJA season in Fig. 2.7. The off-equator stations (Fig. 2.7a and c) have relatively small east versus west 200 mb to 50 mb shear differences with the smallest values of shears occurring during the west phase of the SQBO. Near the equator, however, the east versus west phase

upper tropospheric to lower stratospheric shear differences are large wherein the shear is least during the east phase of the SQBO.

2.3 Temporal Variation of the 50 mb Zonal Winds

The amplitude of the SQBO varies with both latitude and with time. Furthermore, the SQBO has distinct periods of persistence versus change. These temporal tendencies can be illustrated as an annual cycle in the frequency of phase change of the SQBO. The temporal distribution of west to east transitions are shown in Fig. 2.8a. Notice that the SQBO has a tendency to change from west to east during the May through August period. Likewise, the east to west phase transitions in Fig. 2.8b show similar tendencies with the highest incidence of change occurring in the May through June period. The combination of these two frequency distributions is shown in Fig. 2.8c wherein the SQBO tends to show persistence from November to March and change from May to August. This may be important as possible evidence of a link with the El Niño phenomenon which shows similar periods of persistence as well as change.

2.4 Summary of Chapter 2

The contrasting patterns of 200 mb to 50 mb shear caused by the oscillating SQBO tend to persist, in most cases for more than a year and cover broad areas. These shear patterns in the Western Pacific region were studied for each season of the year. The results of this shear analysis for the west phase of the SQBO are as follows.

In DJF:

1. a strip of extremely strong shear values exists in the region extending from roughly 90°E to 180°, 8°N to 8°S, and

2. there are two zonally symmetric areas of minimum shear, one in each hemisphere about 20° poleward of the equator.

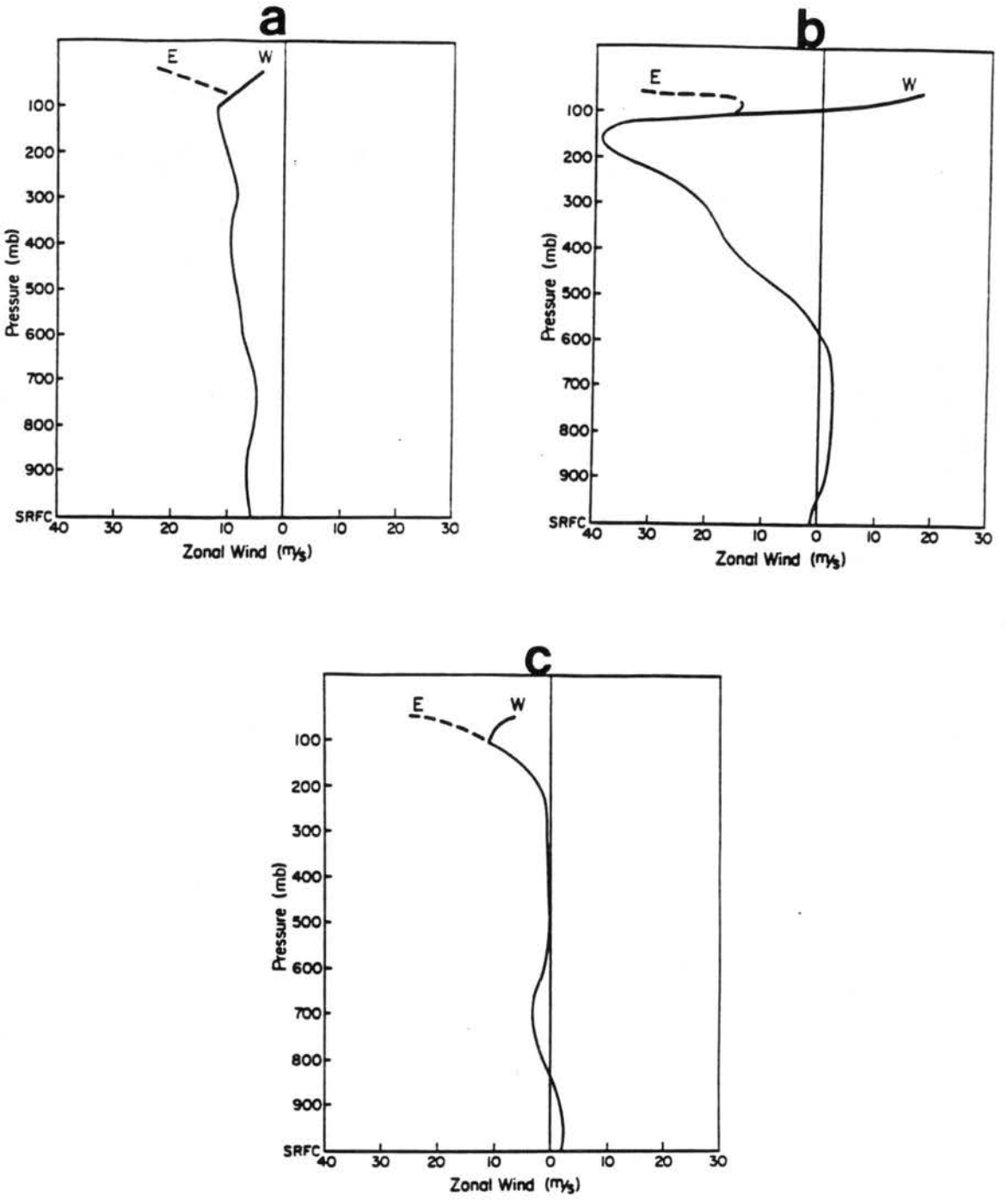

Figure 2.6: Zonal wind profiles during DJF for locations near a) 130°E, 12°N, b) 130°E, Equator, and c)130°E, 12°S. Note that upper tropospheric to lower stratospheric shear is minimized during the west phase of the SQBO 12°N and 12°S, and during the east phase at the equator.

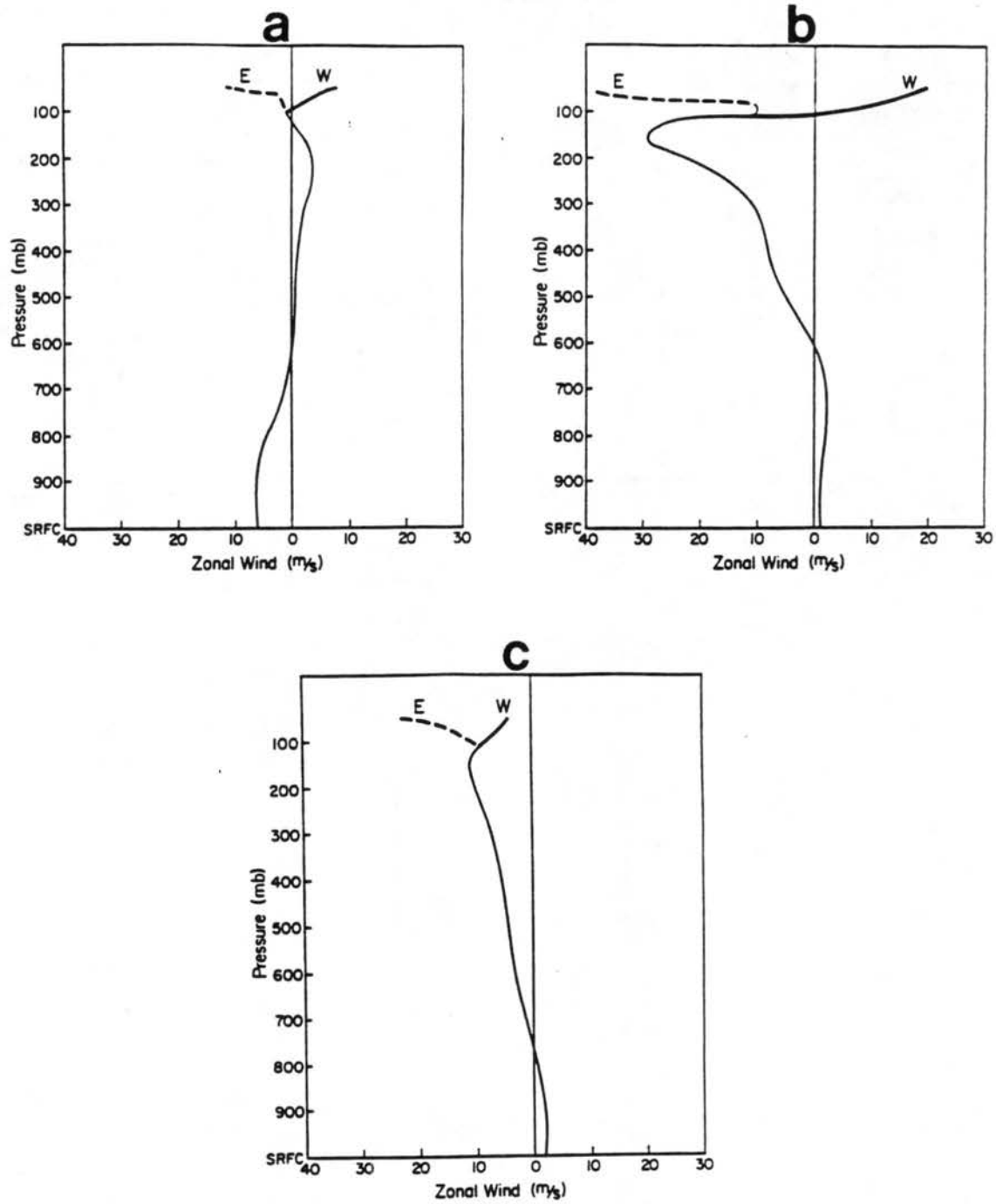

Figure 2.7: As in Fig. 2.6 but for zonal wind profiles during JJA at a) 130°E, 12°N, b) 130°E, Equator, and c) 130°E, 12°S.

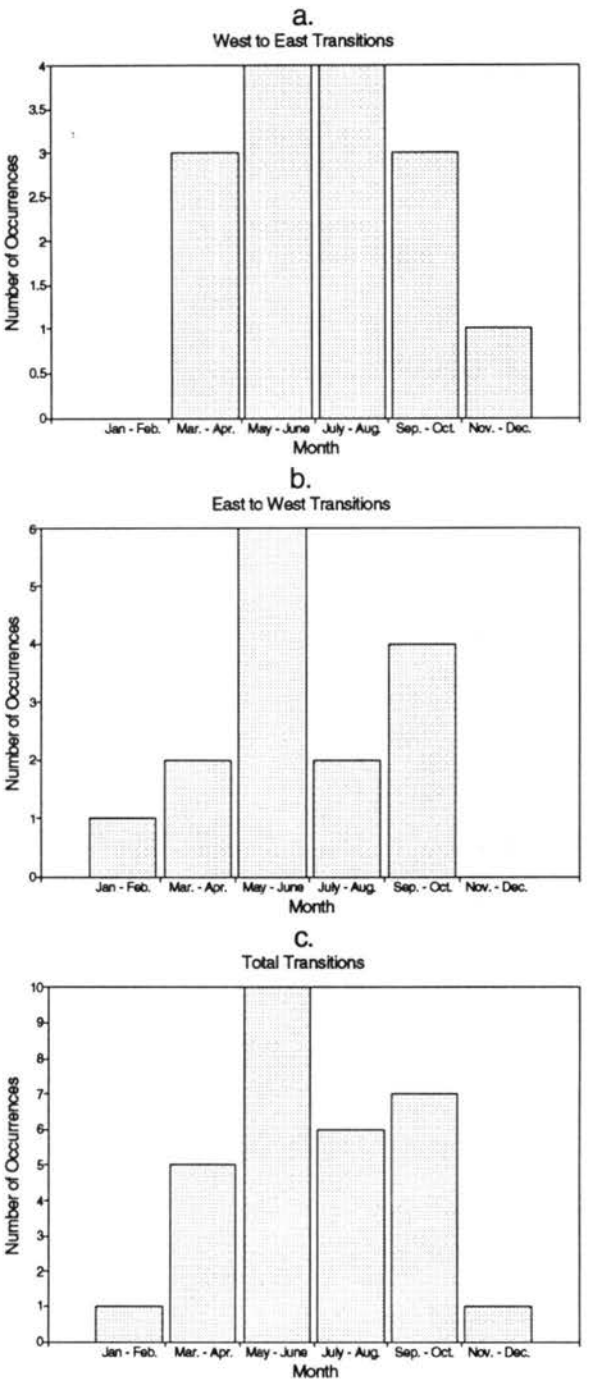

Figure 2.8: Relative frequency of the time of year for SQBO phase change at 50 mb: (a) west phase to east phase transitions; (b) east phase to west transitions, (c) total transitions.

In MAM:

1. there are two zonally symmetric areas of minimum 200 mb to 50 mb shear located at 13°S and 10°N, and
2. a relative shear maximum occurs over the equatorial parts of Indonesia.

In JJA:

1. two areas of very pronounced minimum 200 mb to 50 mb shear are located on either side of the equator, and
2. a relative shear maximum is located in the Western Indonesian region along the equator.

In SON:

1. two broad zonally symmetric areas of minimum shear are located on either side of the equator centered at 10°S and 12°N, and
2. a narrow area of relatively large shear is located in the Western Indonesian region.

The most notable and consistent shear pattern observed during the west phase of the SQBO is of relatively large values of 200 mb to 50 mb shear along the equator and of relative shear minima located just off the equator in all seasons. These on-equator versus off-equator shear differences are particularly pronounced during the DJF season. The upper tropospheric to lower stratospheric shear patterns found to exist during a typical east phase period of the SQBO can be summarized by the following:

In DJF:

1. very small shear values exist near the equator and throughout the West Pacific region from 8°N to 8°S, and

2. maximum values of shear are located approximately at 20°N and 20°S.

In MAM:

1. fairly strong values of shear exist throughout the entire West Pacific region, and
2. there is a relative shear minimum located in a zonally symmetric strip from approximately 12°N to 20°N.

In JJA:

1. relatively strong 200 mb to 50 mb shear is located throughout the Northwest Pacific region with strongest values located near the Dateline and 13°N, and
2. a large region of minimum values of shear is located in the Southern Hemisphere extending from 90°E to 135°E.

In SON:

1. rather strong values of shear exist throughout the entire West Pacific region,
2. relative shear minima located on either side of the equator; one in the Northern Hemisphere covering the Malay Peninsula and the Philippines, the other located in the Southern Hemisphere, covering the area from Northern Australia west to 90° between 10°S and 20°S, and
3. a relative shear maximum is located in the vicinity of the equator and the Dateline.

The east phase of the SQBO forces upper tropospheric to lower stratospheric zonal wind shear that in general is much stronger than that occurring during the west phase (with the exception of the DJF season) over most of the off-equator regions of the West Pacific. In contrast, the equatorial regions ±8° show lower values of 200 mb to 50 mb shear occurring during the east phase of the SQBO.

There are several important points to be made concerning the differences between the 200 mb and 50 mb shear patterns caused by the oscillating zonal winds of the SQBO. First, the shear differences between east and west are greatest during the DJF season. Secondly, the differences are greatest near the equator where the SQBO signal is the strongest. Thirdly, the differences in every season show that the equatorial regions have relatively high shear values during the west phase SQBO periods and relatively small shear values during east SQBO periods. Finally, the SQBO favors persistence during the Boreal Winter and change during the Boreal Summer, much as is observed for many ENSO parameters (Wright, 1985).

These above points, coupled with the temporal persistence of the contrasting phases of the SQBO are the focus of this study. With these long lasting periods of contrasting 200 mb to 50 mb zonal wind shear, there are signs of tropospheric and oceanic differences in the West Pacific region between the contrasting shear periods apparently caused by the SQBO. From the previous study of upper tropospheric to lower stratospheric shear patterns, it can be inferred that associated differences in the troposphere will be located near the equator with the largest differences occurring during the DJF season. The next chapter will discuss the results obtained by stratifying precipitation, surface pressure, and convective anomalies by the sign and amplitude of 200 mb to 50 mb shear in the tropical West Pacific region.

Chapter 3

PRESSURE, PRECIPITATION, AND CONVECTIVE ANOMALIES AND THEIR RELATIONSHIP TO SQBO FORCED ZONAL WIND SHEAR

The oscillation of tropical stratospheric zonal winds creates periods of contrasting upper tropospheric to lower stratospheric zonal wind shear as discussed in chapter 2. In the context of these contrasting wind shear patterns, this chapter examines the distribution of surface station pressure, precipitation and regional convective anomalies in the West Pacific area during the two phases of the SQBO. The results of this study show that upper tropospheric to lower stratospheric zonal wind shear may be an important modulator of deep tropical convection, precipitation and pressure. When this shear is large, surface pressures tend to be higher while precipitation and deep convection are suppressed. In contrast, in regions with small values of this shear, pressures tend to be lower while convection and precipitation appear to be enhanced.

3.1 Surface Station Observations

The World Monthly Surface Station Climatology data set (obtained from NCAR) provided monthly values for surface pressure (20 stations) and monthly precipitation (65 stations) located in the Western Tropical Pacific. The stations chosen represent the most reliable data available, having no more than 5% missing observations and hence, with near continuous data records beginning in 1953. The data were analyzed by comparing years when the SQBO changed phase from west to east with those years that went from east to west. The locations of stations used in surface pressure and precipitation analyses are shown in Fig. 3.1 and in Fig. 3.2, respectively. Station names and latitude/longitude data are listed in Table 3.1.

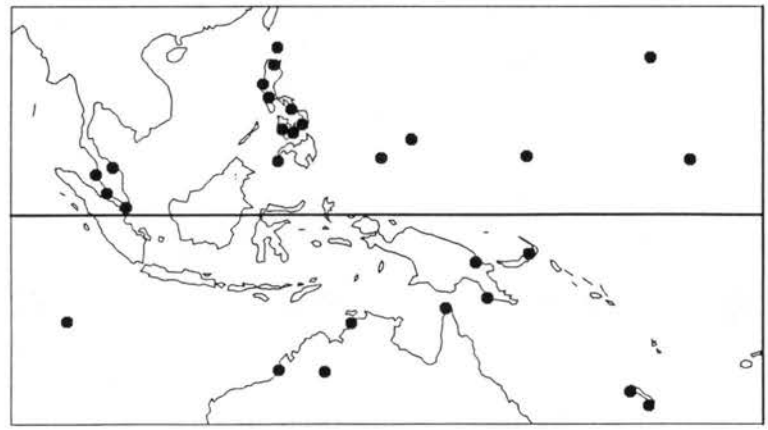

Figure 3.1: Locations of surface stations used for the surface pressure analysis.

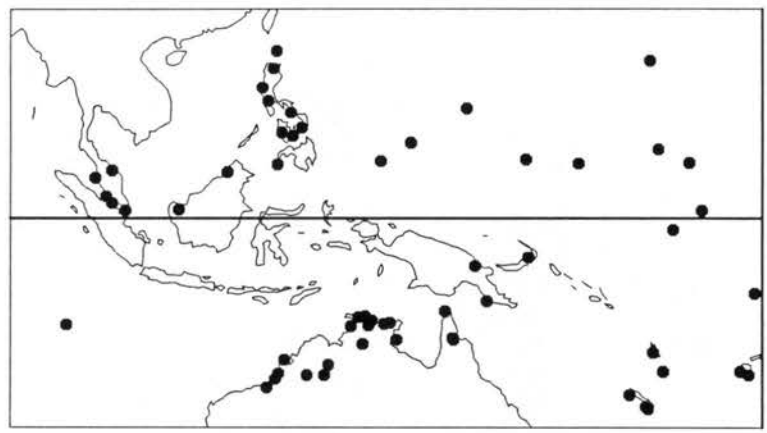

Figure 3.2: Locations of surface stations used for the surface precipitation analysis.

Station data for SQBO transition periods were composited into two groups; one for years with west to east SQBO transitions and another for east to west SQBO transitions. These transition years are: west to east transitions (1956, 1960, 1962, 1965, 1968, 1972, 1974, 1979); east to west transitions (1955, 1957, 1959, 1961, 1971, 1975, 1980, 1982, 1985). These selections were based on years with distinct west or east modes in the lower stratosphere in January, changing to the opposite mode by the following December. In general, the transitions tend to take place between April and July (see Dunkerton and

Table 3.1: List of stations from surface climatology of the world data set used in the analysis.

Station	Latitude o /	Longitude o /	Precipitation	Pressure
Singapore Airport	1 22 N	103 55 E	*	*
Basco	20 27 N	121 58 E	*	*
Aparri	18 22 N	121 38 E	*	*
Dagupan	16 03 N	120 20 E	*	*
Manila Airport	14 31 N	121 00 E	*	*
Legaspi	13 08 N	123 44 E	*	*
Tacloban	11 15 N	125 00 E	*	*
Iloilo	10 42 N	122 34 E	*	*
Cebu	10 20 N	123 58 E	*	*
Zamboanga	6 54 N	122 04 E	*	*
Penang	5 18 N	100 16 E	*	*
Kota Bharu	6 10 N	102 17 E	*	*
Kuala Lumpur	3 07 N	101 33 E	*	
Malacca	2 16 N	102 15 E	*	
Kuching	1 29 N	110 20 E	*	
Kota Kinabaiu	5 57 N	116 03 E	*	*
Cocos Island	12 11 S	96 50 E	*	*
Madang	5 13 S	145 48 E	*	*
Port Morsby	9 26 S	147 13 E	*	*
Rabaul	4 13 S	152 11 E	*	*
Darwin Airport	12 26 S	130 52 E	*	*
Cape Don	11 19 S	131 46 E	*	
Katherine P. O.	14 28 S	132 16 E	*	
Croker Island	11 09 S	132 35 E	*	
Oenpell Mission Stn.	12 19 S	133 03 E	*	
Goulburn Island	11 39 S	133 24 E	*	
Milingimbi	12 05 S	134 55 E	*	
Echo Island	12 01 S	135 34 E	*	
Angurugu	14 00 S	136 40 E	*	
Thursday Island	10 35 S	142 13 E	*	*
Coen Aero	13 45 S	143 07 E	*	
Coen P. O.	13 57 S	143 12 E	*	
Mandora	19 45 S	120 51 E	*	
La Grange Mission	18 41 S	121 46 E	*	
Broome	17 57 S	122 13 E	*	*
Cape Leveque	16 24 S	122 55 E	*	
Fitzroy Crossing	18 11 S	125 35 E	*	
Halls Creek	18 14 S	127 40 E	*	*
Turkey Creek	17 03 S	128 13 E	*	

Table 3.1: Continued.

Station	Latitude o /	Longitude o /	Precipitation	Pressure
Guam	13 33 N	144 50 E	*	
Wake Island	19 17 N	166 39 E	*	*
Truk	7 28 N	151 51 E	*	*
Ponape	6 55 N	158 13 E	*	
Kwajalein	8 44 N	167 44 E	*	
Majuro	7 05 N	171 23 E	*	*
Koror	7 20 N	134 29 E	*	*
Yap	9 29 N	138 05 E	*	*
Ocean Island	0 54 S	169 32 E	*	
Luganville	15 31 S	167 13 E	*	
Vila	17 45 S	168 18 E	*	
Koumac	20 34 S	164 17 E	*	*
La Tontouta	22 01 S	166 13 E	*	
Noumea	22 16 S	166 27 E	*	*
Tarawa	1 21 N	172 55 E	*	
Funifuti	8 31 S	179 13 E	*	
Nandi	17 45 S	177 27 E	*	
Nausori	18 12 S	178 30 E	*	

Baldwin, 1991). After compositing the data, differences between the two composited groups are taken.

Seasonal west phase minus east phase precipitation and pressure differences were spatially stratified into two groups; one for areas situated under low values of upper tropospheric to lower stratospheric zonal wind shear during the west phase of the SQBO and the other of stations located in areas with largest values of 200 mb to 50 mb zonal wind shears during the west phase of the SQBO (for each season). The areas of relatively small shear values during the west phase for each season are schematically shown in Fig. 3.3a-d whereas areas of comparably large shear during the west phase are shown in Fig. 3.4a-d. The stations located in these areas during each season were summed and the median and mean found for both the precipitation (percent difference) and pressure differences.

The DJF west phase minus east phase precipitation differences for stations located in areas of relatively strong west phase 200 mb to 50 mb zonal wind shear are given in Table 3.2. This analysis (see Fig. 3.4a) shows that less precipitation falls in these areas during

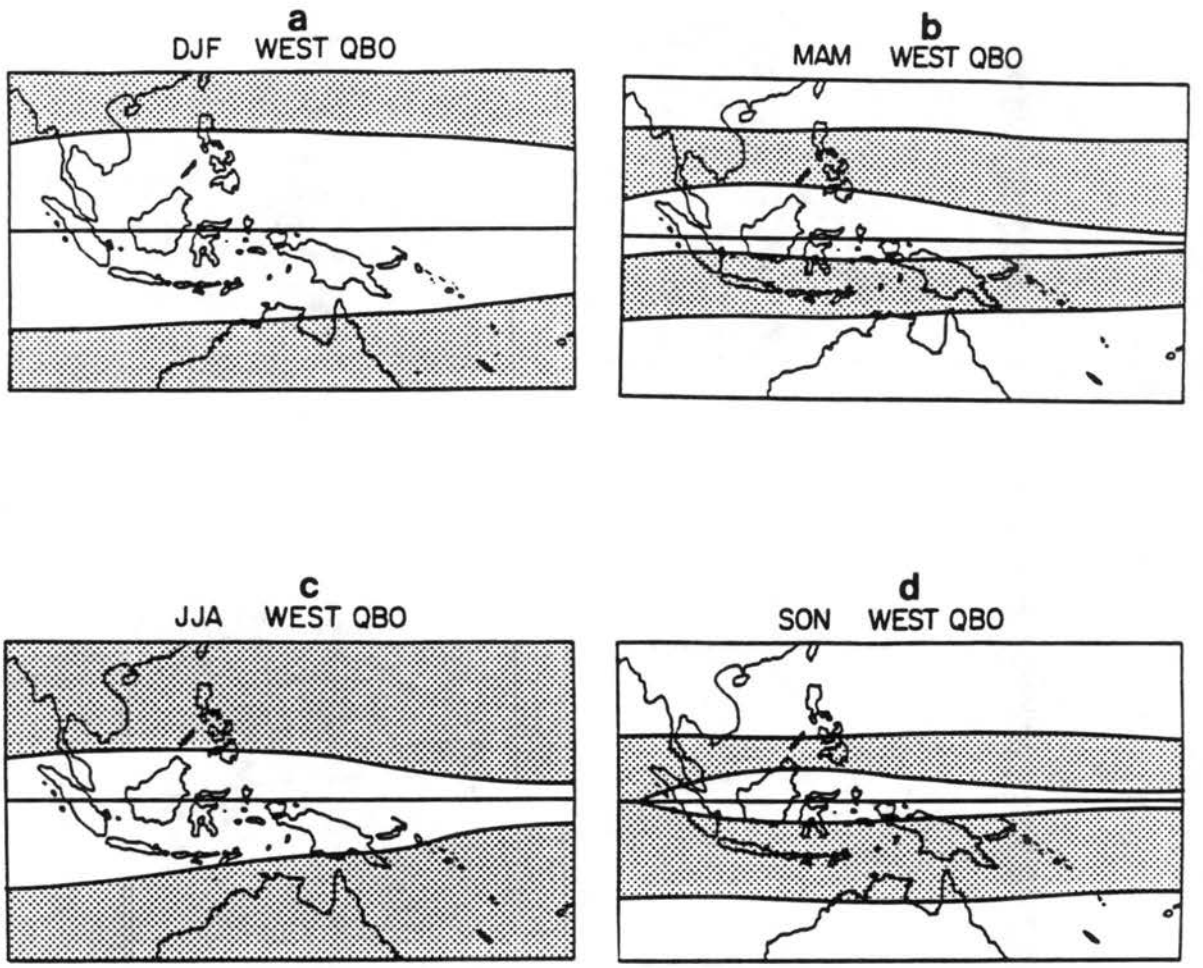

Figure 3.3: Shaded areas depict regions where the upper tropospheric to lower stratospheric zonal wind shear is comparatively small during the west phase of the SQBO in comparison with the east phase of the SQBO for (a) DJF, (b) MAM, (c) JJA and (d) SON.

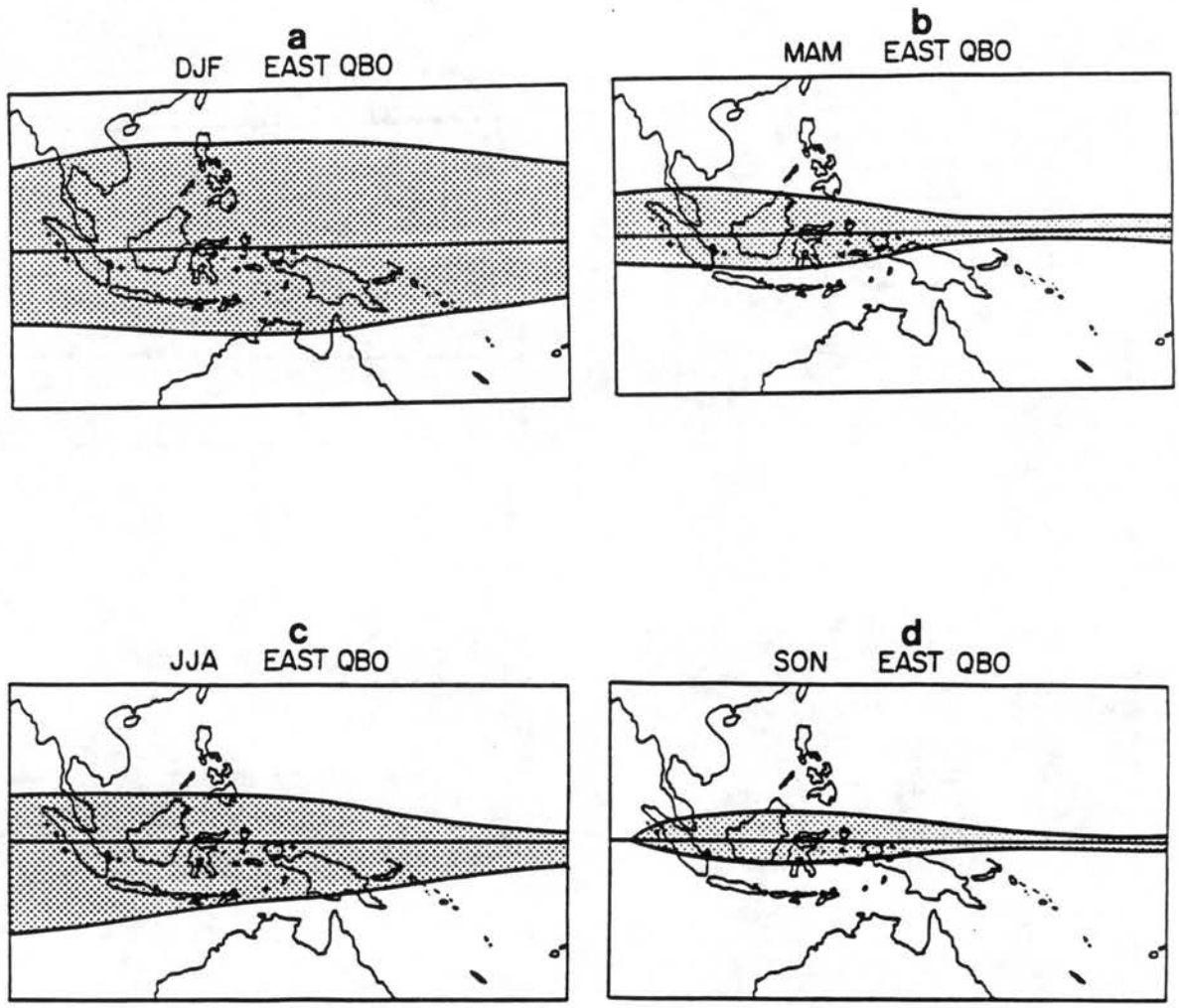

Figure 3.4: Shaded areas depict regions where the upper tropospheric to lower stratospheric zonal wind shear is comparatively large during the west phase of the SQBO in comparison for (a) DJF, (b) MAM, (c) JJA and (d) SON.

the west phase of the SQBO with a mean difference of –4 percent and a median difference of –6 percent. A similar analysis for stations located in regions of weak west phase 200 mb to 50 mb zonal wind shear (see Fig. 3.3a) is shown in Table 3.3. DJF precipitation in this table seems to be greater during the west phase as compared to the east phase with an average difference of 22 percent and a median of 17 percent.

A similar analysis for the west phase minus east phase surface pressure differences for DJF is shown in Table 3.4 and in Table 3.5. Table 3.4 contains the stations for areas with small upper troposphere to lower stratosphere zonal wind shear during the east phase of the SQBO (see Fig. 3.4a). On average, these stations have a west minus east difference of -32×10^{-2} mb with a median of -43×10^{-2} mb. The stations located in areas of weak west phase 200 mb to 50 mb wind shear (see Fig. 3.3a) during the DJF season are shown in Table 3.5. These stations exhibit a mean west minus east pressure difference of -61×10^{-2} mb with a median of -67×10^{-2} mb. These results suggest lower overall DJF surface pressure in the West Pacific region during periods of the westerly SQBO.

Summarizing the results of the precipitation and pressure analyses during the DJF season, we conclude that during the east SQBO (1) precipitation is enhanced approximately 4 percent to 6 percent along the equator in regions where the upper tropospheric to lower stratospheric wind shear is least; (2) precipitation is suppressed by –22 percent to –17 percent in the off-equator regions where 200 mb to 50 mb zonal wind shear is greatest, particularly in Northern Australia; (3) pressure is higher (0.3 mb) throughout the West Pacific region; and (4) the equator to pole pressure gradient is reduced by approximately 0.3 mb. During the west SQBO, (1) precipitation is enhanced by 22 percent to 17 percent in the off-equator areas where the 200 mb to 50 mb shear is least; (2) precipitation is suppressed approximately –5 percent throughout the near equatorial region in association with strong 200 mb to 50 mb zonal wind shear; (3) pressure seems to be lower (–0.3 mb) throughout the entire West Pacific region with the lowest pressure occurring in the off-equator regions; and (4) there is an increased equator to pole pressure gradient of approximately 0.3 mb.

Table 3.2: West phase minus east phase percent difference for precipitation at stations located in areas of strong 200 mb to 50 mb zonal wind shear during the west phase of the SQBO for DJF (see Fig. 3.4a).

Station	Latitude	Longitude	W-E/E Percent Difference
Singapore Airport	1 22 N	103 55 E	27
Legaspi	13 08 N	123 44 E	15
Tacloban	11 15 N	125 00 E	–13
Iloilo	10 42 N	122 34 E	–11
Cebu	10 20 N	123 58 E	–1
Zamboanga	6 54 N	122 04 E	–31
Penang	5 18 N	100 16 E	–5
Kota Bharu	6 10 N	102 17 E	–25
Kuala Lumpur	3 07 N	101 33 E	–6
Malacca	2 16 N	102 15 E	–14
Kuching	1 92 N	110 20 E	–6
Kota Kinabaiu	5 57 N	160 03 E	54
Cocos Island	12 11 S	96 50 E	–11
Madang	5 13 S	145 48 E	–23
Port Morsby	9 26 S	147 13 E	–20
Rabaul	4 13 S	152 11 E	–16
Darwin Airport	12 26 S	130 52 E	0
Cape Don	11 19 S	131 46 E	–13
Croker Island	11 09 S	132 35 E	–7
Oenpell Mission Stn.	12 19 S	133 03 E	4
Goulburn Island	11 39 S	133 24 E	–16
Milingimbi	12 05 S	134 55 E	1
Echo Island	12 01 S	135 34 E	–3
Thursday Island	10 35 S	142 13 E	–14
Guam	13 33 N	144 50 E	–6
Truk	7 28 N	151 51 E	37
Ponape	6 55 N	158 13 E	14
Kwajalein	8 44 N	167 44 E	9
Majuro	7 05 N	171 23 E	–3
Koror	7 20 N	134 29 E	19
Yap	9 29 N	138 05 E	1
Ocean Island	0 54 S	169 32 E	–21
Tarawa	1 21 N	172 55 E	–23
Funifuti	8 31 S	179 13 E	–23
		MEAN	–4
		MEDIAN	–6

Table 3.3: West phase minus east phase percent difference for precipitation at stations located in areas of weak 200 mb to 50 mb zonal wind shear during the west phase of the SQBO for DJF (see Fig. 3.3a).

Station	Latitude	Longitude	W-E/E Percent Difference
Basco	20 27 N	121 58 E	47
Aparri	18 22 N	121 38 E	27
Dagupan	16 03 N	20 20 E	177
Manila Airport	14 31 N	121 00 E	13
Katherine P. O.	14 28 S	132 16 E	–7
Angurugu	14 00 S	136 40 E	9
Coen Aero	13 45 S	143 07 E	12
Coen P. O.	13 57 S	143 12 E	27
Mandora	19 45 S	120 51 E	–24
La Grange Mission	18 41 S	121 46 E	23
Broome	17 57 S	122 13 E	0
Cape Leveque	16 24 S	122 55 E	17
Fitzroy Crossing	18 11 S	125 35 E	7
Halls Creek	18 14 S	127 40 E	–22
Turkey Creek	17 03 S	128 13 E	2
Wake Island	19 17 N	166 39 E	–5
Luganville	15 31 S	167 13 E	31
Vila	17 45 S	168 18 E	36
Koumac	20 34 S	164 17 E	48
La Tontouta	22 01 S	166 13 E	14
Noumea	22 16 S	166 27 E	25
Nandi	17 45 S	177 27 E	27
Nausori	18 12 S	178 30 E	17
		MEAN	22
		MEDIAN	17

Table 3.4: West phase minus east phase SQBO pressure difference (10^{-2} mb) at stations located in areas of strong 200 mb to 50 mb zonal wind shear during the west phase of the SQBO for DJF (see Fig. 3.4a).

Station	Latitude	Longitude	W–E Pressure Difference (10^{-2} mb)
Singapore Airport	1 22 N	103 55 E	7
Legaspi	13 08 N	123 44 E	–64
Tacloban	11 15 N	125 00 E	–88
Iloilo	10 42 N	122 34 E	–43
Cebu	10 20 N	123 58 E	–85
Zamboanga	6 54 N	122 04 E	26
Penang	5 18 N	100 16 E	–7
Kota Bharu	6 10 N	102 17 E	13
Kuala Lumpur	3 07 N	101 33 E	–56
Cocos Island	12 11 S	96 50 E	–17
Truk	7 28 N	151 51 E	–54
Majuro	7 05 N	171 23 E	–35
Koror	7 20 N	134 29 E	–61
Yap	9 29 N	138 05 E	–30
Madang	5 13 S	145 48 E	44
Port Morsby	9 26 S	147 13 E	–71
Rabaul	4 13 S	152 11 E	83
Darwin Airport	12 26 S	130 52 E	–71
Thursday Island	10 35 S	142 13 E	–98
		MEAN	–32
		MEDIAN	–43

Table 3.5: West phase minus east phase SQBO pressure difference (10^{-2} mb) at stations located in areas of weak 200 mb to 50 mb zonal wind shear during the west phase of the SQBO for DJF (see Fig. 3.3a).

Station	Latitude	Longitude	W–E Pressure Difference (10^{-2} mb)
Basco	20 27 N	121 58 E	–28
Aparri	18 22 N	121 38 E	–3
Dagupan	16 03 N	20 20 E	–41
Manila Airport	14 31 N	121 00 E	–114
Wake Island	19 17 N	166 39 E	–75
Koumac	20 24 S	164 17 E	–67
Noumea	22 16S	122 13E	–80
Broome	17 57 S	122 13 E	–81
Halls Creek	18 14 S	127 40 E	–62
		MEAN	–61
		MEDIAN	–67

This same analysis was performed for stations in the West Pacific region for the MAM season. The findings again suggest that in regions of weak 200 mb to 50 mb zonal wind shear, stations receive more rainfall. The west minus east percent differences shown in Table 3.6 include stations located in regions of large west phase 200 mb to 50 mb shear whereas Table 3.7 shows stations in areas of weak west phase shear. The near equator stations listed in Table 3.6 have a mean west minus east difference value of –12 percent and a median of –10 percent, showing less rainfall occurs in this region during the west phase. In contrast, the off-equator stations in Table 3.7 have a mean difference value of 12 percent and a median of 8 percent indicating that more rainfall occurs in these regions during the west phase of the SQBO.

West phase minus east phase differences of seasonal pressure (10^{-2} mb) for MAM suggest that lower pressure occurs throughout the West Pacific region during the west phase of the SQBO; very similar to the differences found for DJF. These results are shown in Table 3.8 for stations in regions where the shear is weak during the east phase of the SQBO. Table 3.9 contains data for stations in low shear west phase areas. Stations located off the equator (Table 3.9) have larger negative west phase anomalies (mean of –10 x 10^{-2}

Table 3.6: West phase minus east phase percent precipitation difference at stations located in areas of strong 200 mb to 50 mb zonal wind shear during the west phase of the SQBO for MAM (see Fig. 3.4b).

Station	Latitude	Longitude	W-E/E Percent Difference
Singapore Airport	1 22 N	103 55 E	2
Penang	5 18 N	100 16 E	–12
Kota Bharu	6 10 N	102 17 E	–13
Kuala Lumpur	3 07 N	101 33 E	–10
Malacca	2 16 N	102 15 E	0
Kuching	1 92 N	110 20 E	–16
Kota Kinabaiu	5 57 N	160 03 E	–11
Madang	5 13 S	145 48 E	–2
Port Morsby	9 26 S	147 13 E	–5
Rabaul	4 13 S	152 11 E	–9
Ocean Island	0 54 S	169 32 E	–35
Tarawa	1 21 N	172 55 E	–29
		MEAN	–12
		MEDIAN	–10

mb and a median of –18 x 10^{-2} mb) as compared to stations located very close to the equator (Table 3.8) which had an average of –6 x 10^{-2} mb and a median of –6 x 10^{-2} mb.

The results of the precipitation and pressure analyses during the MAM season show tendencies wherein during the east phase of the SQBO, (1) precipitation is enhanced 10 percent to 12 percent along and very close to the equator where the SQBO forces the weakest values of 200 mb to 50 mb shear; (2) precipitation is suppressed 8 percent to 12 percent in the off-equator regions where the SQBO causes large values zonal wind shear; (3) surface pressure throughout the West Pacific is approximately 0.1 mb higher; and (3) there is a reduced equator to pole pressure gradient in the tropics. During the west phase of the SQBO, (1) precipitation is enhanced 8 percent to 12 percent in the off-equator regions where the 200 mb to 50 mb zonal wind shear is relatively weak; (2) precipitation is suppressed approximately 10 percent in the vicinity of the equator where the SQBO has caused relatively large values of shear; (3) surface pressure is somewhat lower throughout

Table 3.7: West phase minus east phase percent precipitation difference at stations located in areas of weak 200 mb to 50 mb zonal wind shear during the west phase of the SQBO for MAM (see Fig. 3.3b).

Station	Latitude	Longitude	W-E/E Percent Difference
Dagupan	16 03 N	20 20 E	13
Manila Airport	14 31 N	121 00 E	48
Legaspi	13 08 N	123 44 E	4
Tacloban	11 15 N	125 00 E	8
Iloilo	10 42 N	122 34 E	–2
Cebu	10 20 N	123 58 E	76
Darwin Airport	12 26 S	130 52 E	20
Cape Don	11 19 S	131 46 E	27
Croker Island	11 09 S	132 35 E	7
Oenpell Mission Stn.	12 19 S	133 03 E	1
Goulburn Island	11 39 S	133 24 E	–21
Milingimbi	12 05 S	134 55 E	–25
Echo Island	12 01 S	135 34 E	–4
Thursday Island	10 35 S	142 13 E	–4
Guam	13 33 N	144 50 E	3
Truk	7 28 N	151 51 E	24
Ponape	6 55 N	158 13 E	3
Kwajalein	8 44 N	167 44 E	–2
Majuro	7 05 N	171 23 E	–1
Koror	7 20 N	134 29 E	14
Yap	9 29 N	138 05 E	17
Funifuti	8 31 S	179 13 E	–28
		MEAN	12
		MEDIAN	8

Table 3.8: SQBO west phase minus east phase pressure difference (10^{-2} mb) for stations located in areas of strong west phase 200 mb to 50 mb zonal wind shear during MAM (see Fig. 3.4b).

Station	Latitude	Longitude	W–E Pressure Difference (10^{-2} mb)
Singapore Airport	1 22 N	103 55 E	2
Penang	5 18 N	100 16 E	–14
Kota Bharu	6 10 N	102 17 E	13
Kuala Lumpur	3 07 N	101 33 E	–17
Madang	5 13 S	145 48 E	–6
Rabaul	4 13 S	152 11 E	–12
		MEAN	–6
		MEDIAN	–6

Table 3.9: SQBO west phase minus east phase pressure difference (10^{-2} mb) for stations located in areas of weak west phase 200 mb to 50 mb zonal wind shear during MAM (see Fig. 3.3b).

Station	Latitude	Longitude	W–E Pressure Difference (10^{-2} mb)
Dagupan	16 03 N	20 20 E	11
Manila Airport	14 31 N	121 00 E	17
Legaspi	13 08 N	123 44 E	8
Tacloban	11 15 N	125 00 E	–18
Iloilo	10 42 N	122 34 E	–35
Cebu	10 20 N	123 58 E	–22
Darwin Airport	12 26 S	130 52 E	–4
Thursday Island	10 35 S	142 13 E	–37
		MEAN	–10
		MEDIAN	–18

the West Pacific region by approximately -0.1 mb; and (4) there is an enhanced equator to pole pressure gradient.

Results of the JJA precipitation analyses again show that regions of weak upper tropospheric to lower stratospheric zonal wind shear experience greater amounts of precipitation. These patterns of wind shear forced precipitation anomalies are manifested as greater rainfall in areas along the equator during the SQBO east phase and as greater precipitation in off-equator regions during the west phase of the SQBO. The pressure analysis also agrees with that of the rainfall analysis wherein lower pressure occurs in regions of small 200 mb to 50 mb shear. The west phase minus east phase precipitation analysis is shown in Tables 3.10 and 3.11 for regions of strong and weak SQBO linked west phase shear, respectively. Pressure differences (10^{-2} mb) in Tables 3.12 and 3.13 are associated with strong and weak shear values during the west phase of the SQBO.

Table 3.10: West phase minus east phase percent difference of precipitation for stations located in areas of strong west phase 200 mb to 50 mb zonal wind shear during JJA (see Fig. 3.4c).

Station	Latitude	Longitude	W-E/E Percent Difference
Singapore Airport	1 22 N	103 55 E	7
Penang	5 18 N	100 16 E	–3
Kota Bharu	6 10 N	102 17 E	–14
Kuala Lumpur	3 07 N	101 33 E	–4
Malacca	2 16 N	102 15 E	–4
Kuching	1 92 N	110 20 E	–6
Madang	5 13 S	145 48 E	0
Rabaul	4 13 S	152 11 E	–10
Ocean Island	0 54 S	169 32 E	–11
Tarawa	1 21 N	172 55 E	–9
		MEAN	–5
		MEDIAN	–4

These analyses indicate that during the east phase of the SQBO, (1) precipitation is enhanced approximately 5 percent within areas along the equator in regions of small 200 mb to 50 mb shear; (2) precipitation is suppressed 7 percent to 38 percent in regions

Table 3.11: West phase minus east phase percent difference of precipitation for stations located in areas of weak west phase 200 mb to 50 mb zonal wind shear during JJA (see Fig. 3.3c).

Station	Latitude	Longitude	W-E/E Percent Difference
Basco	20 27 N	121 58 E	67
Aparri	18 22 N	121 38 E	6
Legaspi	13 08 N	123 44 E	–14
Tacloban	11 15 N	125 00 E	7
Iloilo	10 42 N	122 34 E	–4
Cebu	10 20 N	123 58 E	4
Darwin Airport	12 26 S	130 52 E	23
Cape Don	11 19 S	131 46 E	7
Katherine P. O.	14 28 S	132 16 E	–8
Croker Island	11 09 S	132 35 E	62
Oenpell Mission Stn.	12 19 S	133 03 E	–29
Goulburn Island	11 39 S	133 24 E	567
Milingimbi	12 05 S	134 55 E	273
Echo Island	12 01 S	135 34 E	.223
Angurugu	14 00 S	136 40 E	56
Coen Aero	13 45 S	143 07 E	31
Coen P. O.	13 57 S	143 12 E	27
Mandora	19 45 S	120 51 E	–33
La Grange Mission	18 41 S	121 46 E	–60
Broome	17 57 S	122 13 E	–41
Cape Leveque	16 24 S	122 55 E	–38
Fitzroy Crossing	18 11 S	125 35 E	19
Halls Creek	18 14 S	127 40 E	64
Turkey Creek	17 03 S	128 13 E	–10
Guam	13 33 N	144 50 E	–17
Luganville	15 31 S	167 13 E	8
Vila	17 45 S	168 18 E	42
Koumac	20 34 S	164 17 E	12
La Tontouta	22 01 S	166 13 E	–17
Noumea	22 16 S	166 27 E	–22
Nandi	17 45 S	177 27 E	40
Nausori	18 12 S	178 30 E	8
		MEAN	38
		MEDIAN	7

Table 3.12: West phase minus east phase pressure difference (10^{-2} mb) for stations located in areas of strong west phase 200 mb to 50 mb zonal wind shear during JJA (see Fig. 3.4c).

Station	Latitude	Longitude	W–E Pressure Difference (10^{-2} mb)
Singapore Airport	1 22 N	103 55 E	10
Penang	5 18 N	100 16 E	2
Kota Bharu	6 10 N	102 17 E	13
Kuala Lumpur	3 07 N	101 33 E	38
Madang	5 13 S	145 48 E	2
Rabaul	4 13 S	152 11 E	4
		MEAN	10
		MEDIAN	10

Table 3.13: West phase minus east phase pressure difference (10^{-2} mb) for stations located in areas of weak west phase 200 mb to 50 mb zonal wind shear during JJA (see Fig. 3.3c).

Station	Latitude	Longitude	W-E/E Pressure Difference (10^{-2} mb)
Basco	20 27 N	121 58 E	7
Aparri	18 22 N	121 38 E	–1
Legaspi	13 08 N	123 44 E	14
Tacloban	11 15 N	125 00 E	3
Iloilo	10 42 N	122 34 E	15
Cebu	10 20 N	123 58 E	–12
Darwin Airport	12 26 S	130 52 E	–12
Broome	17 57 S	122 13 E	–1
Halls Creek	18 14 S	127 40 E	–18
		MEAN	–1
		MEDIAN	–1

of large upper tropospheric to lower stratospheric shear; (3) surface pressure is lower (0.1 mb) along the equator and slightly higher in off-equator regions. During the west phase of the SQBO, (1) precipitation is enhanced by 7 percent to 38 percent in regions of weak upper tropospheric to lower stratospheric zonal wind shears (i.e., the off-equator regions); (2) precipitation is suppressed by approximately -5 percent along the equator where shear between the upper troposphere and lower stratosphere is large; (3) surface pressure is slightly lower in off-equator areas; and (4) surface pressure is approximately 0.1 mbs higher along the equator.

It is expected that this SQBO forced pattern of enhanced precipitation and lower pressure in areas with weak upper tropospheric to lower stratospheric zonal wind shear continue in SON as is the case for precipitation, but because of the small number of stations reporting pressure data in the $\pm$ 4° equatorial region, pressure results are not considered.

West minus east precipitation percent differences during SON for West Pacific stations where the upper tropospheric to lower stratospheric zonal wind shear is large during the west phase are shown in Table 3.14. These differences again show a tendency for greater precipitation along the equator during the east phase. Table 3.15 shows percent precipitation differences during SON for stations located in the areas of small west phase 200 mb to 50 mb wind shear. More precipitation falls in these areas during the west phase of the SQBO, corresponding to the low upper tropospheric to lower stratospheric zonal wind shear.

In summary, the results of the west phase minus east phase percent differences of precipitation during the SON season show that during the east phase of the SQBO, (1) precipitation was enhanced (6 percent to 15 percent in areas of low 200 mb to 50 mb zonal wind shear (on-equator); and (2) precipitation was suppressed 15 percent to 47 percent in regions of strong 200 mb to 50 mb zonal wind shear, particularly in the off-equator regions. During the west phase of the SQBO, (1) off-equator precipitation is enhanced, particularly

Table 3.14: West phase minus east phase percent difference of precipitation for stations located in areas of strong west phase 200 mb to 50 mb zonal wind shear during SON (see Fig. 3.4d).

Station	Latitude	Longitude	W-E/E Percent Difference
Singapore Airport	1 22 N	103 55 E	−6
Kuala Lumpur	3 07 N	101 33 E	−6
Malacca	2 16 N	102 15 E	10
Kuching	1 92 N	110 20 E	−2
Ocean Island	0 54 S	169 32 E	−39
Tarawa	1 21 N	172 55 E	−45
		MEAN	−15
		MEDIAN	−6

in the pre-monsoon region of North Australia; and (2) precipitation is suppressed slightly near the equator.

From this analysis of precipitation and station pressure, upper tropospheric to lower stratospheric zonal wind shear appears to impose an important modulation on seasonal precipitation. In regions where this shear is small, precipitation is enhanced and the surface pressure tends to be anomalously low. In contrast, areas with large values of SQBO linked shear exhibit reduced precipitation and often a slight increase of surface pressure. These west minus east differences also manifest themselves in measurements of convective anomalies. The next section will examine anomalies of two separate measures of convective activity; Highly Reflective Clouds (HRC) and Outgoing Longwave Radiation (OLR).

3.2 Anomalies in Highly Reflective Clouds and Outgoing Longwave Radiation

In this section, differences in convective anomalies between east and west SQBO periods are examined using HRC and OLR. The results of this analysis are in general agreement with the surface (station) data discussed previously. In regions where the SQBO causes small values of upper tropospheric to lower stratospheric zonal wind shear,

Table 3.15: West phase minus east phase percent precipitation difference at stations located in areas of weak west phase 200 mb to 50 mb zonal wind shear during SON (see Fig. 3.3d).

Station	Latitude	Longitude	W-E/E Percent Difference
Iloilo	10 42 N	122 34 E	−11
Cebu	10 20 N	123 58 E	9
Cocos Island	12 11 S	96 50 E	21
Port Morsby	9 26 S	147 13 E	55
Darwin Airport	12 26 S	130 52 E	15
Cape Don	11 19 S	131 46 E	80
Katherine P. O.	14 28 S	132 16 E	17
Croker Island	11 09 S	132 35 E	90
Oenpell Mission Stn.	12 19 S	133 03 E	40
Goulburn Island	11 39 S	133 24 E	80
Milingimbi	12 05 S	134 55 E	55
Echo Island	12 01 S	135 34 E	197
Angurugu	14 00 S	136 40 E	15
Thursday Island	10 35 S	142 13 E	122
Coen Aero	13 45 S	143 07 E	61
Coen P. O.	13 57 S	143 12 E	255
Truk	7 28 N	151 51 E	−7
Ponape	6 55 N	158 13 E	−6
Kwajalein	8 44 N	167 44 E	−2
Majuro	7 05 N	171 23 E	−6
Koror	7 20 N	134 29 E	2
Yap	9 29 N	138 05 E	−5
Funifuti	8 31 S	179 13 E	4
		MEAN	47
		MEDIAN	15

convection is generally enhanced. In regions where the SQBO causes large values of 200 mb to 50 mb shear, convection is suppressed, particularly during the SON and DJF seasons.

The OLR data used in this study provides a useful tool for monitoring long term variations of convection by sensing the outgoing radiation emitted by the upper most emitting surface. The effective OLR surface can vary, including the actual earth's surface as well as the clouds that inhabit the atmosphere between the satellite and the earth's surface. The earth and cloud surfaces emit radiation at rates proportional to the fourth power of the uppermost temperature. For this reason, deep convective clouds with cold cloud top temperatures appear as low values in the OLR mean and anomaly fields.

Monthly mean OLR observations were obtained from NOAA. The period of coverage spans June 1974 through January 1989. Data for the period spanning March 1978 through December 1978 are missing due to satellite problems during that time period. The data available were derived from polar orbiting satellites which pass over each point of the earth twice a day at 12 hour intervals. Data for both passes are then archived on a 2.5° latitude/longitude grid. Data from both passes are included in the monthly OLR averages as well as in the long term means. These data were further analyzed by computing anomalies and compositing into east and west SQBO periods.

Mean monthly values of OLR (W/m^2) were used along with the long term (15 years, 1974 - 1989) monthly means to create anomaly fields for all the data. These anomaly values were then used to calculate seasonal means; in particular for DJF, MAM, JJA, and SON. These seasonal values then were composited using 50 mb Zonal Wind Anomalies (ZWA) at Singapore (1°N) as the index for the east-west stratification. Compositing was based on these ZWA at 50 mb being either distinctly westerly (> 5 m/s) or distinctly easterly (< -5 m/s). The final results were obtained by computing the difference between the distinctly west cases minus the distinctly east cases.

The HRC data set originated as an attempt by Kilonsky and Ramage (1976) to estimate monthly rainfall amounts over areas of the Tropical Pacific. Under the assumption that most tropical precipitation is associated with areas of organized deep convection and

cloud clusters, Kilonsky and Ramage analyzed mosaics of images obtained from the daytime passes of NOAA polar orbiting satellites. Areas of organized convection generally appear as highly reflective regions in these mosaics. The original HRC data were subjectively (i.e., by hand) identified by using cloud brightness, cloud top temperatures, size, appearance and texture and the local cloud climatology. Whenever possible, both infrared and visual image mosaics were used in the HRC analysis (Grossman and Garcia, 1990).

Following on the original (1976) work of Kilonsky and Ramage, the HRC data set was improved and expanded at NOAA's Environmental Research Laboratories. The revised HRC data set represents a continuous daily record of deep organized convection over the global tropics from January 1971 through December 1988 (Grossman and Garcia, 1990). The data period used for this research extends from January 1971 to December 1985 because of the availability of normalized (corrected for missing data) monthly means from NCAR.

HRC data were generated daily using both the visual and infrared satellite picture mosaics obtained from either NOAA or from the Defense Meteorological Satellite Program (DMSP) polar orbiting satellites. One degree by one degree grid squares covered by areas of organized deep convection identified in the HRC analysis were given a value of one; all other grid squares were given a value of zero. Grid squares are centered at intersections of whole degrees of latitude/longitude and have boundaries at the half-degree marks. For each month, the number of days with HRC cover was summed for each of the 18,360 (51 x 360) grid squares available for the global tropics (25°N to 25°S). These values have a potential monthly range extending from zero to the maximum number of days in each respective month. Because there are occasional data gaps in these mosaics, the number of missing data periods is also digitized and used to create normalized monthly mean values so as to not over/under estimate the amount of HRC coverage (Grossman and Garcia, 1990). These normalized monthly means were used to create monthly and seasonal anomalies as well as east/west SQBO composites. The HRC data were composited much the same way as the OLR data set with the exception that the ± five m/s conditions for distinctly

east or west was not used, but rather by merely westerly (+) and easterly (–) zonal wind anomalies.

The DJF west phase minus east phase composite OLR differences for the West Pacific region are shown in Fig. 3.5 (top). Negative differences in this figure represent regions where deep convection occurs with anomalous frequency during the west phase of the SQBO. During the DJF season, areas of negative differences are located primarily poleward of 10° in both the Northern and the Southern Hemispheres. Nevertheless, all of Northern Australia in this figure is located in an area of negative OLR differences. These anomalously negative regions are strongest in the vicinity of the South Pacific Convergence Zone (SPCZ). In the Northern Hemisphere, these negative differences are primarily poleward of 10° with a strong minimum located near the Northern Philippines. A large area of positive differences is centered near 160°E at the equator and extends meridionally from about 6°S to 11°N and zonally from 140°E to 170°E. This pattern is consistent with the observations of precipitation and surface pressure. In general, the DJF west minus east OLR differences reveal (1) lower values of OLR in the off-equator regions, suggesting that more deep convection occurs in these regions during the west phase of the SQBO, and (2) higher values of OLR along the equator, suggesting that more convection occurs along the equator during the east phase of the SQBO.

West phase minus east phase DJF HRC composite differences are shown in Fig. 3.5 (bottom). During this season, positive HRC differences (i.e., more convection during the west phase) are located primarily poleward of 10° in both Hemispheres with the largest values located near the Philippines and in Northern Australia. Negative differences (hence less convection during the west phase) are located along the equator. These results are consistent with the OLR data and with surface station results. Hence, the HRC west minus east differences can be characterized as having (1) more convection located off the equator, poleward of 10°, during the west phase of the SQBO; (2) more convection occurring along the equator during the east phase of the SQBO; and (3) provide further support for the results of the OLR and surface station analyses.

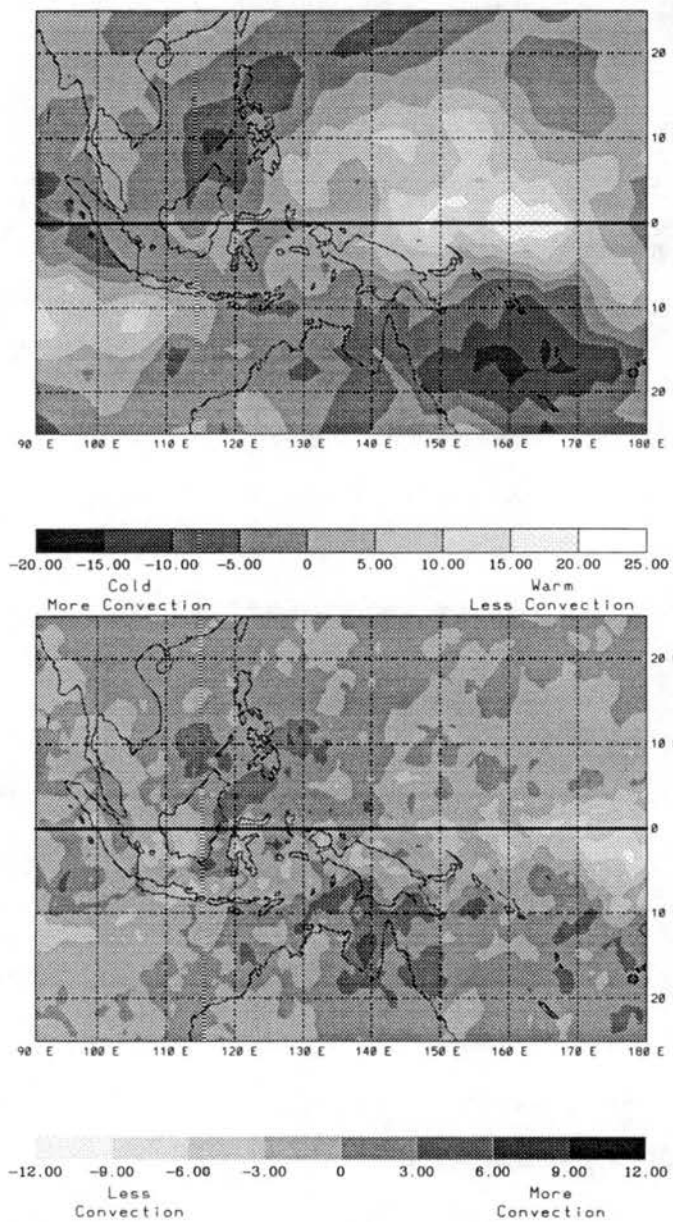

Figure 3.5: West phase minus east phase composite differences for West Pacific OLR (top) expressed in W/m^2, and HRC (bottom) expressed in convective events for DJF. Note that dark shading represents areas where more convection occurs during the west phase of the SQBO and light shading represents areas that have more convection occurring during the east phase of the SQBO.

These results can more clearly be seen in the scatter plot shown in Fig. 3.6. This plot shows the association between west phase minus east phase upper tropospheric to lower stratospheric shear differences versus the zonal mean (20°N to 20°S, 90°E to 180°) values of west phase minus east phase OLR and HRC differences. Figure 3.6a shows zonal 200 mb to 50 mb mean zonal wind shear versus the zonal mean OLR differences whereas Fig. 3.6b shows the zonal mean HRC differences. Both of these plots show a relationship between the 200 mb to 50 mb zonal wind shear and convection such that when this zonal wind shear is weak, convection is enhanced somewhat.

The MAM OLR west phase minus east phase differences show (1) enhanced west phase convection in the off-equator regions of North Australia and between 10°N and 25°N in the Northern Hemisphere, (2) enhanced east phase convection throughout most of Indonesia and along the equator, and (3) further support for surface observations although areas of strong convection does not precisely fit the shear patterns for this season, being slightly displaced from the centers of low shear occurring during the west phase of the SQBO.

These considerations can be seen in the MAM west phase minus east phase OLR differences shown in Fig. 3.7 (top). Here again, enhanced convection during the west phase is represented as negative differences. Negative values in this figure are confined primarily to areas poleward of 10° in both hemispheres. Positive values of OLR are located over most of Indonesia with a maximum located north of New Guinea. Referring again to Figs. 3.3 and 3.4, areas of negative OLR differences are observed located poleward of the areas of lowest west phase 200 mb to 50 mb shear.

West phase minus east phase MAM HRC differences are shown in Fig. 3.7 (bottom). In this figure, enhanced west phase convection is shown in the region east of New Guinea near the equator. Negative HRC values occur in almost all of the off-equator regions. These results conflict with the OLR. The reasons for these differences may be due to differences in how the HRC and OLR data were created or to seasonality of convection in the West Pacific region which, during MAM, has the least overall convection of any individual season. As previously mentioned, HRC is a direct measure of deep convection

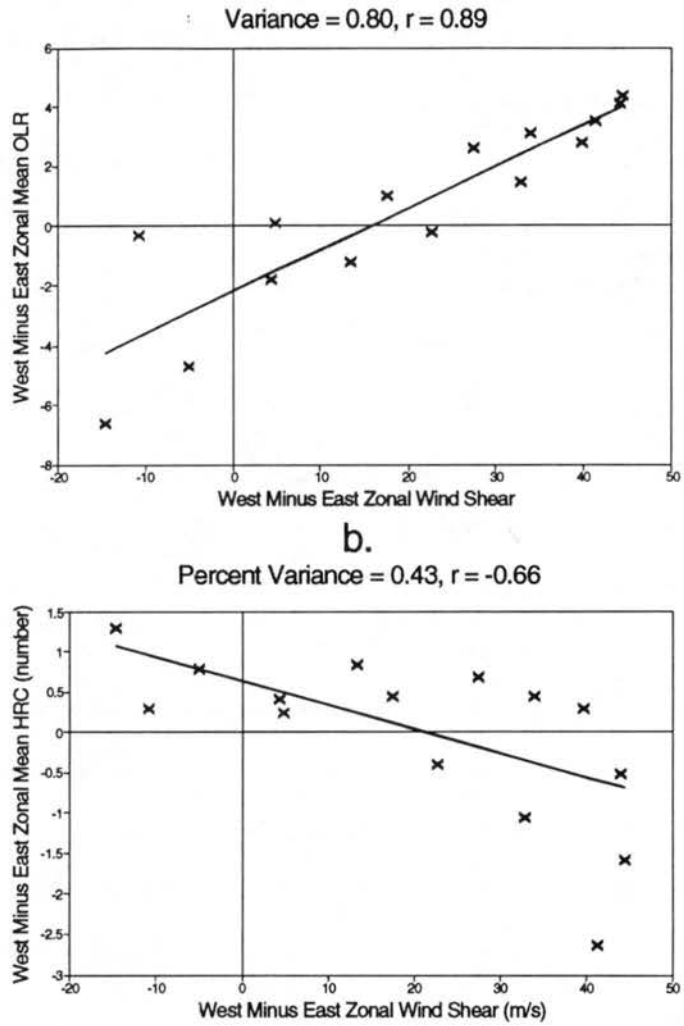

Figure 3.6: Scatter plots of the zonal mean (90°E to 180°) of the difference between the absolute value of west phase and east phase upper tropospheric to lower stratospheric zonal wind shear versus (a) west phase composite OLR minus the east phase composite OLR, expressed as W/m^2 from 90°E to 180°, 20°N to 20°S, and (b) the zonal mean of west phase composite of HRC minus the east phase composite of HRC expressed as units of deep convective events from 20°N to 20°S for the DJF season.

centers whereas OLR is a measure of upward longwave radiation. Moreover, these MAM differences may be associated with slow decay of the SPCZ in April (Meehl, 1987), noting that the SPCZ was stronger than normal in DJF. The MAM HRC west minus east differences may thus be characterized by (1) enhanced convection during the west phase of the SQBO east of New Guinea very close to the equator, and (2) enhanced convection during the east phase of the SQBO, mostly in areas located off the equator.

The JJA west phase minus east phase OLR differences (Fig. 3.8, top) show (1) enhanced convection in the off-equator regions during the west phase of the SQBO, in good agreement with the seasonal 200 mb to 50 mb shear patterns, (2) enhanced convection during the west phase of the SQBO in the Western Indonesian region, most likely due to a strong annual progression of convection as discussed by Meehl (1987), (3) diminished convection during the west phase of the SQBO near the Dateline, and (4) a distribution of anomalies which is predominantly in agreement with the surface station pressure and precipitation analysis discussed previously. Similarly, the JJA west phase minus east phase HRC differences (Fig. 3.8, bottom) show (1) enhanced convection in the Northern Hemisphere in the vicinity of the monsoon trough and poleward of 5°S in the Southern Hemisphere during the west phase of the SQBO, (2) suppressed convection along the equator during the west phase of the SQBO, and (3) enhanced convection in areas of favorable SQBO forced 200 mb to 50 mb zonal wind shear in good agreement with the previously shown west minus east differences of precipitation and pressure observations.

The regions of negative JJA OLR differences shown in Fig. 3.8 (top) represent greater convection occurring during the west phase throughout the West Pacific region. The largest negative differences are located in the vicinity of Indonesia just south of the Equator with secondary minima located just north of 10°N and over Northern Australia. Positive differences in Fig. 3.8 (top) are shown in two strips (one in each hemisphere) extending from a large positive maximum near the Dateline. The locations of the secondary minima and the positive areas agree very well with 200 mb to 50 mb zonal wind shear (see Figs. 3.3 and 3.4); however, the large negative area south of the equator in Indonesia does not.

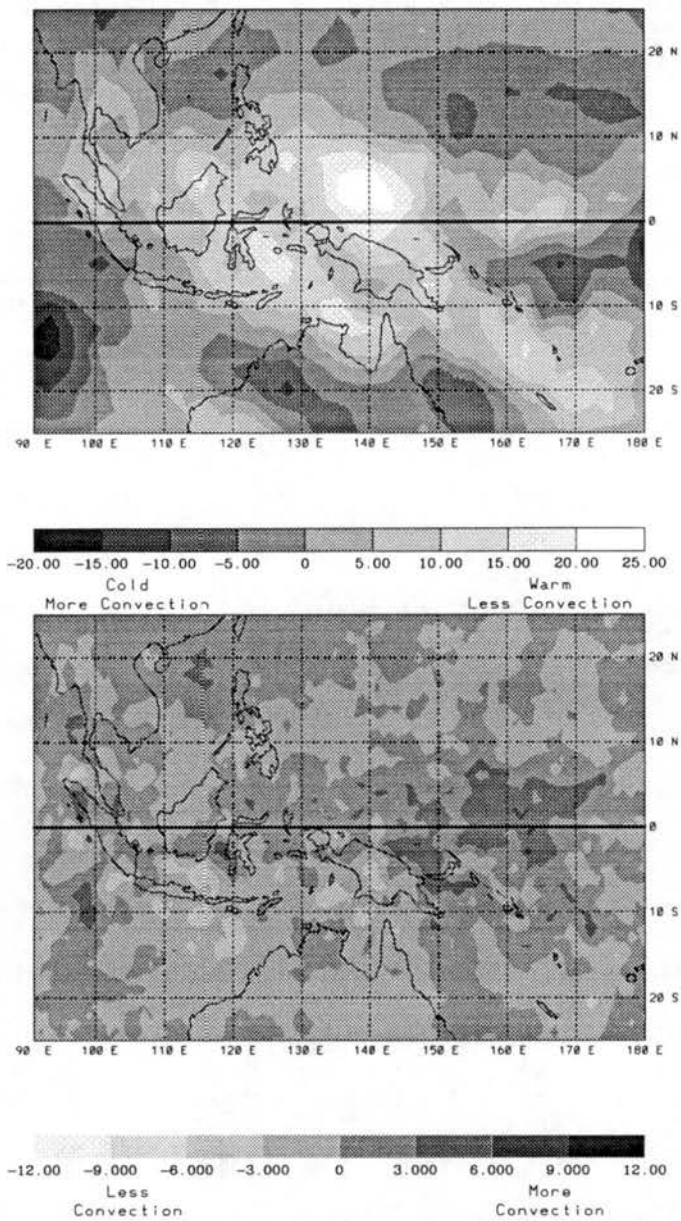

Figure 3.7: West phase minus east phase composite differences for OLR (top) expressed in W/m^2, and HRC (bottom) expressed as convective events for MAM. Note that dark shading represents areas where more convection occurs during the west phase of the SQBO and light shading represents areas that have more convection occurring during the east phase of the SQBO.

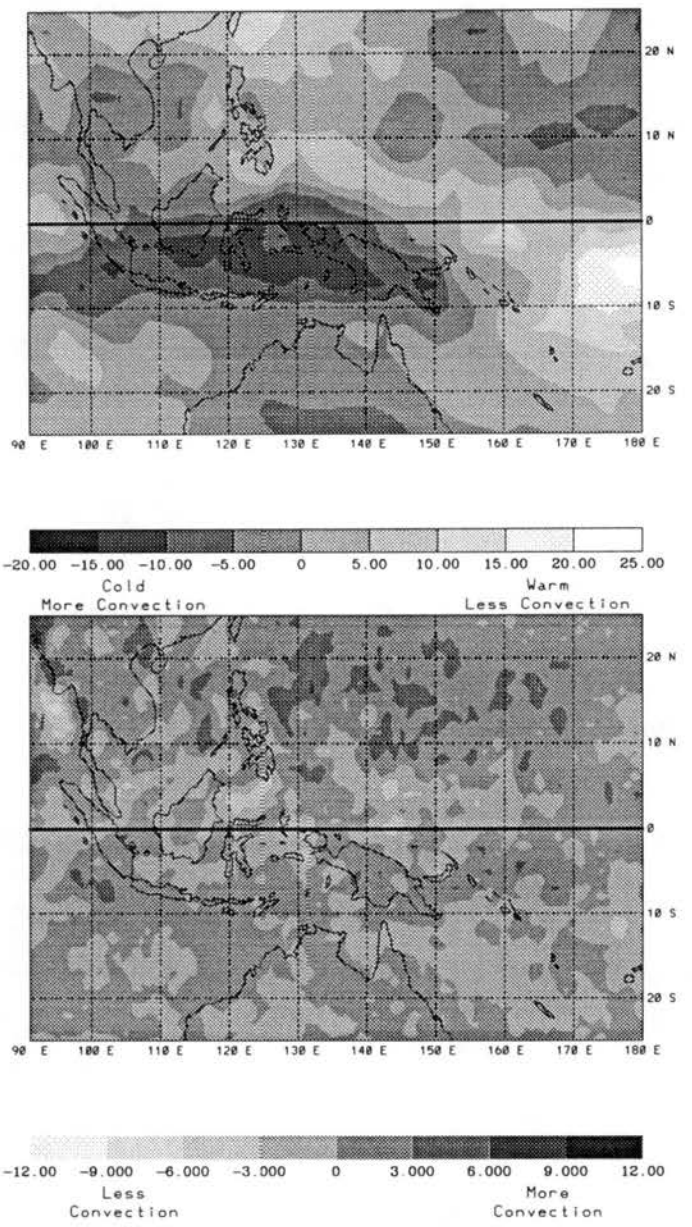

Figure 3.8: West phase composite minus east phase composite differences of OLR (top) expressed in W/m^2, and HRC (bottom) expressed as convective events for JJA. Note that dark shading represents areas where more convection occurs during the west phase of the SQBO and light shading represents areas that have more convection occurring during the east phase of the SQBO.

The west phase minus east phase HRC differences for JJA are shown in Fig. 3.8 (bottom). Large positive difference areas in this figure are located primarily in the Northern Hemisphere in the region of the monsoon trough. Other areas of positive HRC differences are primarily located poleward of 5°S and poleward of 10°N. In contrast, areas of negative differences are located primarily in the region very close to the equator extending from 5°S to about 7°N. These results are in excellent agreement with the surface data analysis wherein regions of strong upper troposphere to lower stratosphere zonal wind shear exhibit signs of suppressed convection.

Figure 3.9 (top) shows the SON west phase minus east phase OLR differences. Negative differences are located in off-equator positions corresponding roughly with the areas of weakest 200 mb to 50 mb zonal wind shear during the west phase SQBO. These negative areas are located primarily in the western part of the West Pacific, including Northern Australia. The most noticeable areas of positive differences are located very close to the Dateline on the equator. The SON OLR west phase minus east phase differences are thus characterized by (1) enhanced convection during the west phase of the SQBO in off-equator regions where the upper tropospheric to lower stratospheric shear is the smallest (see Fig. 3.3d), (2) enhanced convection near the Dateline and along the equator during the east phase of the SQBO, due inpart to favorable 200 mb to 500 mb shear, (3) a general agreement with the distribution of surface precipitation differences examined previously, and (4) enhanced convection in North Australia, an indication of an earlier average onset time for the Australian monsoon (Nicholls *et al.*, 1982).

The HRC west phase minus east phase differences during SON are in excellent agreement with the OLR results, as shown in Fig. 3.9 (bottom). Here again positive values represent areas of enhancement during the west phase of the SQBO. Positive values in this figure are located just off the equator in both hemispheres, corresponding to the areas of small upper tropospheric to lower stratospheric zonal wind shear which occur during the west phase of the SQBO (see Fig. 3.3d). Negative values of these differences are located primarily in a strip very close to the equator; again corresponding to the distribution of

weak upper tropospheric to lower stratospheric zonal wind shear during the east phase of the SQBO. These results are also in good agreement with station precipitation analysis. In summary, these HRC differences show (1) enhanced convection during the west phase of the SQBO just off the equator in areas where the 200 mb to 50 mb shear is relatively small and thus favorable; (2) enhanced convection during the east phase of the SQBO along the equator where the least zonal wind shear occurs between the upper troposphere and the lower stratosphere; and (3) agreement with the precipitation and OLR results discussed previously.

These apparent SQBO forced convection differences can be shown more clearly in a scatter plot of the seasonal zonal mean (20°N to 20°S, 90°E to 180°) 200 mb to 50 mb shear (west minus east) versus the zonal mean of HRC shown in Fig. 3.10. The relationship between 200 mb to 50 mb shear and HRC differences is apparent in this figure such that when this shear is large, HRC is suppressed and when this shear is small, HRC is enhanced, a statistically significant correlation of $r = -0.44$ is observed.

From the previous discussion of west phase minus east phase differences of OLR and HRC, we infer a tendency for more convection (i.e., higher HRC, lower OLR) in regions of weak upper tropospheric to lower stratospheric zonal wind shear. Although these results are not strong for all seasons, there is a good general relationship between this shear and convection during the DJF and SON seasons. These differences also appear to be operating to some degree in all seasons. This trend can be observed when the annual west phase minus east phase differences of OLR and HRC are examined, as shown in Fig. 3.11. The results in Fig. 3.11 suggest that convection is modulated by the amount of 200 mb to 50 mb shear or, more concisely, that convection is modulated by the SQBO. Moreover, scatter plots of zonal annual mean (20°N to 20°S, 90°E to 180°) 200 mb to 50 mb shear versus zonal annual mean values of OLR (Fig. 3.12a) and of HRC (Fig. 3.12b) result in rather striking correlations. Both of these scatter plots show statistically significant correlations of $r = 0.61$ and $r = -0.60$ for the OLR and HRC differences, respectively.

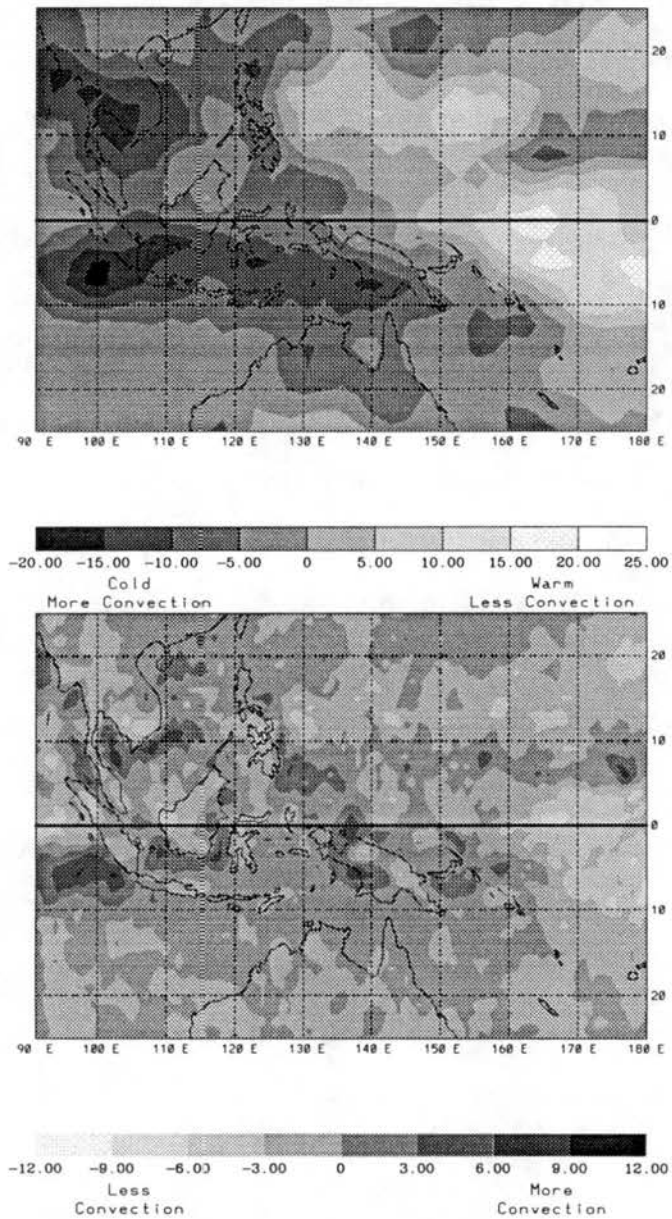

Figure 3.9: West phase composite minus east phase composite differences for OLR (top) expressed in W/m^2, and HRC (bottom) expressed as convective events for SON. Note that dark shading represents areas where more convection occurs during the west phase of the SQBO and light shading represents areas that have more convection occurring during the east phase of the SQBO.

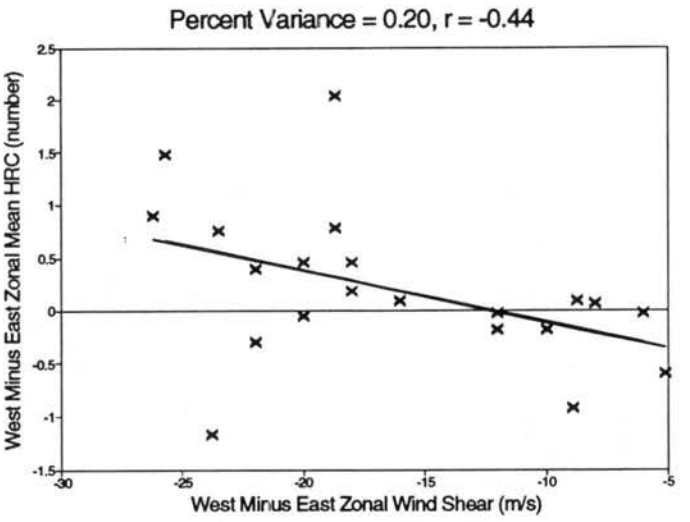

Figure 3.10: Scatter plot of the zonal mean (20°N to 20°S, 90°E to 180°) of the absolute value of west phase minus east phase upper tropospheric to lower stratospheric wind shear versus the zonal mean of the west phase minus east phase HRC differences expressed as units of deep convective events for the SON season.

3.3 Summary

This chapter has examined differences of precipitation, pressure and convection for the west phase and the east phase of the SQBO. The results suggest that distinct patterns of upper tropospheric to lower stratospheric zonal wind shear caused by the contrasting phases of the SQBO result in differences in seasonal precipitation and surface pressure. Results shown here imply that within regions which experience strong 200 mb to 50 mb zonal wind shear convection is suppressed, less precipitation falls, and surface pressure is often slightly higher. In contrast, regions which exhibit small values of upper tropospheric to lower stratospheric shear experience more convection, greater precipitation and slightly lower surface pressure. The effect of 200 mb to 50 mb wind shear are particularly pronounced in the off-equator monsoon regions whereas along the equator, surface pressure differences are often weak and disorganized. These results are more clearly seen in Table 3.16 and Table 3.17 which show seasonal west minus east precipitation and pressure differences for west phase high shear cases (Table 3.16) and west phase low shear cases (Table 3.17) and their location. As can be seen in these tables, the shear patterns are nearly symmetric about the equator, resulting in pressure and precipitation patterns which are

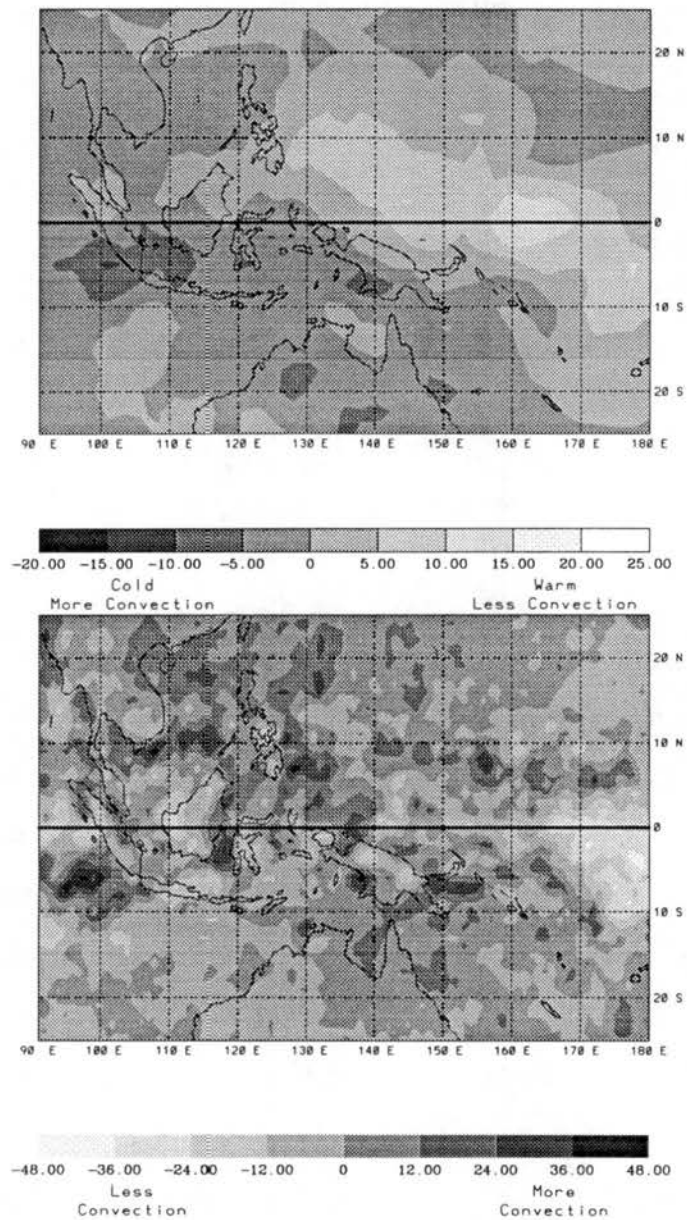

Figure 3.11: West phase composite minus east phase composite differences for OLR (top) expressed in W/m^2, and HRC (bottom) expressed as convective events for the year. Note that dark shading represents areas where more convection occurs during the west phase of the SQBO and light shading represents areas that have more convection occurring during the east phase of the SQBO.

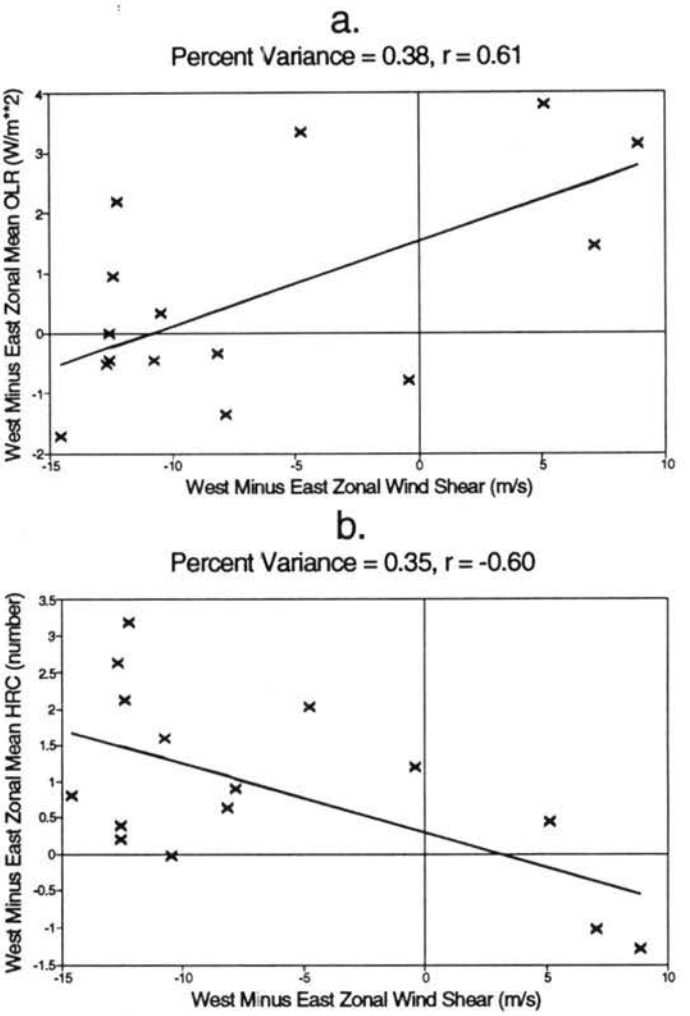

Figure 3.12: Scatter plots of the zonal mean (20°N to 20°S, 90°E to 180°) absolute value of west phase upper tropospheric to lower stratospheric shear minus the zonal mean of the absolute value of east phase 200 mb to 50 mb zonal wind shear versus (a) the zonal mean of west phase minus east phase composite OLR expressed as W/m^2, and (b) the west phase minus east phase composite of HRC, expressed as units of deep convective events for the entire year.

manifest as on-equator and off-equator differences. Consequently, during the west phase of the SQBO, (1) convection and precipitation are enhanced while surface pressure are lower in regions 7° to 25° off the equator, depending upon the seasonal upper tropospheric to lower stratospheric zonal wind shears, and (2) convection and precipitation are suppressed while surface pressure values are often higher in regions near and along the equator where the 200 mb to 50 mb zonal wind shear is large. Conversely, during the east phase of the SQBO, (1) convection along the equator (where upper tropospheric to lower stratospheric zonal wind shear is small) is enhanced, resulting in more precipitation, and (2) in regions located within 7° to 25° in both hemispheres (where 200 mb to 50 mb shear is large) convection and precipitation are suppressed, resulting in slightly higher surface pressure values.

Table 3.16: Mean pressure and precipitation differences for stations located in areas of strong west phase upper tropospheric to lower stratospheric zonal wind shear. For specific station data, see Tables 3.2, 3.6, 3.10, and 3.14 for precipitation and 3.4, 3.8, and 3.12 for pressure.

Strong shear during the west phase of the SQBO
West – East

Season	Latitude Belt	Precipitation (%△)		Pressure (10^{-2} mb)	
		Mean	Median	Mean	Median
DJF	(13.5°N - 12.5°S)	–4	–6	–32	–43
MAM	(6.5°N - 9.5°S)	–12	–10	–6	–6
JJA	(6.5°N - 6°S)	–5	–4	10	10
SON	(4°N - 3°S)	–15	–6	–	–
Annual	(7.5°N - 8°S)	–8	–7	–7	–13

The observed differences in convection and related surface parameters must result in changes in the general circulation. It can be inferred from the observations that the West Pacific monsoons will be stronger during the west phase of the SQBO. However, the question arises as to "how do these convective differences manifest themselves in the greater general circulation fields?" With this question in mind, Chapter 5 will examine 35 years of rawinsonde data in hopes of finding the answer. Another central question of this

Table 3.17: Mean pressure and precipitation differences for stations located in areas of weak west phase upper tropospheric to lower stratospheric zonal wind shear. For specific station data, see Tables 3.3, 3.7, 3.11 and 3.15 for precipitation and 3.5, 3.9, and 3.13 for pressure.

Weak shear during the west phase of the SQBO
West – East

Season	Latitude Belts		Precipitation (%△)		Pressure (10^{-2} mb)	
	Northern Hem.	Southern Hem.	Mean	Median	Mean	Median
DJF	14°N - 25°N	13.5°S - 25°S	22	17	–61	–67
MAM	7°N - 16.5°N	9.5°S - 13°S	12	8	–10	–18
JJA	10°N - 22°N	11°S - 25°S	38	7	–1	–1
SON	7°N - 11°N	9°S - 15°S	47	15	–	–
Annual	9.5°N - 18.5°N	11°S - 19.5°S	30	12	–24	–29

research is, "How can shear between the upper troposphere and the lower stratosphere effect convection?" This problem needs attention from the modeling community. With this need in mind, the next chapter will examine a few possible physical mechanisms whereby large upper tropospheric to lower stratospheric wind shear could suppress convection.

Chapter 4

A THEORY FOR THE OBSERVED QBO MODULATION OF TROPICAL CONVECTION

The previous chapter presented evidence of a modulation of tropical convection and related meteorological quantities, namely precipitation and surface pressure, by SQBO forced variation of the upper tropospheric to lower stratospheric wind shear. Variations of this shear were also examined in relation to the quasi-biennial variations of the stratospheric zonal winds and temperatures. The findings suggest that the shear, and thus the modulation of convection, varies nearly quasi-biennially. Furthermore, this quasi-biennial variation of shear results in a remarkable on versus off equator pattern such that during the west (east) phase of the SQBO, convection is observed to be enhanced off (on) the equator. The purpose of this chapter is to propose a theory for the modulation of tropical convection by the SQBO and the associated variations of upper tropospheric to lower stratospheric wind shear.

Recent studies of tropical and mid latitude deep convection using the concept of Potential Vorticity (PV) have shown that long-lived convective systems have a characteristic dipole (PV) structure, as shown in Fig 4.1 (Hertenstein and Schubert, 1991; Raymond and Jiang, 1990). In Figure 4.1, positive PV anomalies are associated with convergence in the lower tropospheric and negative PV anomalies represent divergence in the upper troposphere. It must be noted that this dipole structure is best observed in a low or no vertical shear situation (Raymond and Jiang, 1990). A link to the QBO is made by suggesting that the actual structure of the PV anomalies may actually be more like a tripole with positive PV anomalies in the lower stratosphere as well (Schubert – personal communication, see Fig. 4.2). If this proves the case (as seems likely) then this triple structure may represent

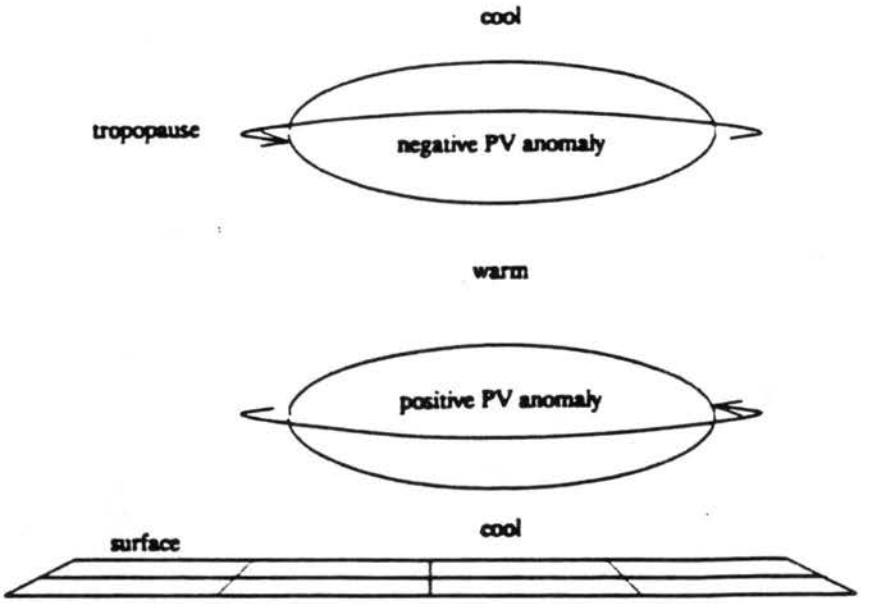

Figure 4.1: Postulated dipole structure of potential vorticity anomalies produced by a region of convection and the associated changes in temperature and wind structure. The circulation is cyclonic around the lower, positive PV anomaly, and anticyclonic around the upper PV anomaly, as shown by the arrows (adapted from Raymond and Jiang, 1990).

the means by which variations of vertical shear between the upper troposphere and the lower stratosphere could effect the tropospheric PV structure and thus convection.

An area of positive PV anomalies in the lower stratosphere, shown in Fig. 4.2, would, in the absence of vertical shear between the upper troposphere and lower stratosphere, promote systematic convergence, sinking, and thus warming in the lower stratosphere and upper troposphere. This process would act to lower pressures and heights in the mid and lower troposphere through hydrostatic adjustments. However, if the convective system is situated in strong upper tropospheric to lower stratospheric wind shear, the tripolar structure would be decoupled from the stratospheric PV anomaly which would be advected away from the area of upper tropospheric divergence. Thus little or no sinking effect would be superposed on the upper troposphere in the sheared situation; the net result being that the mid and lower tropospheric heights and pressures will not be lowered leading to no enhancement of convergence and convection.

It is obvious from this discussion that more observations as well as detailed modeling experiments will be needed to verify this theory. However, the fact remains that the

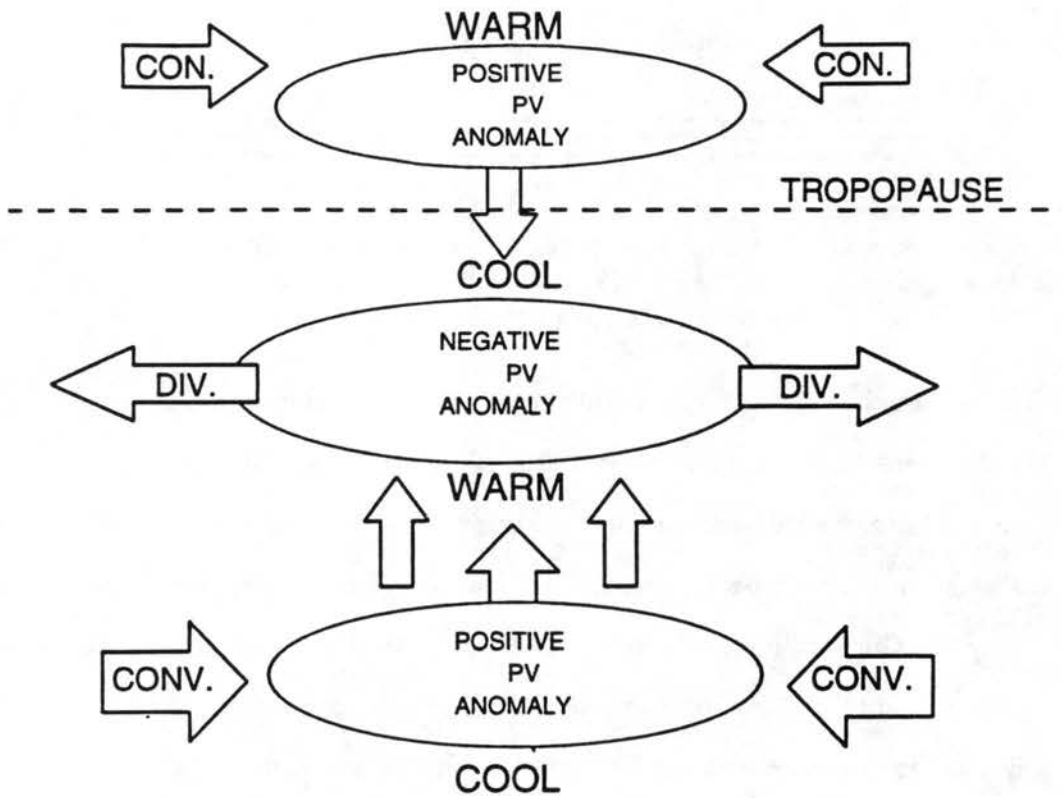

Figure 4.2: Hypothetical structure of potential vorticity (PV) anomalies associated with the thermal structure and circulation in areas of deep persistent tropical convection. Broad arrows indicate the primary vertical and horizontal convergence features and areas of anomalous warming and cooling are also labeled (modified and adapted from Raymond and Jiang, 1990).

convection, precipitation and surface pressure all appear to be modulated by a SQBO forced variations of the upper tropospheric to lower stratospheric wind shear. With these observations at hand, the next step is to further examine the circulation fields in the West Pacific to ascertain the changes caused by this on versus off equator modulation of deep convection. With this purpose in mind, the next chapter will discuss changes in regional circulation patterns associated with the observed SQBO modulation of deep convection.

Chapter 5

CIRCULATION DIFFERENCES BETWEEN EAST AND WEST SQBO PERIODS

The previous chapters have shown that differing phases of the SQBO cause varying rates of upper tropospheric to lower stratospheric zonal wind shear. These differences effect precipitation and surface pressure fields in the West Pacific region, as discussed in Chapter 3. It is thought that differences in surface parameters occurring between the east and west phases of the SQBO are forced by differences in deep convection which are inturn a result of differing values of 200 mb to 50 mb zonal wind shear (see Chapters 3 and 4). In this chapter, data for the east and west phases of the SQBO are examined to ascertain the effects of SQBO forced convection differences cause on the West Pacific region's general circulation. Results shown in this chapter suggest that SQBO linked differences in convection result in stronger Australian monsoon circulations and stronger Walker Circulation manifested as stronger trade winds and upper level westerlies within the West Pacific region.

5.1 Data and Analyses

Rawinsonde station data for the West Pacific warm pool region obtained from NCAR and from Gray project archives were used extensively to identify and assess changes in the general circulation associated with the phases of the SQBO. The available stations generally had more than twenty years of data. Table 4.1 provides a list of the station locations and data availability.

Monthly mean values for winds, heights, and temperatures at various levels were created from the daily rawinsonde station data. These mean values then were composited

Table 5.1: Rawinsonde stations used in this study.

Station	lat	lon	Availability Starting	Ending
Darwin Airport	12 24 S	130 52 E	1/50	5/88
Singapore Airport	1 18 N	103 54 E	1/57	12/85
Honiara	9 25 S	160 03 E	8/58	10/86
Yap	9 29 N	135 05 E	6/51	12/88
Koror	7 20 N	134 29 E	5/52	12/88
Ponape	6 58 N	158 13 E	7/51	12/88
Truk	7 28 N	158 51 E	7/51	12/88
Kwajalein	8 44 N	167 44 E	5/52	11/74
Majuro	7 05 N	171 23 E	2/55	12/86
Clark AFB	15 10 N	120 33 E	3/51	2/71
Guam	13 33 N	144 50 E	10/52	12/86
Wake Island	19 17 N	166 30 E	1/57	12/78

with respect to the phase of the QBO using the 50 mb zonal wind anomalies of Koror (7°N) as a criteria for the phase. Data from other tropical rawinsonde station were used to fill in missing data periods and extend the length of the Koror 50 mb data set from March, 1951 through December, 1988. The method by which the (rawinsonde station) data was stratified was by distinctly west and distinctly east. This was done because the transitions between SQBO phases are often noisy and typically take several months. Hence, the term "distinctly" simply means that the amplitude of the anomalies were greater than 5 m/s, east or west. This stratification allows speculation on changes in the general circulation during two completely different upper tropospheric to lower stratospheric shear situations. Data for all available levels were analyzed in this fashion. All stations had the WMO standard levels and many of the stations had extra levels at 950 mb ,800 mb, 750 mb, 600 mb, 400 mb, 350 mb, 175 mb, 125 mb, and 80 mb. Hence, these rawinsonde composites gave information for both troposphere and stratosphere.

The composites were used to examine aspects of the Pacific Walker Trade-Circulation as well as circulation features associated with the Australian monsoon. To examine differences between the Walker Circulation during each of the two phases of the SQBO, West Pacific stations were used to create meridional cross-sections of the near equatorial circu-

lation. The next section will discuss west phase minus east phase differences occurring in the Walker Trade Circulation during all seasons.

5.2 Equatorial West Pacific Meridional Cross-sections

Using data from near equatorial rawinsonde stations at Singapore, Koror, Truk, Ponape and Majuro meridional cross-sections of zonal and meridional winds with pressure were created in order to look at the west phase minus east phase circulation differences in the West Pacific. This section will discuss these differences with particular attention to variations of the Walker Circulation.

The west phase minus east phase composite difference of zonal and meridional winds for the DJF season is shown in Fig. 5.1. In this figure the 850 mb circulation differences indicate that, from Truk eastward, the trade winds are slightly stronger and with more of a southerly component during periods of QBO westerlies at 50 mb. In contrast, during the QBO west phase 850 mb winds west of Koror are slightly westerly, but again the winds are more southerly. At Singapore, the low level winds tend to be more northerly indicating cross equatorial flow in that region during the west SQBO periods. These wind differences are compatible with the prior analysis of convection which suggested more west phase off-equator convergence and thus more convection.

In the upper atmosphere during DJF, winds in the eastern half of Fig. 5.1 show a more southerly component, suggesting a stronger local Hadley Circulation with more mass transport toward the winter hemisphere. At Singapore, on the other hand, winds above 200 mb show stronger easterly flow, indicative of a stronger equatorial easterly jet in association with an anomalously intense Australian monsoon circulation. Stronger mid level westerlies at Singapore are indicative of enhanced mid-level convergence in the extreme Western Pacific equatorial region, between 100°E and 130°E.

These results support the of previously described observations of precipitation, pressure and convective anomalies. Furthermore, they indicate that cold ENSO type conditions occur during the west phase of the SQBO. Thus, these DJF circulation differences

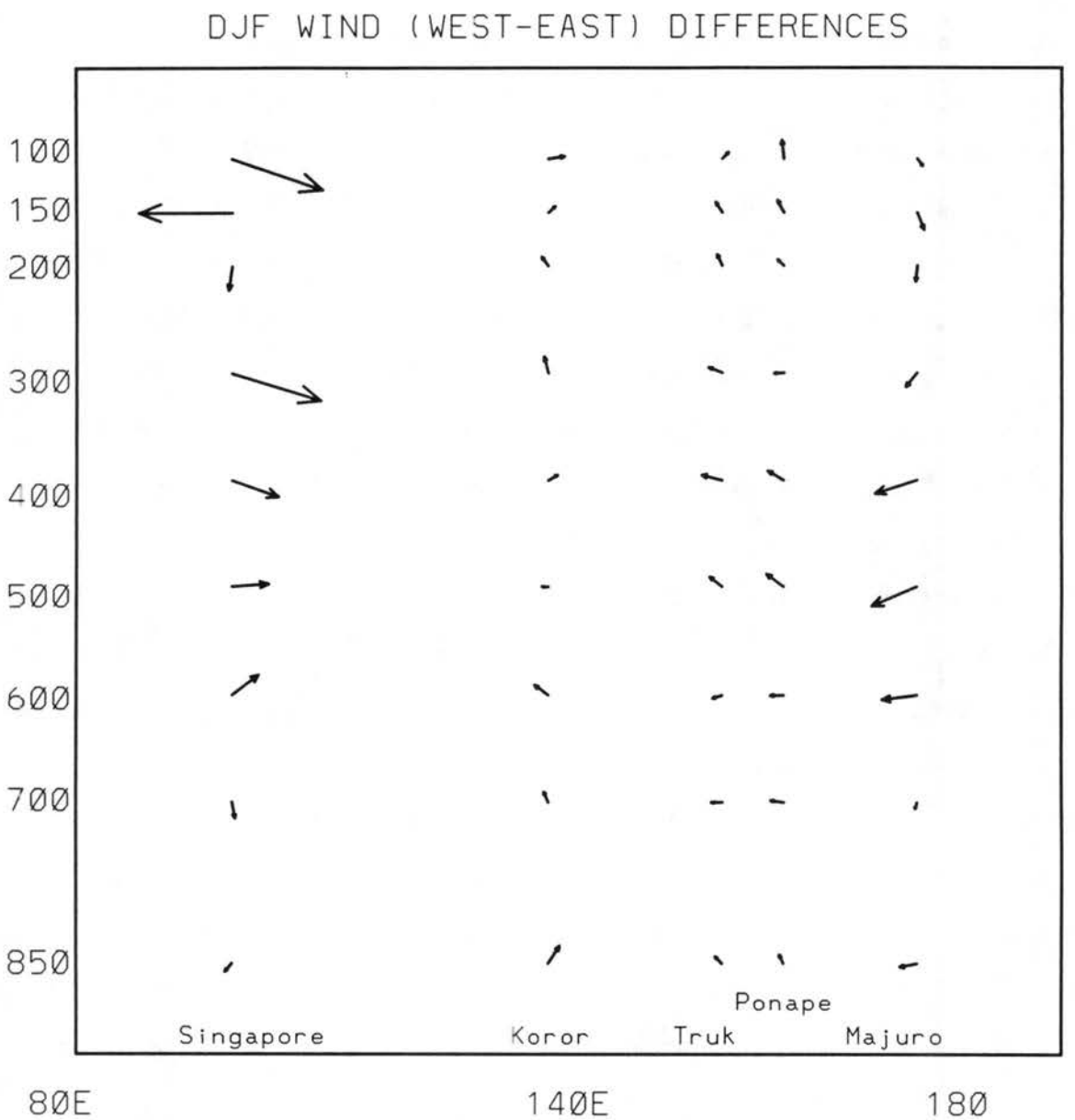

Figure 5.1: West phase minus east phase DJF composite of rawinsonde stations located close to the equator in the West Pacific region. The composite consist of average zonal and meridional winds for periods of distinctly west (> 5 m/s) and distinctly east (< -5 m/s) zonal winds at 50 mb.

suggest: (1) that the local Walker/Hadley Circulation is stronger than average during the west phase of the SQBO and weaker than average during the east phase of the SQBO, (2) that west phase of the SQBO acts to enhance off-equator convergence, particularly, in the lower levels of the atmosphere, and (3) that a stronger Australian monsoon circulation occurs as inferred from both a stronger easterly component in the upper levels at Singapore and that a stronger southerly component occurs at 200 mb to 150 mb over the eastern portion of the West Pacific during the west phase of the SQBO.

The composite MAM west phase minus east phase West Pacific circulation differences are shown in Fig. 5.2. In this figure, the trade winds show a westerly bias, indicating weaker (easterly) trades occur during the west phase of the SQBO. These differences may be associated with a slower than average decay of the South Pacific Convergence Zone (SPCZ) as discussed by Meehl (1987). The delay in this transition is thought to be slow because the convection associated with the SPCZ is stronger than average during the DJF season and thus lasts longer as it breaks up near the equator.

At the upper levels in Fig. 5.2, composite anomaly differences over the eastern half of the West Pacific cross-sections are predominantly westerly, suggesting a stronger than average westerly return flow for the Walker Circulation. This inturn suggest that, even though the trades are weaker, there must be strong low level convergence and deep convection in the Western Equatorial Pacific during this season. These result again suggest that a cold ENSO type climatology occurs during the west phase of the SQBO. These west minus east phase differences in circulation suggest: (1) that more convergence is occurring in the Western Pacific during periods of westerly stratospheric anomalies, (2) trade winds east of 140°E are weaker in association with the persistent remains of a stronger than average SPCZ during the west phase of the SQBO, and (3) the upward branch of the local Walker Circulation is stronger during the west phase of the SQBO.

The JJA west phase minus the east phase composite is shown in Fig. 5.3. The low level trade wind flow appears much stronger during the west phase of the SQBO, manifested in this figure as easterly anomalies throughout the lower troposphere (700–850

mb). These low level differences also show more southerly wind components, suggesting stronger Northern Hemisphere off-equator low level convergence is occurring. The upper levels in Fig. 5.3 show westerly differences throughout the West Pacific, suggesting a stronger upper branch of the local Walker Circulation. This implies that stronger monsoon activity is occurring during the west phase of the SQBO in the off-equator regions. Results for the JJA season again show a cold ENSO type circulation climatology occurring during the west phase of the SQBO. Overall the JJA results suggest that: (1) stronger trade winds exist throughout the West Pacific region, (2) a stronger local Walker Circulation exists, and that (3) stronger off-equator convergence, particularly monsoon activity, occurs during the west phase of the SQBO.

The SON west phase minus east phase differences are shown in Fig. 5.4. As in JJA, the SON low level wind differences in Fig. 5.4 show that enhancement of the trade wind easterlies occurs during the west phase of the SQBO. There are also signs of increased low level and mid-level convergence occurring between Singapore and Koror during the west phase of the SQBO. The upper level wind differences, shown in Fig. 5.4, suggest that stronger westerlies occur east of 140°E during the west phase of the SQBO . West of 140°E (at Singapore), 150 mb and 200 mb wind differences are more easterly, suggesting an anomalously early start may occur for the Australian northwest monsoon. These upper level observations tend to support the differences in convection shown in Chapter 3. The results for SON show that the local Walker Circulation is enhanced during the west phase of the SQBO, suggesting a cold ENSO pattern is more likely during the west phase of the SQBO. Summarizing these results for the SON season, (1) the Walker Circulation is enhanced when the SQBO is in its west phase, (2) the Australian monsoon may tend to have an anomalously early starting date during the west phase of the SQBO, and (3) the west phase of the SQBO has a climatology much like the circulations that exist during cold ENSO outbreaks.

The results shown in Fig. 5.1 through Fig. 5.4 suggest that during periods o the west phase SQBO, is dominant that circulation patterns are more favorable for cold ENSO

conditions to occur. In particular, these results suggest that during the west phase of the SQBO (1) the local West Pacific Walker Circulation is stronger than average, (2) off-equator low level convergence is enhanced, (3) equatorial low level convergence is confined to an area west of 130°E, (4) the Australian monsoon has an earlier starting time, and a stronger circulation than average, and thus (5) a cold ENSO type climatology exists. Conversely, during the east phase of the SQBO: (1) the Pacific Walker Circulation is weaker than average, (2) the Australian monsoon is weaker than average, and (3) conditions favorable for the onset and maintenance of warm ENSO events often exist.

5.3 Differences in the Australian Monsoon Circulation

The observations of convection and precipitation throughout Chapter 3 suggested a stronger Australian monsoon occurs during the west phase of the SQBO. In this section, the circulation differences which occur in the Australian monsoon during each phase of the SQBO are examined. Using the available soundings, in particular Darwin (12°S, 130°E) and Honiara (9°S, 160°E), the results suggest stronger monsoon circulation during the west phase composite as compared to the east phase composite. On closer examination, the west phase composite shows a southerly shift in the 200 mb ridge and 850 mb trough associated with the SPCZ and the Northern Australian summer monsoon. Table 5.2 gives the wind speed and direction for both Honiara and Darwin at 200 mb and at 850 mb for the DJF composites. Figure 5.5 schematically shows the estimated mean position of the monsoon trough for the west phase (a), and the east phase (b) composite. The position of the monsoon trough is quite notably different (i.e., more southerly during the west phase), especially over the SPCZ and Australian continent.

These SQBO related monsoon changes are more evident when the monthly anomalies of 850 mb zonal winds are calculated for the four month active monsoon period which spans DJFM. These data (i.e., Fig. 5.6) are smoothed using a seven year running mean. The motivation for this smoothing is to isolate 4 to 8 year variations related to the strong and moderate El Niño events. This running mean then is subtracted from the unsmoothed

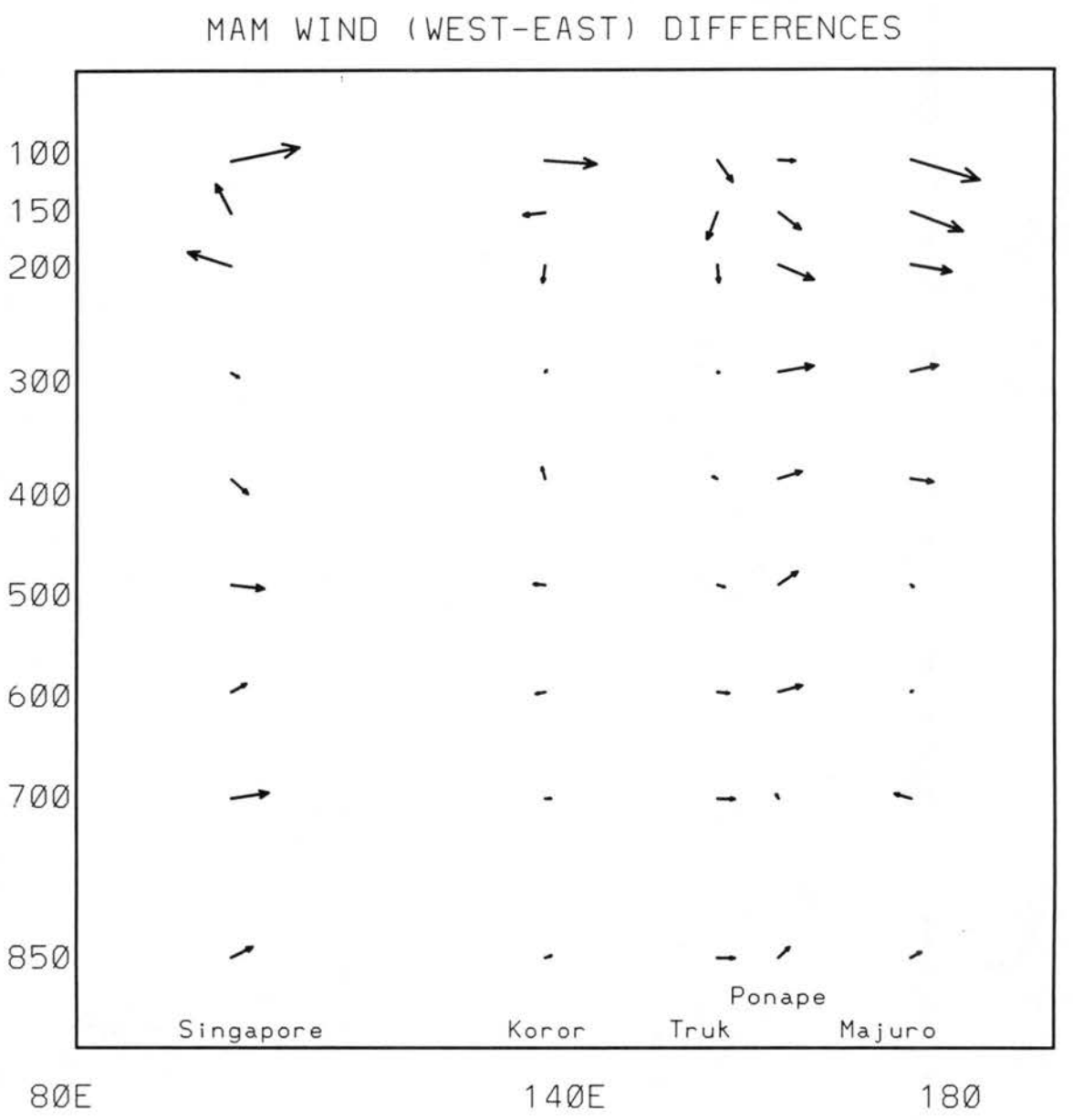

Figure 5.2: West phase minus east phase MAM composite of rawinsonde stations located close to the equator in the West Pacific region. The composite consist of average zonal and meridional winds for periods of distinctly west (> 5 m/s) and distinctly east (< -5 m/s) zonal winds at 50 mb.

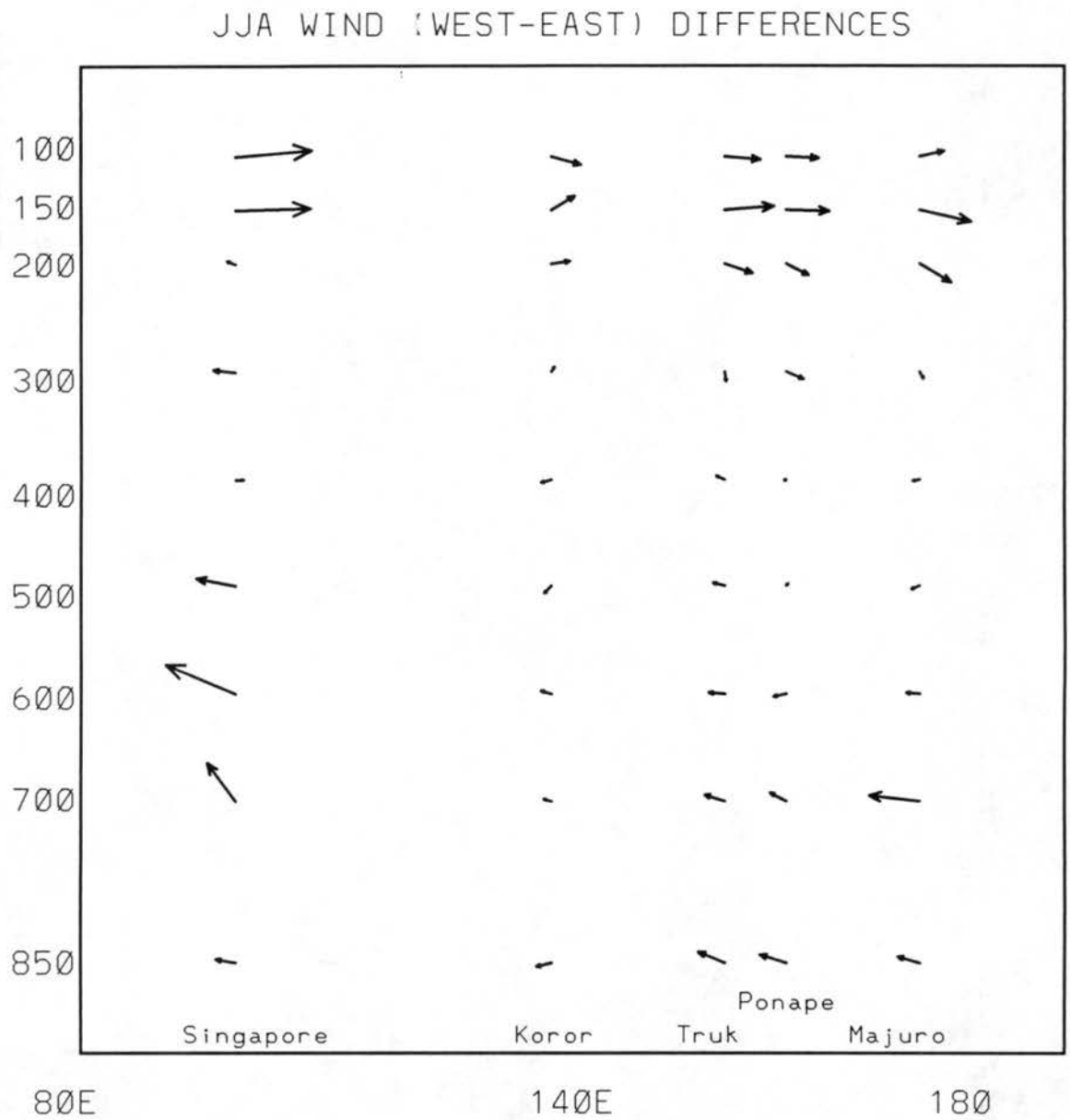

Figure 5.3: West phase minus east phase JJA composite of rawinsonde stations located close to the equator in the West Pacific region. The composite consist of average zonal and meridional winds for periods of distinctly west (> 5 m/s) and distinctly east (< -5 m/s) zonal winds at 50 mb.

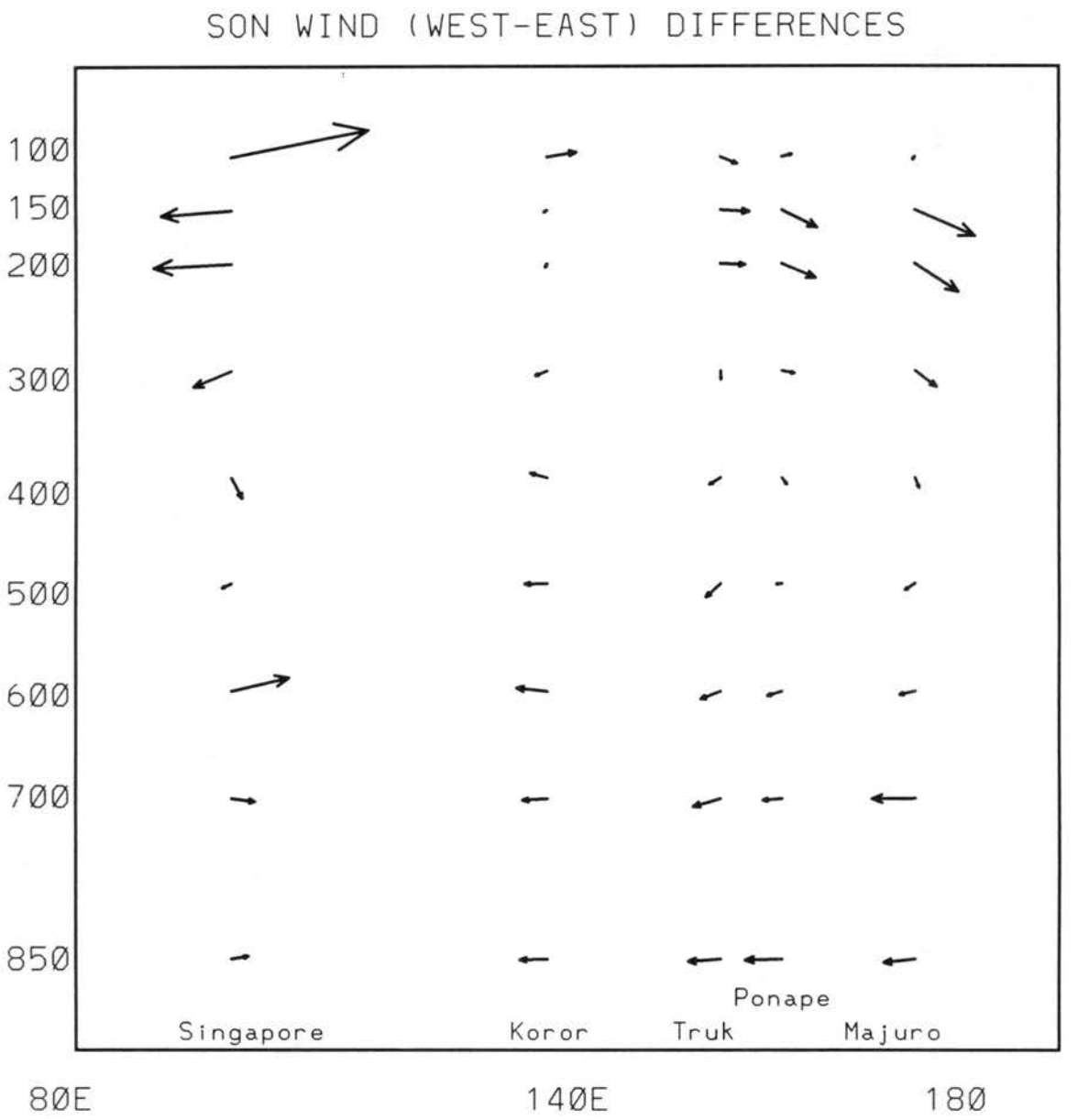

Figure 5.4: West phase minus east phase SON composite of rawinsonde stations located close to the equator in the West Pacific region. The composite consist of average zonal and meridional winds for periods of distinctly west (> 5 m/s) and distinctly east (< -5 m/s) zonal winds at 50 mb.

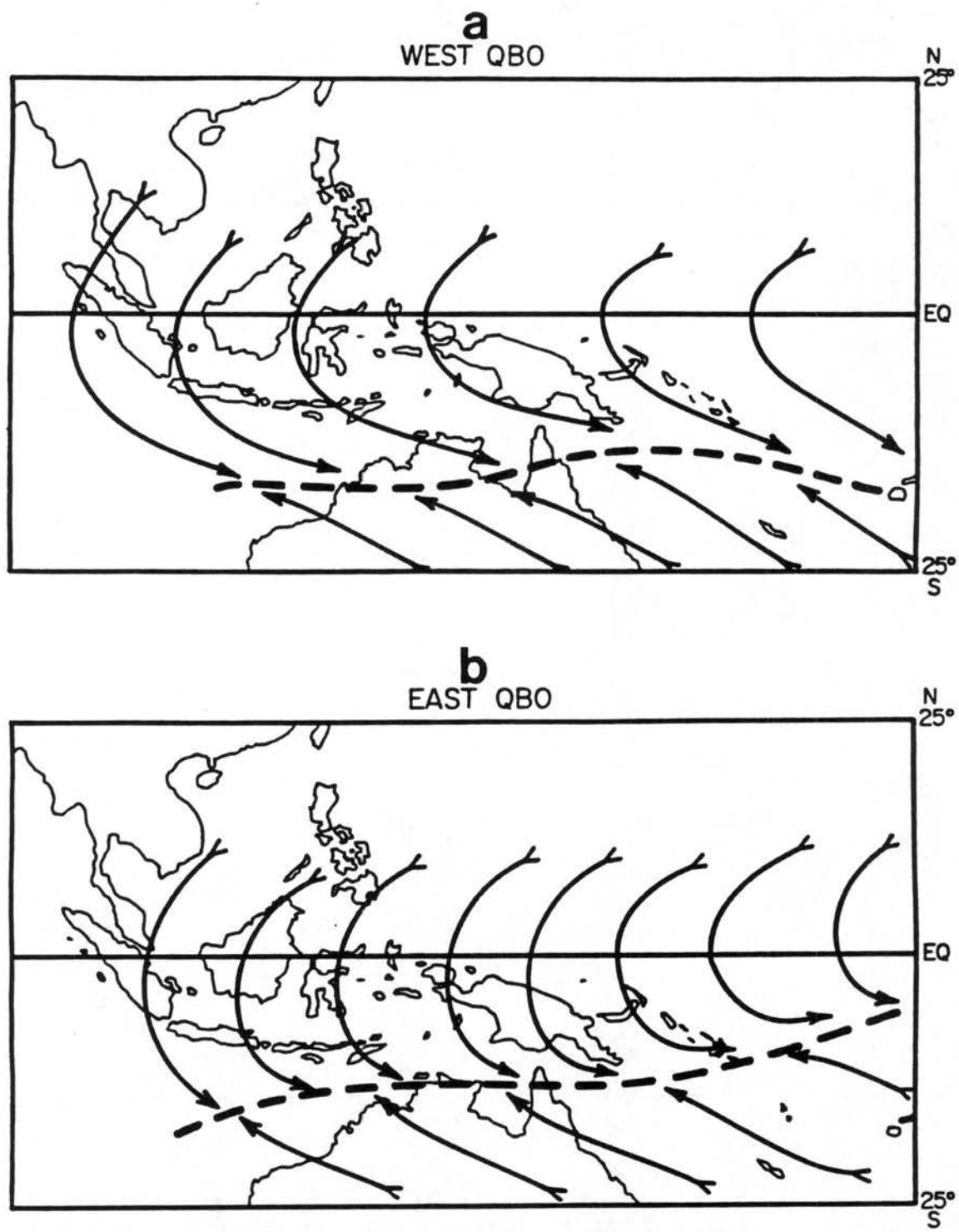

Figure 5.5: Schematic of the estimated position of the Australian monsoon trough inferred from Darwin and Honiara rawinsonde averages during DJF for a) the distinctly west (> 5 m/s) 50 mb composite, b) the distinctively east (< -5 m/s) 50 mb composite.

Table 5.2: Wind speed (kts) and direction at 200 mb and at 850 mb from the east and west phase composites at Honiara and Darwin during the DJF season.

	Pressure	west		east	
	mb	dir	speed	dir	speed
Honiara	850	275	3	250	2
	200	105	3	285	4
Darwin	850	250	3	calm	calm
	200	95	7	90	4

values of the 850 mb ZWA's. The results from smoothing are then plotted against 50 mb ZWA during the previous October, as shown in Fig. 4.6. This process yielded a significant linear correlation (r = 0.37), thus explaining approximately 14% of the variance of the smoothed data. These results suggest that a fairly consistent year to year variation of the Northern Australian monsoon strength occurs for the different phases of the SQBO.

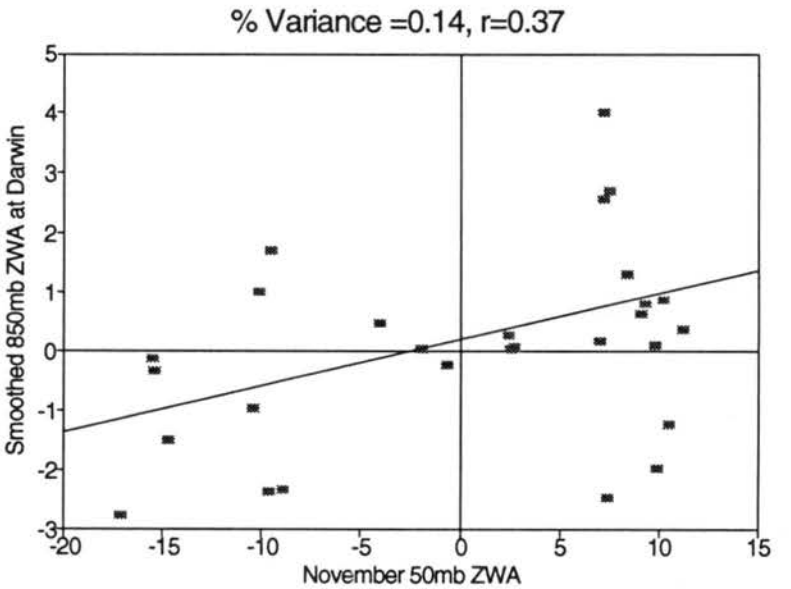

Figure 5.6: Regression of smoothed (seven year running mean applied) DJFM 850 mb ZWA at Darwin versus the previous November value of 50 mb ZWA. The relationship shows a correlation of r = 0.37, explaining 14% of the variance.

In summary, these results suggest that a distinct SQBO modulation of the strength of the Australian monsoon circulation occurs such that: (1) a more robust monsoon circulation exist in Northern Australia during the west phase of the SQBO, and (2) a

mean monsoon trough poleward of the average position occurs during the west phase of the SQBO.

5.4 Summary of Chapter 5

This chapter discusses tropospheric circulation patterns associated with the two phases of the SQBO. It is felt that these circulation differences are forced by the modulation of convection in response to the variations of upper tropospheric to lower stratospheric zonal wind shear associated with the SQBO. The circulation features examined in this chapter suggest that the SQBO promotes contrasting differences such that during the west phase of the SQBO: (1) the Australian summer monsoon circulation is stronger and is located poleward of its climatological mean position, (2) the local West Pacific Walker Circulation appears stronger in all seasons, and (3) enhanced low level convergence occurs along the equator in the equatorial West Pacific west of 140°E. During the east phase of the SQBO: (1) the Australian monsoon has a weaker overall circulation and is positioned equatorward of the climatological long term mean, (2) the local Walker Circulation is weaker, and (3) suppressed low level convergence occurs in regions west of 140°E along the equator.

All of these latter (east phase) conditions are consistent with conditions favorable to the onset, intensification, and prolonged maintenance of ENSO warm events and similarly of cold ENSO events during the former (west) phase of the SQBO (Rasmusson and Carpenter, 1982; Wallace and Desser, 1985; Wright, 1985). Because of this relationship between the general circulation and the SQBO, the question becomes, "Does the SQBO signal show up in the ENSO parameters?" With this in mind, the next chapter will examine the relationship between these parameters and ENSO and summarize the results of this study.

Chapter 6

SYNTHESIS AND DISCUSSION

Chapters 2 and 3 showed that the SQBO, by causing varying amounts of upper tropospheric (200 mb) to lower stratospheric (50 mb) zonal wind shears, may affect deep tropical convection and thus affect both precipitation and surface pressures over large areas of the tropics. Furthermore, it was shown that these shear patterns are primarily manifested as low vertical shears in the vicinity of the tropopause occurring along the equator during the east phase of the SQBO and as low vertical shear near the tropopause located in off-equator regions during the west phase of the SQBO. The findings imply that convection and rainfall are enhanced (often causing lower surface pressures) in regions where this 200 mb to 50 mb zonal wind shear is lowest. This modulation results in more convection and rainfall in regions located off the equator region during the west phase of the SQBO and in regions on the equator during the east phase of the SQBO. The influence of this apparent modulation of deep tropical convection upon some aspects of the West Pacific general circulation were discussed in Chapter 5. Among these effects were a stronger equatorial West Pacific Walker Circulation and a stronger Australian monsoon circulation occurring during the west phase of the SQBO. In this chapter, a synthesis of these results is performed followed by a discussion of the significance of the results in relation to ENSO variability.

6.1 Synthesis of Results

The results presented in this paper suggest that there is indeed a link between stratospheric circulations, specifically the SQBO, and circulations in the troposphere. This link is believed to be involved in the modulation of deep convection in the tropics. The strato-

sphere is observed to be extremely dry. Therefore, because the tropical tropopause is so cold and hence dry, it is thought that regions of deep tropical convection are the likely centers of upward mass exchange between the troposphere and the stratosphere, thereby creating a link between the two (Newell and Gould-Stuart, 1981; Johnson and Kriete, 1982; Danielson, 1982; Dobson *et al.*, 1946; Selkirk and Newell, 1989). It is suggested that this mass exchange leads to a tri-polar Potential Vorticity (PV) structure in the vertical associated with deep convection. This tri-polar structure will be effected by varying rates of shear between the upper troposphere and lower stratosphere such that large shear perturbs the PV structure and inhibits convection whereas small shear would appear to enhance convection.

Collectively, the influence of the tropospheric annual cycle and of the quasi-biennial and annual cycles of the stratosphere conspire to create large areas of relatively weak or strong 200 mb to 50 mb zonal wind shear. The stratospheric quasi-biennial cycle is the dominant variable creating differing amounts of 200 mb to 50 mb zonal wind shears. Because of the strength of this quasi-biennial variability, the 200 mb to 50 mb shears appear as a uniform quasi-biennial pattern, varying only about 5° latitudinally during the year. The net result is a zonally symmetric shear pattern such that during the west phase of the SQBO (shown in Fig. 6.1), areas of small upper tropospheric to lower stratospheric zonal wind shears are located 8° to 18° off the equator in both hemispheres and areas of large 200 mb to 50 mb zonal wind shear occur within approximately 7° of the equator. Conversely, during the east phase of the SQBO, (shown in Fig. 6.2) areas of small upper tropospheric to lower stratospheric shear are located within 7° of the equator and, areas of large 200 mb to 50 mb wind shear are located in regions 8° to 18° off the equator.

Comparisons of rainfall pressures and convective anomalies occurring during differing phases of the SQBO suggest that this link between the stratosphere and the troposphere exists. This link appears to be the result of a modulation of deep tropical convection by varying rates of upper tropospheric to lower stratospheric zonal wind shear. Stations located in areas of low shear during the west phase of the SQBO (i.e., off-equator regions

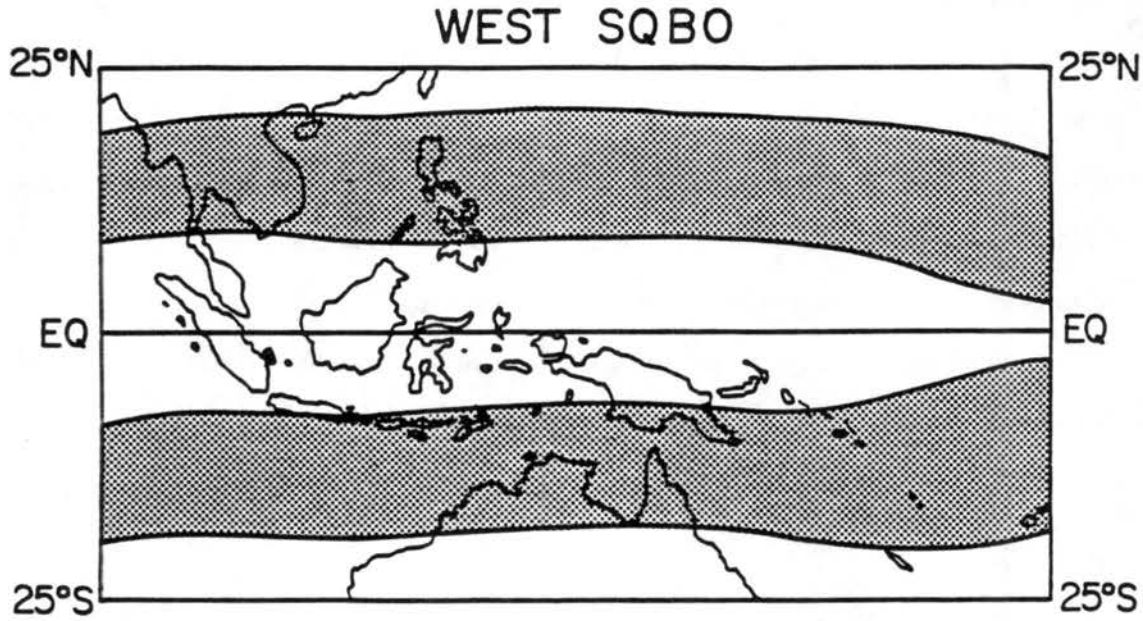

Figure 6.1: Pattern of upper tropospheric to lower stratospheric zonal wind shear pattern associated with the west phase of the SQBO. Shaded areas have comparatively weak 200 to 50 mb shear during the QBO west phase.

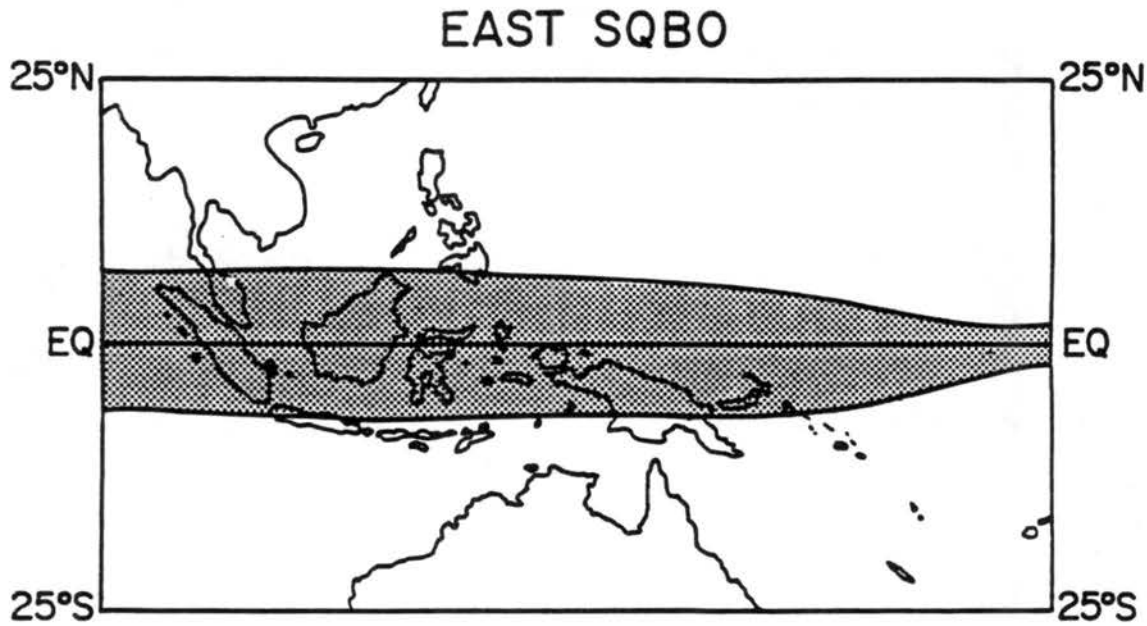

Figure 6.2: As in Fig. 6.1 but for the upper tropospheric to lower stratospheric zonal wind shear pattern associated with the east phase of the SQBO. The shaded area again indicates those areas with comparatively weak shear.

listed in Table 6.1), show that greater rainfall and lower pressure occurs in these areas during the west phase of the SQBO. In contrast, stations located in regions of strong west phase shear (i.e., on-equator), shown in Table 6.2, have more rainfall during the east phase of the SQBO. Furthermore, the analysis of convective anomalies using HRC and OLR data are consistent with those of rainfall results, indicating that deep convection occurs more often in regions with less than 200 mb to 50 mb shear. In summary, the analysis of precipitation, pressure and convective anomalies suggest that in regions that experience strong upper tropospheric to lower stratospheric zonal wind shear that: (1) deep tropical convection is somewhat suppressed, (2) surface pressures are somewhat but not always slightly higher, and (3) less precipitation falls.

Table 6.1: Results obtained for pressure and precipitation stations in areas of weak upper tropospheric to lower stratospheric zonal wind shear during the west phase of the SQBO. See Tables 3.3, 3.7, 3.11 and 3.15 for precipitation and 3.5, 3.9, and 3.13 for pressure.

Weak shear during the west phase of the SQBO
West – East

Season	Latitude Belts		Precipitation (%△)		Pressure (10^{-2} mb)	
	Northern Hem.	Southern Hem.	Mean	Median	Mean	Median
DJF	14°N - 25°N	13.5°S - 25°S	22	23	–61	–67
MAM	7°N - 16.5°N	9.5°S - 13°S	12	8	–10	–18
JJA	10°N - 22°N	11°S - 25°S	38	7	–1	–1
SON	7°N - 11°N	9°S - 15°S	47	15	–	–
Annual	9.5°N - 18.5°N	11°S - 19.5°S	30	13	–24	–29

As a result of these shear patterns, areas of enhanced convection and rainfall seem to be located off the equator during the west phase of the SQBO and on the equator during the east phase of the SQBO. Surface pressure, however, only seems to follow convection and precipitation in the off-equator monsoon regions. (As surface pressure gradients are difficult to maintain very close to the equator, convection along the equator does not always result in lower surface pressures.) These findings agree with Kuma (1990) who shows that the intra-seasonal oscillation seems to operate more efficiently during the QBO east phase (more specifically, during low upper tropospheric to stratospheric zonal wind shear

Table 6.2: Results obtained for pressure and precipitation stations in areas of strong upper tropospheric to lower stratospheric zonal wind shear during the west phase of the SQBO. See Tables 3.2, 3.6, 3.10, and 3.14 for precipitation and 3.4, 3.8, and 3.12 for pressure.

Strong shear during the west phase of the SQBO
West – East

Season	Latitude Belt	Precipitation (%Δ)		Pressure (10^{-2} mb)	
		Mean	Median	Mean	Median
DJF	(13.5°N - 12.5°S)	–4	–6	–32	–43
MAM	(6.5°N - 9.5°S)	–12	–10	–6	–6
JJA	(6.5°N - 6°S)	–5	–4	10	10
SON	(4°N - 3°S)	–15	–6	–	–
Annual	(7.5°N - 8°S)	–8	–7	–7	–13

situations) of the SQBO at Singapore (1.5°N). The net result of this convection modulation is a change in the general circulation, as was discussed in Chapter 5. These changes in convection appear to relate to the West Pacific Walker Circulation such that generally during the west phase of the SQBO, the Walker Circulation is generally stronger than during the east phase of the SQBO. Another more obvious result, is that the Australian monsoon is stronger during the west phase of the SQBO. The most impressive result, however, is the apparent weakening of the West Pacific trade winds, as shown in Table 6.3 during the east phase of the SQBO (except for MAM).

In summary, results show that during the west phase of the SQBO: (1) trade winds are stronger, (2) Walker circulation is stronger, (3) convergence is stronger along the equator west of 140°E, and (4) the Australian monsoon is stronger with and the monsoon trough is located further poleward.

The net result observed for parameters examined for the SQBO west phase (shown in Fig. 6.3) is that off-equator convection and precipitation along the equator west of 140°E, the Central Pacific trades and the equatorial Walker Circulation are all enhanced. These results portray a cold ENSO type climatology, the details of which are discussed in the next section. During the east phase of the SQBO, the West Pacific climatology is almost opposite that of the west phase climatology as shown in Fig. 6.4. In Fig. 6.4, anomalous

Table 6.3: Distinctly west (50 mb u > 5 m/s), distinctly east (50 mb u < 5 m/s), and differences for 850 mb and surface winds used in this study.

		850 mb zonal winds (m/s)				
Station		DJF	MAM	JJA	SON	ANN
	West	−8.7	−7.0	−5.3	−3.8	−6.2
Ponape	East	−8.6	−7.4	−4.5	−2.7	−5.8
(7N,155E)	W−E	−0.1	+0.4	+ 0.8	−1.1	−0.4
	West	−6.0	−4.3	+0.8	+1.1	−2.1
Koror	East	−6.4	−4.5	+1.3	+2.0	−1.9
(7N,134E)	W−E	+0.4	+0.2	−0.5	0.9	−0.2
	West	−8.1	−6.4	−1.2	−1.3	−4.2
Yap	East	−8.4	−6.7	−1.0	−0.4	−4.1
(9N,138E)	W−E	+0.3	+0.3	−0.2	−0.9	−0.1
	West	−7.9	−5.9	−3.7	−2.5	−5.0
Truk	East	−7.7	−6.4	−2.9	−1.5	−4.6
(7N,152E)	W−E	−0.2	+0.5	−0.8	−1.0	−0.4
	West	−8.2	−7.5	−6.5	−4.9	−6.8
Majuro	East	−7.7	−7.8	−5.9	−4.0	−6.3
(7N,172E)	W−E	−0.5	+0.3	−0.6	−0.9	−0.5
	West	−9.0	−7.7	−4.7	−4.5	−6.5
Guam	East	−8.8	−7.8	−3.9	−4.4	−6.2
(13N,145E)	W−E	−0.2	+0.1	−0.8	−0.1	−0.3
	West	−4.4	−5.4	−5.9	−6.4	−5.5
Wake Island	East	−4.5	−5.9	−5.9	−6.6	−5.8
(19N,167E)	W−E	−0.1	+0.5	0.0	+0.2	+0.3
	West	−1.7	−1.9	−6.3	−3.8	−2.6
Honiara	East	+1.1	−1.7	−5.2	−3.8	−2.4
(9S,160E)	W−E	+0.6	−0.2	−1.1	0.0	−0.2
	West	+1.4	−5.1	−6.4	−5.5	−3.9
Darwin	East	+0.1	−5.4	−5.7	−5.9	−4.2
(12S,130E)	W−E	+1.3	+0.3	−0.7	+0.4	+0.3
		Surface Zonal Wind (m/s)				
	West	−3.7	−4.2	−3.4	−2.8	−3.5
Tarawa	East	−3.3	−3.9	−2.6	−2.3	−3.0
(2N,173E)	W−E	−0.4	−0.3	−0.8	−0.5	−0.5

convection is confined to the very near equator region, trade winds are anomalously from the west and the Walker Circulation along the equator is relatively weak. These conditions are typical of a warm ENSO type climatology.

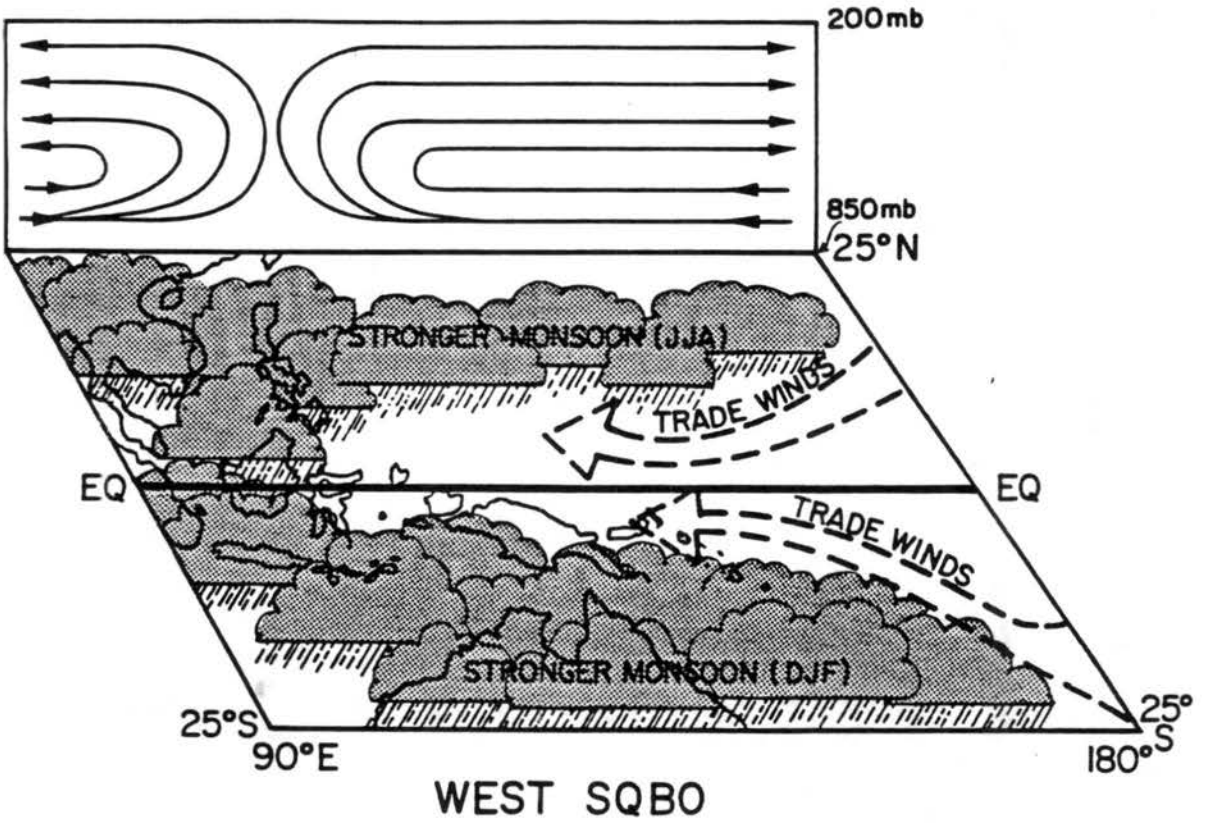

Figure 6.3: Conceptual illustration of anomalous convection and circulation due to effects of the upper tropospheric to lower stratospheric zonal wind shear anomalies occurring during the west phase of the SQBO. The anomalous state of the regional Walker Circulation is shown at the top of the drawing.

6.2 Discussion of Results in Relation to ENSO Variability

The results of this analysis suggest that the west phase of the SQBO, by modulating deep tropical convection, creates conditions in the West Pacific region which are associated with cold ENSO events whereas the east phase of the SQBO promotes the opposite conditions. This modulation of convection relates well to changes in the local Walker Circulation, particularly the trade winds. The modulation of the trades is most likely the result of enhanced (suppressed) convection near the equator during the east (west) phase

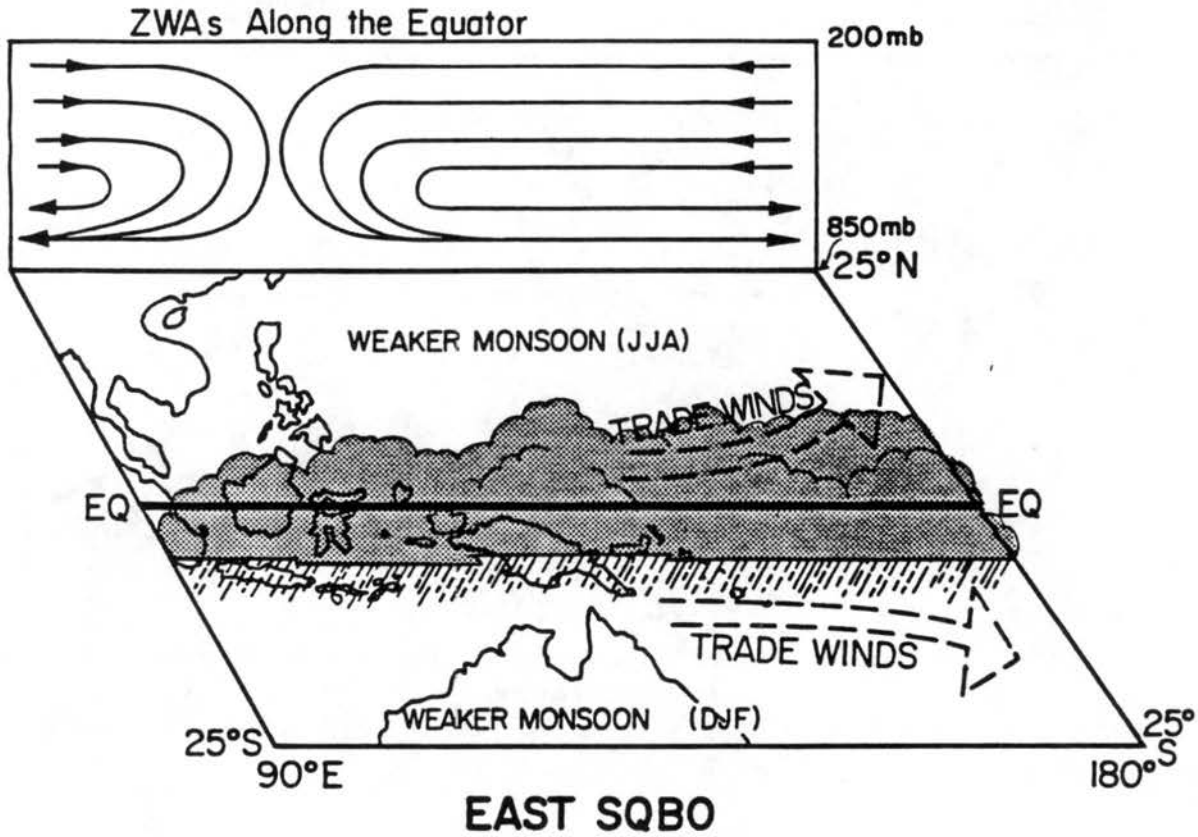

Figure 6.4: As in Fig. 6.3 but for convection and circulation due to the upper tropospheric to lower stratospheric zonal wind shear anomalies during the east phase of the SQBO.

of the SQBO. Furthermore, the enhanced convection along the equator during the east phase of the SQBO indicates that convection can progress eastward more easily in association with active modes of the 30-60 day oscillation. Observations of a stronger more robust intra-seasonal oscillation occurring during the east phase of the SQBO were noted by Kuma (1990). The implications of the stronger 30-60 day oscillation occurring during the east phase of the SQBO are important. Work done by Lau and Chan (1988) indicate that inter-annual variations of the intra-seasonal oscillation may be a key component of ENSO variability; their results show that periods of strong 30-60 day oscillations precede the occurrence of warm ENSO events.

The trade winds, as they are effected by the equatorial convection, act as the instrument by which the 30-60 day oscillation can influence ENSO variability. During cold ENSO periods the trade winds are stronger. These stronger trades tend to push warm surface waters near the dateline toward the west. As this westward drift is more saline, these warm dense waters are subduction under the less dense waters of similar temperatures in the warm pool area. This subduction acts to recharge the heat energy of the warm pool by deepening the thermocline (Lucas and Lundstrom, 1987). An enhanced mode of this recharge process can occur during the west phase of the SQBO when equatorial convection is somewhat suppressed, resulting in stronger than average trade winds along the equator.

The situation along the equator during the east phase of the SQBO is essentially reversed. During these periods, convection along the equator is enhanced, causing weaker trade winds. By weakening the trade winds, upwelling along the equator is reduced leading to accumulation of warm surface waters along the equator in Pacific Ocean east of 140°E. Weakening the trade winds also leads to equatorial ocean Kelvin waves being generated (Wyrtki, 1975). Oceanic Kelvin waves are well recognized as a principle cause of anomalous equatorial ocean currents that facilitate the movement of the warm pool eastward (Phillander, 1990).

By these arguments, it quickly becomes evident that by causing varying amounts of 200 mb to 50 mb zonal wind shears (and thus modulating deep tropical convection)

the SQBO causes prolonged periods of contrasting conditions. During the east phase of the SQBO, convection is enhanced along the equator, resulting in a stronger 30-60 day oscillation and the weaker trade winds. This condition facilitates the production of oceanic Kelvin waves and promotes conditions favorable for the onset of warm ENSO. In contrast, the west phase of the SQBO causes more off-equator convection, especially in monsoon regions. This latter condition act has two effects: (1) the trades are stronger indicating periods favorable for recharge or cold ENSO periods, and (2) pressure anomalies in the off-equator region become lower, causing a strengthening of the east-west pressure gradient across the Pacific Ocean. The latter conditions favor cold ENSO periods.

The trade winds are stronger during the east phase of the SQBO during MAM; this due to a slow decay of the SPCZ. However, this effect in itself may be an important factor in the timing of ENSO as the SQBO often changes phase between the MAM and SON seasons. This association may thus be linked to why ENSO parameters favor change between MAM and SON. The results suggest that the occurrence a warm ENSO event is most favorable when the SQBO in the lower stratosphere changes from west to east between March to June, as it typically does. Consequently, the results offer a theory for the strong biennial component of ENSO! The SQBO, by modulating convection within the framework of the tropospheric annual cycle results in a biennial signal, that often changes phase and has variable amplitude as described by Rasmusson *et al.* (1990).

6.3 Summary of Chapter 6

This Chapter has presented observational evidence of a link between the SQBO and tropospheric parameters for the equatorial Pacific region. More specifically, deep convection appears to be effected by differing rates of upper tropospheric to lower stratospheric wind shear which oscillate with the SQBO. This convective modulation is observed in composites of OLR and HRC and in precipitation data throughout the West Pacific region. Furthermore, anomalous convection due to low values of 200 mb to 50 mb shear seems to create lower surface pressures in off-equator regions. This feedback, however,

does not seem to operate well along the equator. The lack of this feedback along the equator could be due to the difficulties inherent in maintaining pressure gradients very close to the equator. Nevertheless, the results suggest that a different SQBO related mechanism may be at work along the equator. Evidence of a stratospheric-tropospheric link, notably one that effects deep tropical convection, has important implications. First, this SQBO convection modulation may explain many of the recently documented quasi-biennial and biennial modes of ENSO, global precipitation, and of the tropical 30-60 day oscillation. Second, the SQBO may be an important factor for predicting monsoon strength. Finally, the results suggest the potential importance for the inclusion of the SQBO in climate variability studies, particularly those related to tropical convection.

ACKNOWLEDGEMENTS

This work represents culmination of the labors, and hopes of many. I owe many thanks to those who have helped with the research and preparation of this manuscript. I would especially like to thank my advisor, Dr. William M. Gray, whose enthusiasm and energy allowed for the fairly expedient finish of this work. I am in much debt to Barbara Brumit and Laneigh Walters whose typing and correction making saved me many months of hard work. I would also like to thank John D. Sheaffer for his help and careful editing of the manuscript and advisement on much of the precipitation and pressure data sources and analysis. I would like to express thanks to Dr. Gramme Stephens for supplying outgoing longwave radiation data; Bob Grossman for helping explain and acquire the highly reflective cloud data set; and much gratitude goes to William Thorson for acquiring all the rawinsonde data. Others deserving of thanks are Wayne Schubert, Darren Jackson, Rennie Selkirk and Russell Elsberry whose comments and suggestions helped me along the way.

REFERENCES

Angell, J. K., 1992: Evidence of a relation between El Niño and QBO, and for an El Niño in 1991–92. *Geophys. Res. Lett.*.

Barnett, T., 1989: A solar–ocean relation: Fact or fiction. Proceedings of the Thirteenth annual Climate Diagnostics Workshop, Cambridge, MA, October, US Dept. of Commerce, PB89–178115.

Barnett, T., 1990: A solar–ocean relation: Fact or fiction. *Geophys. Res. Lett.*, 16, 803–806.

Barnett, T., 1991: The interaction of multiple time scales in tropical climate system. *J. Climate, 3*, 269–285.

Chellia's CAC Global Tropospheric Climatology, 1979–1988: CAC 10 year climate diagnostics data base.

Danielsen, E. F., 1982: A dehydration mechanism for the stratosphere. *Geophys. Res. Lett.*, 9, 601–604.

Desser, C. and J. M. Wallace, 1990: Large-scale atmospheric circulation features of warm and cold episodes in the tropical Pacific. *J. Climate*, 3, 1254–1281.

Dobson, G. M., A. W. Brewer and B. Cwilong, 1946: Meteorology of the lower stratosphere. *Proc. Roy. Soc. London*, A185, 144–175.

Dunkerton, T. J. and D. P. Delisi, 1985: Climatology of the equatorial lower stratosphere. *J. Atmos. Sci.*, 42, 376-396.

Dunkerton, T. J. and M. P. Baldwin, 1991: Quasi-biennial modulation of planetary-wave fluxes in the Northern Hemisphere winter. *J. Atmos. Sci.*, 48, 1043–1061.

Gray, W. M., 1984: Atlantic seasonal hurricane frequency: Part I: El Niño and 30 mb quasi-biennial oscillation influences. *Mon. Wea. Rev.*, 112, 1649–1668.

Gray, W. M., 1988: Environmental influences on tropical cyclones. *Aust. Met. Mag.*, 36, 3, 127–139.

Gray, W. M., J. D. Sheaffer, and J. A. Knaff, 1992a: Influence of the stratospheric QBO on ENSO variability. *J. Meteor. Soc. Japan*, 70, 975–995.

Gray, W. M., J. D. Sheaffer, and J. A. Knaff, 1992b: Hypothesized mechanism for stratospheric QBO influences on ENSO variability. *Geophy. Res. Lett.*, 19, 2, 107–110.

Gray, W. M., J. D. Sheaffer and J. A. Knaff, 1991: Hypothesized mechanism for stratospheric QBO influence on ENSO variability. Paper presented for the 5th Conference on Climate Variations, Denver, CO, October 14-18.

Grossman, R. and O. Garcia, 1990: The distribution of deep convection over ocean and land during the Asian summer monsoon. *J. Climate*, 3, 1032–1044.

Hertenstein, R. F. and W. H. Schubert, 1991: Potential vorticity anomalies associated with squall lines. *Mon. Wea. Rev.*, 119, 1663–1672.

Holland, G. J., 1986: Interannual variability of the Australian summer monsoon at Darwin. *Mon. Wea. Rev.*, 114, 594–604.

Johnson, R. H., and D. C. Kriete, 1982: Thermodynamic and circulation characteristics of winter monsoon tropical mesoscale convection. *Mon. Wea. Rev.*, 110, 1898–1910.

Kilonsky, B. and C. S. Ramage, 1976: A technique for estimating tropical open-ocean rainfall from satellite observations. *J. Appl. Meteor.*, 15, 972–975.

Knaff, J. A., W. M. Gray, and J. D. Sheaffer, 1991: Evidence for an association between the stratospheric QBO and ENSO. Preprints, 5th AMS Conference on Climate Variations, Denver, Colorado, October, 1991.

Kuma, K., 1990: A quasi-biennial oscillation in the intensity of the intra-seasonal oscillation. *Int. J. of Climatology*, 10, 263-278.

Lau, K. M. and D. J. Sheu, 1988: Annual cycle, quasi-biennial oscillation on global precipitation. *J. Geophys. Res.*, 93, 10975-10988.

Lau, K. and P. Chan, 1988: Intraseasonal and interannual variations of tropical convection: A possible link between the 40–50 day oscillation and ENSO? *J. Atmos. Sci.*, 45, 506–521.

Lukas, R. and E. Lindstrom, 1987: The mixed layer of the western equatorial Pacific ocean dynamics of the oceanic surface mixed layer. Proceedings of the 'Aha Huliko's Hawaiian Winter Workshop, Honolulu, Hawaiian, January 14-16, 1987.

Maruyama, T., 1991: Annual and QBO–synchronized variations of lower stratospheric equatorial wave activity over Singapore during 1961–1989. *J. Meteor. Soc. Japan*, 69, 219–231.

Maruyama, T. and Y. Tsuneoka, 1988: Anomalously short duration of easterly wind phase of the QBO at 50 hPa in 1987 and its relationship to an El Niño event. *J. Meteor. Soc. Japan*, 66, 629-633.

Meehl, G. A., 1987: The annual cycle and interannual variability in the Tropical Pacific and Indian Ocean regions. *Mon. Wea. Rev.*, 115, 27–50.

Mukherjee, R. B., K. Indra, R. S. Reddy, and B. H. V. Ramanamurty, 1985: QBO in stratospheric zonal wind and Indian Summer Monsoon. *Mon. Wea. Rev.*, 113, 1421–1423.

Nicholls, N., J. L. McBride and R. J. Ormerod, 1982: On predicting the onset of the Australian wet season at Darwin. *Mon. Wea. Rev.*, 110, 14–17.

Phillander, G., 1989: El Niño and La Niña. *Amer. Sci.*, 77, 451–459.

Phillander, G., 1990: El Niño, La Niña, and the southern oscillation. Academic Press, Inc., San Diego, California, 293 pp.

Rasmusson, E. M. and T. H. Carpenter, 1982: Variations in tropical sea surface temperature and surface wind fields associated with the southern oscillation/El Niño. *Mon. Wea. Rev.*, 110, 354–384.

Rasmusson, E. M., X. Wang and C. F. Ropelewski, 1990: The biennial component of ENSO variability. *J. Marine Systems*, 1, 1, 15 pp.

Raymond, D. J. and H. Jiang, 1990: A theory for long lived mesoscale convective systems. *J. Atmos. Sci.*, 47, 24, 3067–3077.

Selkirk, H. B. and R. E. Newell, 1989: Diagnostic studies in relation to the NASA stratosphere-troposphere exchange project. Final report under NASA Grant NAGW-703 Massachusetts Institute of Technology, Cambridge, MA, 187 pp.

Shapiro, L. J., 1989: The relationship of the quasi-biennial oscillation to Atlantic tropical storm activity. *Mon. Wea. Rev.*, 117, 1545-1552.

Trenberth, K. E., 1980: Atmospheric quasi–biennial oscillation. *Mon. Wea. Rev.*, 108, 1370–1377.

US Department of Commerce, NOAA, and CAC, 1991: Monthly averaged OLR derived from Polar Orbinins Satellites.

US Department of Commerce, NOAA, NCDC, National Environmental Satellite, Data, and Information Service, 1971-1983, 1989, 1990: Monthly Climatic Data for the World, Asheville, NC, 24-36, 42, 43, No. 1-12.

Wright, P.B., 1985: The Southern Oscillation: An ocean-atmosphere feedback system? *Bull. Amer. Meteor. Soc.*, 66, 398-412.

Wyrtki, K., 1975: El Niño–the dynamic response of the equatorial Pacific Ocean to atmospheric forcing. *J. Phy. Oceanography*, 5, 572–584.

Yasunari, T., 1989: A possible link of the QBO's between the stratosphere, troposphere and the surface temperature in the tropics. *J. Meteor. Soc. Japan*, 67, 483-493.

PROJECT REPORTS FROM W. M. GRAY'S FEDERALLY SUPPORTED RESEARCH
(SINCE 1967)

CSU Dept. of Atmos. Sci. Report No.	Report Title, Author, Date, Agency Support
104	The Mutual Variation of Wind, Shear and Baroclinicity in the Cumulus Convective Atmosphere of the Hurricane (69 pp.). W. M. Gray. February 1967. NSF Support.
114	Global View of the Origin of Tropical Disturbances and Storms (105 pp.). W. M. Gray. October 1967. NSF Support.
116	A Statistical Study of the Frictional Wind Veering in the Planetary Boundary Layer (57 pp.). B. Mendenhall. December 1967. NSF and ESSA Support.
124	Investigation of the Importance of Cumulus Convection and ventilation in Early Tropical Storm Development (88 pp.). R. Lopez. June 1968. ESSA Satellite Lab. Support.
Unnumbered	Role of Angular Momentum Transports in Tropical Storm Dissipation over Tropical Oceans (46 pp.). R. F. Wachtmann. December 1968. NSF and ESSA Support.
Unnumbered	Monthly Climatological Wind Fields Associated with Tropical Storm Genesis in the West Indies (34 pp.). J. W. Sartor. December 1968. NSF Support.
140	Characteristics of the Tornado Environment as Deduced from Proximity Soundings (55 pp.). T. G. Wills. June 1969. NOAA and NSF Support.
161	Statistical Analysis of Trade Wind Cloud Clusters in the Western North Pacific (80 pp.). K. Williams. June 1970. ESSA Satellite Lab. Support.
—	A Climatology of Tropical Cyclones and Disturbances of the Western Pacific with a Suggested Theory for Their Genesis/Maintenance (225 pp.). W. M. Gray. NAVWEARSCHFAC Tech. Paper No. 19-70. November 1970. (Available from US Navy, Monterey, CA). US Navy Support.
179	A diagnostic Study of the Planetary Boundary Layer over the Oceans (95 pp.). W. M. Gray. February 1972. Navy and NSF Support.
182	The Structure and Dynamics of the Hurricane's Inner Core Area (105 pp.). D. J. Shea. April 1972. NOAA and NSF Support.
188	Cumulus Convection and Larger-scale Circulations, Part I: A Parametric Model of Cumulus Convection (100 pp.). R. E. Lopez. June 1972. NSF Support.
189	Cumulus Convection and Larger-scale Circulations, Part II: Cumulus and Meso-scale Interactions (63 pp.). R. E. Lopez. June 1972. NSF Support.
190	Cumulus Convection and Larger-scale Circulations, Part III: Broadscale and Meso-scale Considerations (80 pp.). W. M. Gray. July 1972. NOAA-NESS Support.
195	Characteristics of Carbon Black Dust as a Tropospheric Heat Source for Weather Modification (55 pp.). W. M. Frank. January 1973. NSF Support.
196	Feasibility of Beneficial Hurricane Modification by Carbon Black Seeding (130 pp.). W. M. Gray. April 1973. NOAA Support.
199	Variability of Planetary Boundary Layer Winds (157 pp.). L. R. Hoxit. May 1973. NSF Support.
200	Hurricane Spawned Tornadoes (57 pp.). D. J. Novlan. May 1973. NOAA and NSF Support.

CSU Dept. of Atmos. Sci. Report No.	Report Title, Author, Date, Agency Support
212	A Study of Tornado Proximity Data and an Observationally Derived Model of Tornado Genesis (101 pp.). R. Maddox. November 1973. NOAA Support.
219	Analysis of Satellite Observed Tropical Cloud Clusters (91 pp.). E. Ruprecht and W. M. Gray. May 1974. NOAA/NESS Support.
224	Precipitation Characteristics in the Northeast Brazil Dry Region (56 pp.). R. P. L. Ramos. May 1974. NSF Support.
225	Weather Modification through Carbon Dust Absorption of Solar Energy (190 pp.). W. M. Gray, W. M. Frank, M. L. Corrin, and C. A. Stokes. July 1974.
234	Tropical Cyclone Genesis (121 pp.). W. M. Gray. March 1975. NSF Support.
—	Tropical Cyclone Genesis in the Western North Pacific (66 pp.). W. M. Gray. March 1975. US Navy Environmental Prediction Research Facility Report. Tech. Paper No. 16-75. (Available from the US Navy, Monterey, CA). Navy Support.
241	Tropical Cyclone Motion and Surrounding Parameter Relationships (105 pp.). J. E. George. December 1975. NOAA Support.
243	Diurnal Variation of Oceanic Deep Cumulus Convection. Paper I: Observational Evidence, Paper II: Physical Hypothesis (106 pp.). R. W. Jacobson, Jr. and W. M. Gray. February 1976. NOAA-NESS Support.
257	Data Summary of NOAA's Hurricanes Inner-Core Radial Leg Flight Penetrations 1957-1967, and 1969 (245 pp.). W. M. Gray and D. J. Shea. October 1976. NSF and NOAA Support.
258	The Structure and Energetics of the Tropical Cyclone (180 pp.). W. M. Frank. October 1976. NOAA-NHEML, NOAA-NESS and NSF Support.
259	Typhoon Genesis and Pre-typhoon Cloud Clusters (79 pp.). R. M. Zehr. November 1976. NSF Support.
Unnumbered	Severe Thunderstorm Wind Gusts (81 pp.). G. W. Walters. December 1976. NSF Support.
262	Diurnal Variation of the Tropospheric Energy Budget (141 pp.). G. S. Foltz. November 1976. NSF Support.
274	Comparison of Developing and Non-developing Tropical Disturbances (81 pp.). S. L. Erickson. July 1977. US Army Support.
—	Tropical Cyclone Research by Data Compositing (79 pp.). W. M. Gray and W. M. Frank. July 1977. US Navy Environmental Prediction Research Facility Report. Tech. Paper No. 77-01. (Available from the US Navy, Monterey, CA). Navy Support.
277	Tropical Cyclone Cloud and Intensity Relationships (154 pp.). C. P. Arnold. November 1977. US Army and NHEML Support.
297	Diagnostic Analyses of the GATE A/B-scale Area at Individual Time Periods (102 pp.). W. M. Frank. November 1978. NSF Support.
298	Diurnal Variability in the GATE Region (80 pp.). J. M. Dewart. November 1978. NSF Support.
299	Mass Divergence in Tropical Weather Systems, Paper I: Diurnal Variation; Paper II: Large-scale Controls on Convection (109 pp.). J. L. McBride and W. M. Gray. November 1978. NOAA-NHEML Support.

CSU Dept. of Atmos. Sci. Report No.	Report Title, Author, Date, Agency Support
—	New Results of Tropical Cyclone Research from Observational Analysis (108 pp.). W. M. Gray and W. M. Frank. June 1978. US Navy Environmental Prediction Research Facility Report. Tech. Paper No. 78-01. (Available from the US Navy, Monterey, CA). Navy Support.
305	Convection Induced Temperature Change in GATE (128 pp.). P. G. Grube. February 1979. NSF Support.
308	Observational Analysis of Tropical Cyclone Formation (230 pp.). J. L. McBride. April 1979. NOAA-NHEML, NSF and NEPRF Support.
—	Tropical Cyclone Origin, Movement and Intensity Characteristics Based on Data Compositing Techniques (124 pp.). W. M. Gray. August 1979. US Navy Environmental Prediction Research Facility Report. Tech. Paper No. CR-79-06. (Available from the US Navy, Monterey, CA). Navy Support.
—	Further Analysis of Tropical Cyclone Characteristics from Rawinsonde Compositing Techniques (129 pp.). W. M. Gray. March 1981. US Navy Environmental Prediction Research Facility Report. Tech. Paper No. CR-81-02. (Available from the US Navy, Monterey, CA). Navy Support.
333	Tropical Cyclone Intensity Change—A Quantitative Forecasting Scheme. K. M. Dropco. May 1981. NOAA Support.
—	Recent Advances in Tropical Cyclone Research from Rawinsonde Composite Analysis (407 pp.). WMO Publication. W. M. Gray. 1981.
340	The Role of the General Circulation in Tropical Cyclone Genesis (230 pp.). G. Love. April 1982. NSF Support.
341	Cumulus Momentum Transports in Tropical Cyclones (78 pp.). C. S. Lee. May 1982. ONR Support.
343	Tropical Cyclone Movement and Surrounding Flow Relationships (68 pp.). J. C. L. Chan and W. M. Gray. May 1982. ONR Support.
346	Environmental Circulations Associated with Tropical Cyclones Experiencing Fast, Slow and Looping Motions (273 pp.). J. Xu and W. M. Gray. May 1982. NOAA and NSF Support.
348	Tropical Cyclone Motion: Environmental Interaction Plus a Beta Effect (47 pp.). G. J. Holland. May 1982. ONR Support.
—	Tropical Cyclone and Related Meteorological Data Sets Available at CSU and Their Utilization (186 pp.). W. M. Gray, E. Buzzell, G. Burton and Other Project Personnel. February 1982. NSF, ONR, NOAA, and NEPRF Support.
352	A Comparison of Large and Small Tropical Cyclones (75 pp.). R. T. Merrill. July 1982. NOAA and NSF Support.
358	On the Physical Processes Responsible for Tropical Cyclone Motion (200 pp.). Johnny C. L. Chan. November 1982. NSF, NOAA/NHRL and NEPRF Support.
363	Tropical Cyclones in the Australian/Southwest Pacific Region (264 pp.). Greg J. Holland. March 1983. NSF, NOAA/NHRL and Australian Government Support.
370	Atlantic Seasonal Hurricane Frequency, Part I: El Nino and 30 mb QBO Influences; Part II: Forecasting Its Variability (105 pp.). W. M. Gray. July 1983. NSF Support.

CSU Dept. of Atmos. Sci. Report No.	Report Title, Author, Date, Agency Support
379	A Statistical Method for One- to Three-Day Tropical Cyclone Track Prediction (201 pp). Clifford R. Matsumoto. December, 1984. NSF/NOAA and NEPRF support.
—	Varying Structure and Intensity Change Characteristics of Four Western North Pacific Tropical Cyclones. (100 pp.). Cecilia A. Askue and W. M. Gray. October 1984. US Navy Environmental Prediction Research Facility Report No. CR 84-08. (Available from the US Navy, Monterey, CA). Navy Suppor
—	Characteristics of North Indian Ocean Tropical Cyclone Activity. (108 pp.). Cheng-Shang Lee and W. M. Gray. December 1984. US Navy Environmental Prediction Research Facility Report No. CR 84-11. (Available from the US Navy, Monterey, CA). Navy Support.
391	Typhoon Structural Variability. (77 pp.). Candis L. Weatherford. October, 1985. NSF/NOAA Support.
392	Global View of the Upper Level Outflow Patterns Associated with Tropical Cyclone Intensity Change During FGGE. (126 pp.). L. Chen and W. Gray. October, 1985. NASA support.
394	Environmental Influences on Hurricane Intensification. (156 pp.). Robert T. Merrill. December, 1985. NSF/NOAA Support.
403	An Observational Study of Tropical Cloud Cluster Evolution and Cyclogenesis in the Western North Pacific. (250 pp.). Cheng-Shang Lee. September, 1986. NSF/NOAA support.
—	Recent Colorado State University Tropical Cyclone Research of Interest to Forecasters. (115 pp.). William M. Gray. June, 1987. US Navy Environmental Prediction Research Facility Contractor Report CR 87-10. Available from US Navy, Monterey, CA. Navy support.
428	Tropical Cyclone Observation and Forecasting With and With and Without Aircraft Reconnaissance. (105 pp.) Joel D. Martin. May, 1988. USAF, NWS, ONR support.
429	Investigation of Tropical Cyclone Genesis and Development Using Low-level Aircraft Flight Data. (94 pp.) Michael G. Middlebrooke. May, 1988. USAF, NSF support.
436	Environmental and convective influence on tropical cyclone development vs. non–development. (105 pp.) Patrick A. Lunney. December, 1988.
446	The structural evolution of typhoons. (198 pp.). Candis Weatherford. September, 1989. NSF/NOAA and ONR Support
457	Relationships between tropical cyclone deep convection and the radial extent of damaging winds. (109 pp.) Daniel N. Shoemaker. October, 1989. AFGL Support.
468	Associations between West Pacific equatorial zonal winds and East Pacific SST anomalies. (103 pp.) Christopher C. Collimore. May, 1990. NSF Support.
480	An observational analysis of tropical cyclone recurvature. (124 pp.). Stephen J. Hodanish. May, 1991. ONR Support.
484	West African monsoonal rainfall and intense hurricane associations. (270 pp.). Christopher W. Landsea. October, 1991. NSF Support.